

**Preparation, Characterization, and Evaluation of  
Thermophysical Properties of Si<sub>3</sub>N<sub>4</sub> Based Nanofluid for Heat  
Transfer**



By

Sana Saleem

(Registration No: 00000402830)

Department of Thermal Energy Engineering

US-Pakistan Center for Advanced Studies in Energy (USPCAS-E)

National University of Sciences & Technology (NUST)

Islamabad, Pakistan

(2024)

**Preparation, Characterization, and Evaluation of  
Thermophysical Properties of Si<sub>3</sub>N<sub>4</sub> Based Nanofluid for Heat  
Transfer**



By

Sana Saleem

(Registration No: 00000402830)

A thesis submitted to the National University of Sciences and Technology, Islamabad,

in partial fulfillment of the requirements for the degree of

Master of Science in

Thermal Energy Engineering

Supervisor: Dr. Majid Ali

Co Supervisor: Dr. Sana Yaqub

US-Pakistan Center for Advanced Studies in Energy (USPCAS-E)

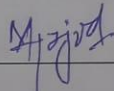
National University of Sciences & Technology (NUST)

Islamabad, Pakistan

(2024)

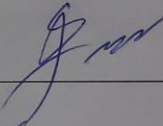
### THESIS ACCEPTANCE CERTIFICATE

Certified that the final copy of MS Thesis written by Ms. Sana Saleem (Registration No. 402830), of USPCASE, has been vetted by the undersigned, found complete in all respects as per NUST Statutes/ Regulations/ Masters Policy, is free of plagiarism, errors, and mistakes and is accepted as partial fulfillment for award of Master's degree. It is further certified that necessary amendments as pointed out by GEC members and foreign/ local evaluators of the scholar have also been incorporated in the said thesis.

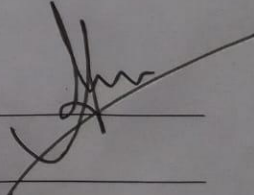
Signature: \_\_\_\_\_ 

Name of Supervisor Dr Majid Ali

Date: \_\_\_\_\_ 26/12/2024

Signature (HOD): \_\_\_\_\_ 

Date: \_\_\_\_\_ 06/01/2025

Signature (Dean/ Principal) \_\_\_\_\_ 

Date: \_\_\_\_\_ 7/1/25

TEE

FORM TH-4

**International University of Sciences & Technology**  
**MASTER THESIS WORK**

We hereby recommend that the dissertation prepared under our supervision by Sana Saleem & Registration Number 00000402830 Titled: Preparation, Characterization, and Evaluation of Thermophysical Properties of Si<sub>3</sub>N<sub>4</sub> Based Nanofluid for Heat Transfer be accepted in partial fulfillment of the requirements for the award of MS Thermal Energy Engineering degree with A grade.

**Examination Committee Members**

1. Name: Dr. Nadia Shahzad ✓

Signature: \_\_\_\_\_

2. Name: Ghulam Ali ✓

Signature: \_\_\_\_\_

3. Name: Dr. Sehar Shakir ✓

Signature: \_\_\_\_\_

Supervisor's name: Dr. Majid Ali ✓

Signature: \_\_\_\_\_

Date: 19/12/2024

Co-Supervisor's name: Dr. Sana Yaqub ✓

Signature: \_\_\_\_\_

\_\_\_\_\_  
Head of Department

06/01/2025  
Date

**COUNTERSIGNED**

\_\_\_\_\_  
Dean/Principal

Date: \_\_\_\_\_

## CERTIFICATE OF APPROVAL

This is to certify that the research work presented in this thesis, entitled "Preparation, Characterization, and Evaluation of Thermophysical Properties of Si<sub>3</sub>N<sub>4</sub> Nanofluid for Heat Transfer." was conducted by Ms. Sana Saleem under the supervision of Dr. Majid Ali. No part of this thesis has been submitted anywhere else for any other degree. This thesis is submitted to the Us-Pakistan Center For Advanced Studies in Energy (USPCAS-E) in partial fulfillment of the requirements for the degree of Master of Science in the Field of Thermal Energy Engineering, Department of Thermal Energy Engineering National University of Sciences and Technology, Islamabad

Student Name: Sana Saleem

Signature: Sana Saleem

Examination Committee:

a) GEC Member 1: Dr. Ghulam Ali  
(Professor, USPCAS-E NUST)

Signature: Ghulam Ali

b) GEC Member 2: Dr. Nadia Shahzad  
(Associate Professor, USPCAS-E NUST)

Signature: Nadia Shahzad

c) GEC Member 3: Dr. Sehar Shakir  
(Assistant Professor, USPCAS-E NUST)

Signature: Sehar Shakir

Supervisor Name: Dr. Majid Ali

Signature: Majid Ali

Co-Supervisor Name: Dr. Sana Yaqub

Signature: Sana Yaqub

Name of HOD: Dr. Asif Hussain Khoja

Signature: Asif Hussain Khoja

Name of Principal/Dean: Dr. Adeel Waqas

Signature: Adeel Waqas

### AUTHOR'S DECLARATION

I Sana Saleem hereby state that my MS thesis titled "Preparation, Characterization, and Evaluation of Thermophysical Properties of  $\text{Si}_3\text{N}_4$  nanofluid for Heat Transfer" is my own work and has not been submitted previously by me for taking any degree from National University of Sciences and Technology, Islamabad or anywhere else in the country/ world.

At any time if my statement is found to be incorrect even after I graduate, the university has the right to withdraw my MS degree.

Name of Student: Sana Saleem

Date: Sana Saleem ,

### PLAGIARISM UNDERTAKING

I solemnly declare that the research work presented in the thesis titled "Preparation, Characterization, and Evaluation of Thermophysical Properties of Si<sub>3</sub>N<sub>4</sub> nanofluid for Heat Transfer" is solely my research work with no significant contribution from any other person. Small contribution/ help wherever taken has been duly acknowledged and that complete thesis has been written by me.

I understand the zero-tolerance policy of the HEC and the National University of Sciences and Technology (NUST), Islamabad towards plagiarism. Therefore, I as an author of the above titled thesis declare that no portion of my thesis has been plagiarized and any material used as reference is properly referred/cited.

I undertake that if I am found guilty of any formal plagiarism in the above-titled thesis even after the award of MS degree, the University reserves the right to withdraw/ revoke my MS degree and that HEC and NUST, Islamabad have the right to publish my name on the HEC/University website on which names of students are placed who submitted plagiarized thesis.

Student Signature: Sana Saleem .

Name: Sana Saleem

## **ACKNOWLEDGEMENTS**

All praise is due to Allah Almighty, the most Gracious and Merciful, for granting me the strength to successfully complete this challenging yet rewarding journey of obtaining my MS degree. I am deeply grateful for the resilience that sustained me and the invaluable life lessons I have learned along the way. As my research comes to an end, I want to extend my heartfelt appreciation to my supervisors, Dr. Majid Ali and Dr. Sana Yaqub, for their unwavering guidance and support throughout my MS program.

I am profoundly thankful to my guidance and evaluation committee members Dr. Seher Shakir, Dr. Ghulam Ali, and Dr. Nadia Shahzad—for their insightful contributions that have significantly enhanced my research. My sincere thanks go to my faculty for their unwavering support during the challenging period following my father's passing. Their assistance and encouragement played a key role in my successful completion of the degree. I also appreciate Mr. Abdul Rehman for his invaluable assistance and support during my research. My gratitude extends to the entire teaching and non-teaching faculty and lab engineers at the U.S.-Pakistan Center for Advanced Studies in Energy for their consistent support, which greatly enriched my research experience.

I am especially thankful to my family, whose strength, support, and unwavering encouragement have constantly motivated me. Lastly, I am deeply grateful to my friends and colleagues for their continuous support and encouragement, which has uplifted me throughout this journey.



## TABLE OF CONTENT

<b>ACKNOWLEDGEMENTS</b>	<b>VIII</b>
<b>TABLE OF CONTENT</b>	<b>IX</b>
<b>LIST OF TABLES</b>	<b>XII</b>
<b>LIST OF FIGURES</b>	<b>XIII</b>
<b>LIST OF SYMBOLS, ABBREVIATIONS AND ACRONYMS</b>	<b>XIV</b>
<b>ABSTRACT</b>	<b>XV</b>
<b>CHAPTER 1: INTRODUCTION</b>	<b>1</b>
<b>1.1. Heat Transfer Fluids</b>	<b>1</b>
<b>1.2. Development of Nanofluids</b>	<b>2</b>
<b>1.3. Research Motivation</b>	<b>4</b>
<b>1.4. Applications of Nanofluids</b>	<b>7</b>
1.4.1. Thermal Applications of Nanofluids	8
<b>1.5. Problem Statement and Research Objectives</b>	<b>9</b>
<b>1.6. Research Limitations</b>	<b>10</b>
<b>Summary</b>	<b>10</b>
<b>Dissertation Organization</b>	<b>10</b>
<b>CHAPTER 2: LITERATURE REVIEW</b>	<b>12</b>
<b>2.1. Nanofluids as Heat Transfer Fluids</b>	<b>12</b>
<b>2.2. Nanoparticle Synthesis Approaches and Methods</b>	<b>12</b>
2.2.1. Top-Down Approach	13
2.2.1.1. Mechanical Milling & Ball Milling Process	14
2.2.1.2. Thermal Evaporation	15
2.2.1.3. Laser Ablation	16
2.2.1.4. Sputtering	16
2.2.2. Bottom-Up Approaches	16
2.2.2.1. Chemical Vapour Deposition (CVD)	17
2.2.2.2. Hydrothermal Method	17
2.2.2.3. Co-Precipitation	18
2.2.2.4. Sol-Gel Method	18
<b>2.3. Nanofluids Preparation Techniques</b>	<b>18</b>
2.3.1. Single-step Method of Nanofluid Preparation	19
2.3.1.1. Direct Evaporation Method	20
2.3.1.2. Physical Method	20
2.3.1.3. Chemical Method	21
2.3.2. Two-Step Method	21

2.3.2.1. Ultrasonic Sonicator	22
2.3.2.2. High-pressure homogenizer	22
2.3.2.3. Mechanical Stirring	22
<b>2.4. Stability of Nanofluid</b>	<b>23</b>
2.4.1. Stability Measuring Techniques	24
2.4.2. 3w Method	24
2.4.3. Sedimentation and Centrifugation	24
2.4.4. Zeta potential Measurement	25
2.4.5. Absorbance and Transmittance Analysis	26
2.4.6. Electron Microscopy	26
2.4.7. Dynamic Light Scattering	27
<b>2.5. Destabilization Factor and Mode</b>	<b>27</b>
2.5.1. Aging	28
2.5.2. Concentration	28
2.5.3. Share Rate	29
2.5.4. Phase Change	29
2.5.5. Solution Chemistry	30
2.5.6. Surfactant	30
<b>2.6. Thermal Conductivity</b>	<b>31</b>
2.6.1. Particle Size	31
2.6.2. Particle Shape	31
2.6.3. Particle Material and Base Fluid	32
2.6.4. Temperature	32
2.6.5. Additives	32
2.6.6. Acidity (pH)	33
2.6.7. Clustering	33
<b>2.7. Viscosity</b>	<b>33</b>
2.7.1. Volume Concentration	34
2.7.2. Morphology	35
2.7.3. Shear Rate	35
2.7.4. Temperature	35
<b>2.8. Recent Studies of Different Research Groups</b>	<b>36</b>
<b>2.9. Why silicon nitride?</b>	<b>41</b>
<b>2.10. Research Gap</b>	<b>41</b>
<b>Summary</b>	<b>41</b>
<b>CHAPTER 3: EXPERIMENTAL PROCEDURES</b>	<b>42</b>
<b>3.1. Materials</b>	<b>42</b>
<b>3.2. Preparation of Nanofluids</b>	<b>42</b>
<b>3.3. Characterization and Stability</b>	<b>44</b>
<b>3.4. Thermophysical Properties of Nanofluid</b>	<b>45</b>
<b>Summary</b>	<b>46</b>
<b>CHAPTER 4: RESULTS AND DISCUSSION</b>	<b>48</b>
<b>4.1. Phase Analysis</b>	<b>48</b>
<b>4.2. Impact of Temperature on Ultra-Sonication</b>	<b>48</b>
<b>4.3. Stability Analysis Using Visual Sedimentation Method</b>	<b>49</b>

<b>4.4. Stability Analysis using UV-VIS Spectroscopy</b>	<b>51</b>
<b>4.5. Stability Analysis using Zeta Potential</b>	<b>53</b>
<b>4.6. Thermal Conductivity</b>	<b>55</b>
<b>4.7. Rheological Behavior of Nanofluids</b>	<b>57</b>
<b>4.8. Viscosity</b>	<b>60</b>
<b>Summary</b>	<b>65</b>
<b>CHAPTER 5: CONCLUSIONS AND RECOMMENDATION</b>	<b>66</b>
<b>5.1. Conclusions</b>	<b>66</b>
<b>5.2. Future Recommendation</b>	<b>67</b>
<b>REFERENCES</b>	<b>68</b>
<b>LIST OF PUBLICATION</b>	<b>97</b>

## LIST OF TABLES

	<b>Page No.</b>
Table 1.1. Liquid Metals Thermodynamics properties [15]. .....	5
Table 2.1. Zeta potential values .....	25
Table 2.2. Literature review of Silicon and nitride base nanofluids. ....	40
Table 3.1. Characteristics of the nanoparticles, base fluids, and surfactants .....	42
Table 3.2. Specifications details of the instruments used. ....	45
Table 4.1. A summary of previous literature on nanofluid. ....	63

## LIST OF FIGURES

	Page No.
Fig. 1.1. Benefits of suspension of Nano-sized particles.....	3
Fig. 1.2. Thermal conductivity of nanoparticles, at room temperature [21].....	7
Fig. 1.3. Applications of Nanofluids [36]. .....	8
Fig. 1.4. Thermal applications of Nanofluids. ....	9
Fig. 2.1. Top-down and Bottom-up synthesis technique for nanostructure.....	13
Fig. 2.2. Schematic diagram of ball milling technique. ....	15
Fig. 2.3. Preparation Method (a) Single-step method (b) Two-step method [62] .....	19
Fig. 3.1. Preparation of nanofluid by two-step method. ....	44
Fig. 4.1. XRD pattern of Si <sub>3</sub> N <sub>4</sub> nanoparticles. ....	48
Fig. 4.3. Visual analysis of prepared nanofluids on (a) day 1, (b) day 20, (c) day 40, and month 5 .....	51
Fig. 4.4. UV-visible spectra of prepared nanofluids over various time intervals. ....	53
Fig. 4.5. Zeta potential graph of prepared nanofluids.....	55
Fig. 4.6. Thermal conductivity of nanofluid with the influence of temperature (a) Si <sub>3</sub> N <sub>4</sub> /DIW, (b) Si <sub>3</sub> N <sub>4</sub> /60DIW, (c) Si <sub>3</sub> N <sub>4</sub> /60EG, and (d) Si <sub>3</sub> N <sub>4</sub> /EG. ....	57
Fig. 4.7. Rheological behavior of nanofluid at different temperatures (a) Si <sub>3</sub> N <sub>4</sub> /DIW, (b) Si <sub>3</sub> N <sub>4</sub> /DIW/OLAM, (c) Si <sub>3</sub> N <sub>4</sub> /EG, (d) Si <sub>3</sub> N <sub>4</sub> /EG/OLAM, (e) Si <sub>3</sub> N <sub>4</sub> /60DIW, (f) Si <sub>3</sub> N <sub>4</sub> /60DIW/OLAM, (g) Si <sub>3</sub> N <sub>4</sub> /60EG, and (h) Si <sub>3</sub> N <sub>4</sub> /60EG/OLAM. ....	60
Fig. 4.8. Viscosity of nanofluid at shear rate (a) 100s <sup>-1</sup> , (b) 150s <sup>-1</sup> , (c) 180s <sup>-1</sup> and (d) 220s <sup>-1</sup> . .....	62

## LIST OF SYMBOLS, ABBREVIATIONS AND ACRONYMS

Si <sub>3</sub> N <sub>4</sub>	Silicon Nitride
DIW	De-ionized Water
EG	Ethylene Glycol
OLAM	Oleyl amine
SDS	Sodium Dodecyl Sulfate
SDBS	Sodium Dodecyl Benzene Sulfonate
Vol.	Volume
UV-VIS	Ultraviolet-visible Spectroscopy
TC	Thermal conductivity

## ABSTRACT

Nanofluids are effective heat transfer fluids, exhibiting enhanced heat transfer than conventional fluids such as deionized water (DIW) and ethylene glycol (EG). In this study, nanofluids with a volume concentration of 0.06% were prepared by dispersing silicon nitride ( $\text{Si}_3\text{N}_4$ ) nanoparticles in DIW, EG, and different ratios (60:40 and 40:60) of DIW-EG using a two-step method. The phase and structural analysis of the nanoparticles were conducted using X-ray diffraction and scanning electron microscopy. The stability of the prepared nanofluids was investigated using visual sedimentation, zeta potential, and UV-VIS spectroscopy measurements. Thermo-physical properties such as thermal conductivity and viscosity of  $\text{Si}_3\text{N}_4$ /DIW,  $\text{Si}_3\text{N}_4$ /EG,  $\text{Si}_3\text{N}_4$ /DIW-EG (60:40), and  $\text{Si}_3\text{N}_4$ /DIW-EG (40:60) were evaluated across a temperature range from 30°C to 80°C. The results showed that  $\text{Si}_3\text{N}_4$ /DIW exhibited high stability as compared to  $\text{Si}_3\text{N}_4$ /DIW-EG (60:40), followed by  $\text{Si}_3\text{N}_4$ /EG and  $\text{Si}_3\text{N}_4$ /DIW-EG (40:60) nanofluids. The maximum thermal conductivity enhancements of 14% and 9.4% were observed for  $\text{Si}_3\text{N}_4$ /DIW and  $\text{Si}_3\text{N}_4$ /DIW-EG (40:60) nanofluids, respectively. The rheological properties of  $\text{Si}_3\text{N}_4$  nanofluids exhibited Newtonian behavior in DIW, EG, and the (60:40 and 40:60) DIW-EG mixtures, with and without surfactant, as indicated by a linear relationship between shear stress and shear rate. However, adding OLAM to the  $\text{Si}_3\text{N}_4$ /EG nanofluid changed its flow behavior from Newtonian to dilatant. At a constant volume fraction, the viscosity of the nanofluid decreased with increasing temperature, with the most significant reduction in viscosity relative to the base fluid observed at 80°C. The visual sedimentation, zeta potential, and UV-VIS spectroscopy, results indicated that  $\text{Si}_3\text{N}_4$ /DIW/OLAM nanofluid remained stable up to 5 months. Overall, the results suggest that  $\text{Si}_3\text{N}_4$ /DIW/OLAM is the most suitable nanofluid for enhancing heat transfer and energy efficiency in industrial applications.

**Keywords:**  $\text{Si}_3\text{N}_4$ -nanofluids; Surfactants; Stability; Thermal conductivity; Rheology; Viscosity

## CHAPTER 1: INTRODUCTION

### 1.1. Heat Transfer Fluids

Conventional heat transfer fluids for example oil, water, and ethylene glycol play a vital role in many industrial applications like power generation, chemical processes, heating and cooling processes, biomedical, microelectronics, and transportation. The thermal properties of conventional heat transfer fluid possess low thermal conductivity compared to solid materials. That is the main reason for enhanced heat transfer. Using fins, variation of surface, suction/vaccination of fluid, and electrical or magnetic fields have made it to a dead stop. So novel technologies with the upcoming strength for thermo-physical properties of traditional fluids have been the domain of noble research [1]. Heat transfer fluid transports heat to the storage tank as well as the steam generator. Therefore, they should have low viscosity and high thermal capacity for efficiency. Water, artificial oil, and liquid salt are heat transfer fluids. Water is a high-quality heat transfer fluid as it has a high thermal range and low viscosity. It is economical because it is used in direct steam generation saves the price of the heat exchanger. However, it is unbalanced and hard to control at high temperatures. Oil has a higher boiling point than water and is preferred for accumulating high-pressure conditions. The problem with heavy oil is that rapid hydrocarbon breakdowns when heated within  $400^{\circ}\text{C}$  so that is the temperature limit at which concentrated solar power (CSP) can work. Molten salt is a mixture of sodium nitrate and potassium nitrate and can significantly control higher temperatures up to  $550^{\circ}\text{C}$  compared to other fluids like water and oil. These properties allow steam turbines to run with enhanced efficiency. One of the major drawbacks of this heat-transfer fluid is the risk of freezing salt in extended receiver length [2]. Some of the characteristics which is important to choose heat transfer fluid.

- I. Low viscosity eases fluid flow and reduces pumping expenses.
- II. Select non-corrosive fluid to decrease pipe replacement and lower maintenance costs.
- III. High thermal conductivity and thermal diffusivity will enhance the rate of heat transfer across the fluid.



High boiling and freezing points of fluid will help to keep the fluid in the same phase while exchanging heat by these complications of equipment design decrease [3].

This thesis will discuss the analysis of the stability of NFs for heat transfer improvement as one of the key uses of nanotechnology for energy efficiency development.

## **1.2. Development of Nanofluids**

Nanofluids are a fluid in which nanometer-size particles are smaller than 100 nm suspended in a liquid medium. Nanofluid exhibits enhanced thermos-physical properties like thermal conductivity, viscosity, thermal diffusivity, and heat transfer coefficient compared to their base fluid. The main factor of nanofluid is its good thermal conductivity. They exhibit exciting applications in diverse fields of science and technology. Efficient production of nanofluids with controllable microstructures enabled through chemical solution method. The capability to design microstructure that could have the potential to control chemical reactions that happen quickly and require precision of a high degree. The industrial production of nanofluids depends on future research improvements to become achievable. They offer us feasible solutions for our latest technological issues. The technology can only develop if the manufacturing costs are enhanced and better stability is attained for nanofluids [4]. The scientist Maxwell examined that millimeter or micrometer-sized particles disperse in fluids enhance the thermal conductivity, and then investigated to increase thermal properties of fluids achieved. Although micro particles settled speedily in the fluid leading to corrosion and clogging in the flow medium, regulate further research into suspensions in fluids [5]. Choi et al. developed that the addition of metal and metal oxide particles to the base fluid improves the thermal conductivity significantly [6]. Further nanocomposite has enabled the production of hybrid nanomaterial and researchers have been investigating hybrid nanofluid properties. It analyzed various factors that affect thermal conductivity like type of nanoparticle, amount of nanoparticles, types of base fluid, size of nanoparticles, temperature, addition of surfactants, pH variations, and ultra-sonication time analyzed in previous research. The preparation of hybrid nanocomposites and hybrid nanofluid show excellent physical characteristics and stability as compared to mono nanofluid. On the other way, nanofluid contains only one type of nanoparticle more likely to form clusters [7]. Compared

to micro and Milli-sized particles, the importance and benefits of Nano-sized have been investigated and it could be listed as shown in Fig. 1.1.

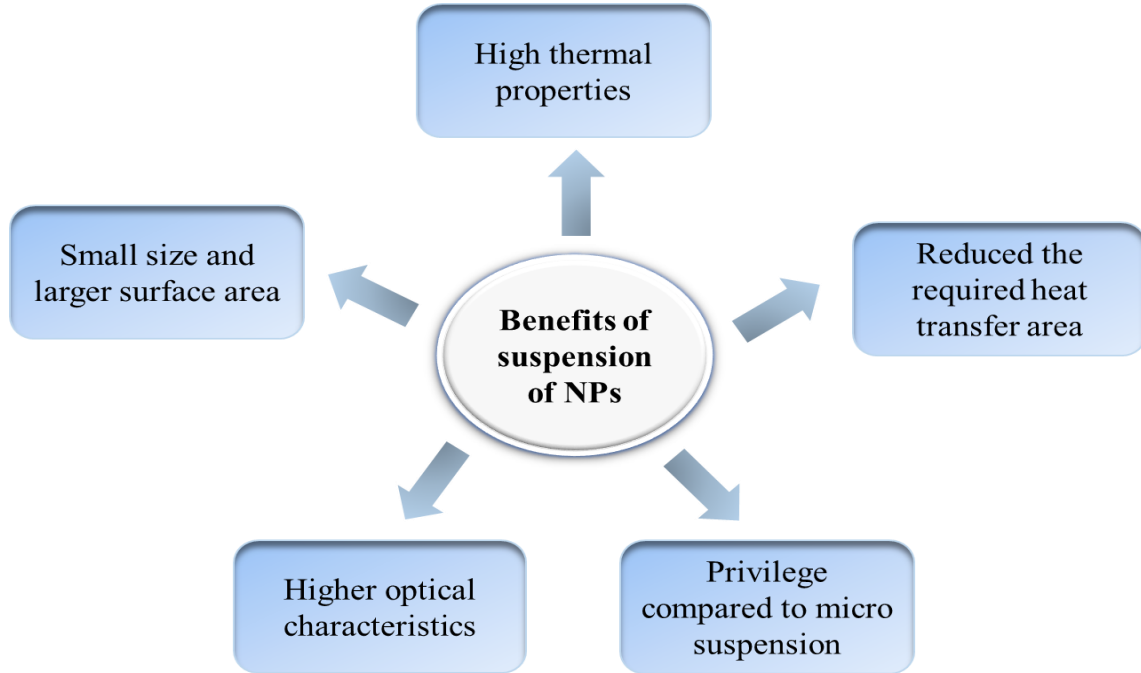


Fig. 1.1. Benefits of suspension of Nano-sized particles.

Some of the challenges for nanofluids that cause homogeneous dispersion. Firstly, enhancing the similarity between nanomaterials. Secondly, enhancing base fluids by leveraging the combined characteristics of two phases could be a promising solution. The shape and structure of nanoparticles play a significant role in improving nanofluid properties. Therefore, developing advanced nanofluid synthesis methods that allow for controlled microscopic structures will present a remarkable research challenge. Thirdly, suspension stability is a critical problem for practical applications and scientific research. More research is needed on the long-term stability of nanofluids for practical conditions and after thousands of thermal cycles. Fourthly the thermal performance of nanofluids at high temperature need more investigation. This limits the potential application area of nanofluid in high-temperature energy storage and high-temperature solar energy absorption. More work is needed on the high-temperature performance of Nanofluids by using surfactants which may produce more foams. Lastly, the stability of nanofluid strongly depends on the shape and properties of the added nanoparticles [8]. There should be good

compatibility to achieve long-term stability between nanoparticles and the base fluids hydrophilic nanoparticles are easily dispersed in polar solvents and hydrophobic in non-polar solvents. Stability affects not only the thermos-physical properties but also the performance of thermal systems. These days, using surfactants in hybrid nanofluids decreases the fluid's surface tension, enhances Brownian motion, and improves heat transfer properties [9].

### **1.3. Research Motivation**

In recent years, nanofluids have obtained important motivation owing to their potential to transform different areas, along with engineering, pharmaceutical, and environmental science. Nowadays, the cooling of mechanical and electrical components has become problematic in fast-growing technology. Due to the advancement of faster speeds and reduced volumes of heat-exchanging devices, the heat required to reject is increasing continuously, and more output power is needed for engines. However, for heat transfer, three ways are used for heating or cooling applications, but the advantages of heat flux of convection and conduction is the best and most effective ways of consuming fluids. Heat transfer fluids have many civil and industrial applications. The poor thermal conductivity of these fluids is a confined factor in cooling systems design. The increase of power with the decrease in the size of equipment is considered to be innovative heat transfer technology. Moreover, the ability of nanofluids to work as modern functional fluids in different fields, like biomedicine and renewable energy, has raised interest in their advancement. There are two ways to meet the cooling/heating requirements. Designing advanced heat exchanging devices, for example, micro-channels, extending the surfaces by fins, improving the heat transfer properties of the fluids, and homogenized spot cooling [10].

While enhancing the design of heat-exchange devices has traditionally been a reliable method to improve heat transfer rates, its potential has now reached a limit [11]. With the growing demand for machines and devices to function efficiently, there is an urgent need to discover advanced heat transfer fluids that offer higher thermal conductivity and superior cooling capabilities. Current research and development efforts are focused on enhancing the heat transport properties of conventional fluids. [12].

Liquid metals become increasingly popular for its unique properties like electrical and thermal conductivity, melting point, low freezing and low viscosity. These properties make it ideal for different applications including chemical synthesis, flexible electronics and biomedicines [13]. The resulting functional materials can significantly expand the application range of low melting liquid metals like alloying and fabrication of micro-droplets and have a wide range of applications in areas like 3D printing, soft robotics, and drug delivery. Liquid metals usually have high thermal conductivity, which make them off from other fluids such as oil, water, glycols [14]. Thermo-physical properties of liquid metals are shown in Table 1.1.

Table 1.1. Liquid Metals Thermodynamics properties [15].

<b>Name of liquid metal</b>	<b>Density/m<sup>-3</sup></b>	<b>Melting point /°C</b>	<b>Thermal conductivity /W.(m.°C)</b>	<b>Specific heat/kJ.(kg.K)<sup>-1</sup></b>
Mercury	13.546	-38.87	8.34	0.139
Potassium	664	63.2	54.0	0.78
Sodium	926.9	97.83	86.9	1.38
Lithium	51.5	186	41.3	4.389
Tin	6.940	232	15.08	0.257

The current cooling techniques convectional conduction and force-air convection techniques may not be enough for advanced electronic systems. However, researchers are exploring new solutions such as thermoelectric cooling, liquid cooling, heat pipes, and vapor chambers. Recently using liquid metals or alloys with a low melting point as coolant has shown potential to reduce the chip temperature significantly. However, the techniques raised many fundamental and practical problems that must be addressed. The focus will be on the thermal properties of liquid metals with low melting points or their alloys and their potential applications in chip cooling. The liquid metal cooling method should be revolutionized by computer chip

cooling due to its advantages over traditional coolants [15]. To improve thermal conductivity, Maxwell suggested the concept of the addition of more thermally conductive powdered particles into fluids. Firstly Maxwell's idea was conceptual, and the next studies of many researchers achieved little success [5]. The factor which increase the thermal conductivity was the size of particles, and the synthesis methods for tiny particles available at that time could not control the size effectively. S.U.S Choi and J Eastman in the 1990s, prepared nanofluid with suspension of metallic particles having nanometer size in EG (ethylene glycol) and oils, respectively, as well as suspension of carbon nanotube. The results were varied but inspiring as seen in measurements of nanofluids prepared by Choi and Eastman in 1996, 1997 and 1999 respectively [4] [6] [16]. To prepare nanofluids from the literature, it is predicted that the particle concentration is commonly from 0.1% to 10% which enhance thermal conductivity. According to the research for instance at a volume concentration of 0.01(1 vol%), CNT- ethylene glycol suspensions showed a 12.4% thermal conductivity. On the other hand, synthetic engine oil suspensions displayed a 30% enhancement in thermal conductivity at a volume fraction of 0.02% [17].

The most extensive studied extensively studied NPs are the ZnO, TiO<sub>2</sub>, and Al<sub>2</sub>O<sub>3</sub>. Over the last decade, zinc oxide (ZnO) has attained pronounced interest from the research community, due to its exponential physical properties, mainly its enormous thermal and electrical conductivity [18]. However, the major problem with using ZnO is its long-term stability and thermos-physical properties. Additionally, ZnO nanoparticles exhibit anti-microbial properties, making them ideal for use in different applications in nanofluid technology, including industrial and biomedical fields [19] [20].

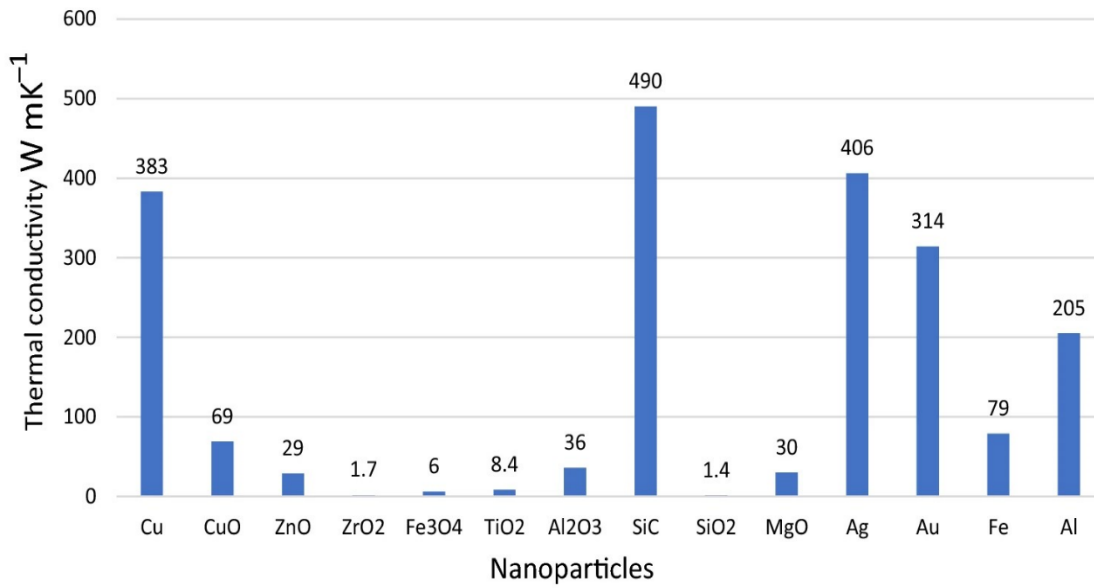


Fig. 1.2. Thermal conductivity of nanoparticles, at room temperature [21].

#### 1.4. Applications of Nanofluids

Nanofluids have become a popular subject of study of engineering materials due to their unique composition of nano-sized additives and base fluids. Their exceptional thermal properties and potential applications make them exciting prospects for researchers [22]. In literature nanoparticles are various types, such as metallic, nonmetallic, and intermetallic compounds (such as Ni [23], Cu [24], Au [25], Ag [26], and others.) Additionally, there are different kinds of ceramic compounds like carbide oxides and sulfides or carbon-based materials such as carbon nanotubes [17], graphene, or graphene oxide [27].

Base fluids are water, ethylene glycol, propylene glycol [28], water-ethylene glycol mixture [29], polyethylene-water [30], engine oil [31] vegetable oil [32], and others. After the introduction of the concept of nanofluids, the potential features of nanofluids have attracted the attention of many researchers across different areas. That's why a lot of researchers are working toward various purposes and applications.

In the literature, the number of applications of nanofluids in diverse areas such as biomedical, electronics, mechanical, heat transfer, automotive, energy, and others have been

described in Fig. 1.3, showing some possible applications of nanofluids in various fields. Other applications are solar fields, nanofluid detergent magnetic sealing, reactor heat exchangers, optical fields, electronic cooling, and petroleum industries [33]. Recently nanofluids have been synthesized by dispersing nanoparticles in conventional lubricating oil that successfully improve the anti-wear property as a result at which friction is reduced. Based on the research, it has been found that the minimum quantity of lubricants is suitable for green machining. This technique has been utilized with vegetable oils, mineral oils, and nanofluid-based cutting fluids across various machining processes, including drilling, turning, and grinding. It has demonstrated effectiveness in enhancing surface quality and reducing cutting forces, tool wear, coefficient of friction, and cutting zone temperature compared to both wet and dry machining methods [33, 34].

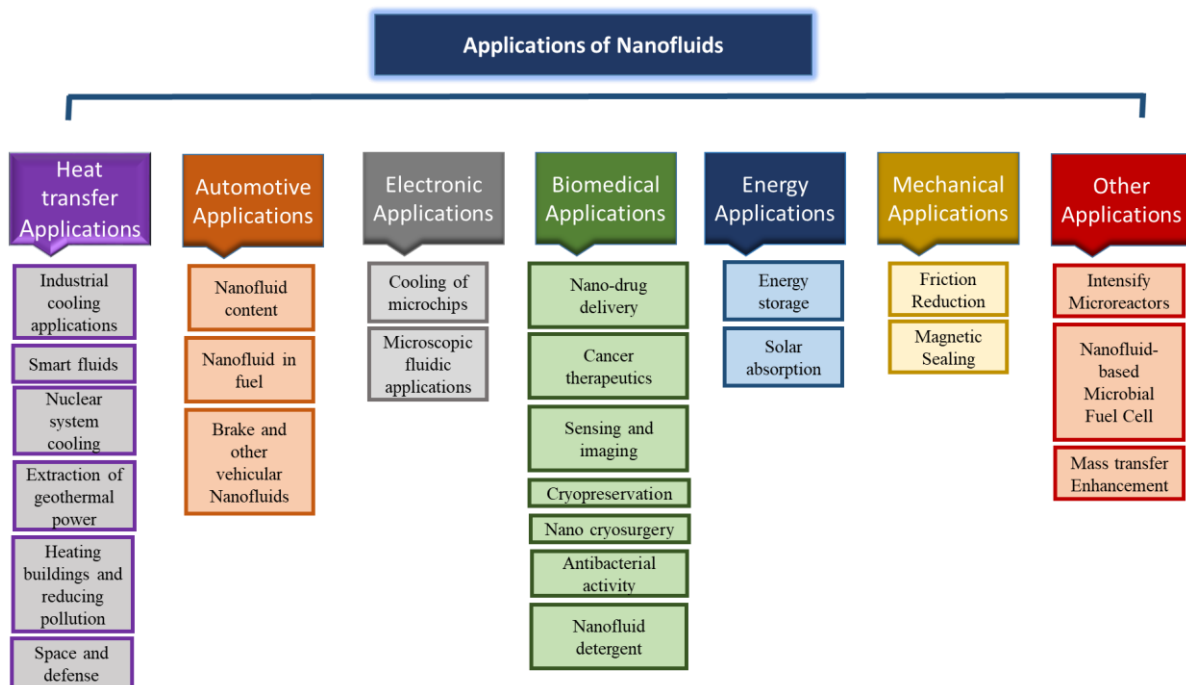


Fig. 1.3. Applications of Nanofluids [36].

#### 1.4.1. Thermal Applications of Nanofluids

Nanofluids have emerged as an innovative solution for enhancing the efficiency and cost-effectiveness of thermal systems across commercial, residential, and industrial applications. The

benefits of enhanced efficiency in thermal systems are the reduction of, lower energy consumption, environmental impact, and lower cost. As a result, hybrid nanofluids are being increasingly used in thermal systems like solar collectors, heat exchangers, and hybrid photovoltaic-thermal (PVT) solar systems with a focus on the life cycle approach [37]. Nanofluid can be used in transport systems like automotive and automobiles to cool the engine [38] in metal processing they can be utilized in metal cutting [35]. They can also be used as an efficient coolant in data science and compact electronic cooling systems [37,38].

Several studies have highlighted the promise of nanofluids in energy-related applications such as in the fabrication of innovative phase change materials (PCM) for storing thermal energy and also for solar absorption in solar collectors in which the introduction of nanofluids could improve the absorption properties of working fluids [41].

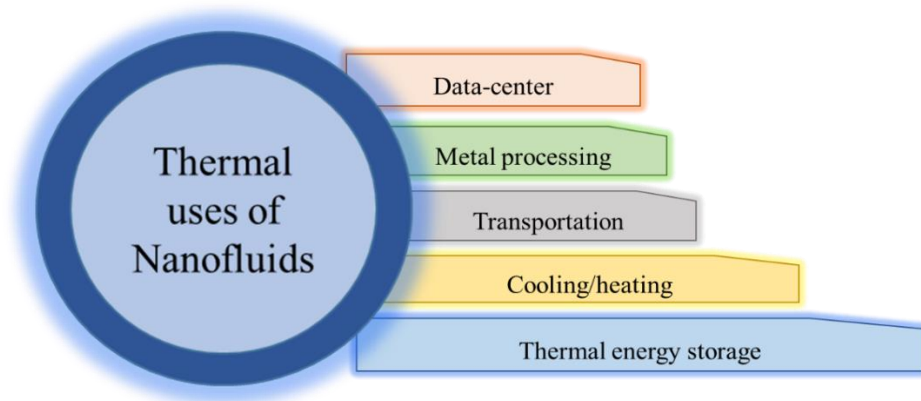


Fig. 1.4. Thermal applications of Nanofluids.

## 1.5. Problem Statement and Research Objectives

In the context of climate change and the pursuit of sustainability goals, there is an increasing need for energy-efficient systems across various applications. Traditional heat transfer fluids are being replaced by nanofluids, which integrate more conductive nanoparticles, to enhance heat transfer efficiency. However, the stability of these nanofluids remains a significant challenge, limiting their widespread use. This study focuses on addressing this issue, as the existing literature does not adequately explore the stability of nanofluids, the role of surfactants, and the effect of



different base fluids on the thermophysical properties and stability of  $\text{Si}_3\text{N}_4$  nanofluids. The addition of surfactants helps reduce the intermolecular forces between nanoparticles, thereby improving their suspension in the base fluid.

- Preparation of silicon nitride-based nanofluids by two-step method.
- Effect of surfactants on stability of prepared nanofluids.
- Determination of thermophysical properties and rheology analysis of various combinations of base fluids.

## **1.6. Research Limitations**

The extensive research on nanofluids reveals several limitations that make their use quite specialized. The base fluid must be carefully selected according to the temperature range and the nanoparticle's chemical nature. The addition of surfactants can increase viscosity, and high nanoparticle concentrations can reduce the effectiveness of Zeta potential and UV-vis spectroscopy for stability analysis. Furthermore, the high cost of nanoparticles is a significant hurdle, particularly for small-scale applications.

## **Summary**

To achieve efficient heat transfer, fluids with high thermal conductivity like water and ethylene glycol are often used. Adding nan-sized particles to these fluids can further improve efficiency. These nanoparticles enhance heat transfer by increasing convection through Brownian motion. The particles' size, shape, and type influence their dispersion and thermophysical properties. Inadequate dispersion can lead to agglomeration, reducing Brownian motion and thermal conductivity. Techniques such as ultrasonication, pH adjustments, and surfactant addition are applied to stabilize nanofluids. This study investigates various surfactants for stabilizing  $\text{Si}_3\text{N}_4$  hybrid nanofluids and assesses their impact on the nanofluids thermophysical and rheological characteristics.

## **Dissertation Organization**

Thesis write up is separated into six main sections as;

Chapter 1 gives the introduction of research work, motivation behind the selection of this topic and what to do in this work, objective statement of work and limitation of current study.

Chapter 2 covers the literature review regarding nanofluids preparation techniques, different techniques used to enhance performance of thermal system and describes the parameters effecting the performance of such systems. This chapter also covers the role of stable nanofluids for heat transfer enhancement and study of various factors effecting the stability and stability enhancement techniques.

Chapter 3 presents the experimentation method adopted for preparation, characterization methods for nanofluids, and testing methods used to find the stability and thermophysical properties of nanofluids.

Chapter 4 discusses the results obtained from various characterization techniques (XRD, SEM,), of nanoparticles for nanofluids. Results obtained from nanofluids preparation methods of suspended nanoparticles with and without using surfactant to evaluate the stability and thermophysical properties of nanofluids are also mentioned in this section.

Chapter 5 concludes the outcomes research project and elaborates possible future prospective and probable recommendations of current work.

## **CHAPTER 2: LITERATURE REVIEW**

### **2.1. Nanofluids as Heat Transfer Fluids**

There has been a growing interest in research studies related to nanofluids in recent years. This is because of the increasing demand for nanofluids as a heat transfer in various applications [38]. Nanofluids are suspensions of nanoparticles in base fluids. With the rising need for more high efficiency of thermal systems, researchers are exploring the potential of nanofluids as a promising option [42]. The enhancement in thermal conductivity examined in these fluids with nanoparticles was unexpected. Alternative heat transfer mechanisms have been investigated, as suspensions with micrometer-sized particles do not show such a pronounced improvement. To develop a comprehensive theory, efforts are being made to understand this difference [33].

Nanofluids are fluids composed of a mixture of solid and liquid phases. The addition of powdered nanoparticles to the specific fluid can increase the thermal conductivity of the fluid, thereby enhancing its heat transfer characteristics. It has been proven that adding a single nanoparticle to the base fluid can improve its heat transfer and flow characteristics. In recent years, researchers have focused on studying nanofluids containing composite nanoparticles, which are made up of more than two nanoparticles in the base fluid. Studies have shown that hybrid or composite nanofluids enhance the base fluid's thermal and rheological characteristics more than mono-nanoparticle-based nanofluids [43]. The stability of nanofluid is a main challenge that needs to be addressed for its widespread industrial use. Without proper stability, the performance of the system will gradually decrease over time. Therefore, it is essential to address the long-run stability of nanofluid and ensure its successful for industrial use. It is essential to study the stability of nanofluids under various conditions such as shear rate, pressure, confinement, temperature, salinity, composition, magnetic field, etc. [44].

### **2.2. Nanoparticle Synthesis Approaches and Methods**

When it comes to nanomaterial composition, understanding the properties of the material is crucial. This includes chemical, physical, optical, and mechanical properties, which all play a key role in determining how the material can be behave and used. Chemical properties like surface energy, oxidation process, chemical potential, and catalysis play important roles in shaping the composition of nanomaterials. On the other hand, the physical properties of nanomaterials are dependent on factors like shape, size, color, and particle morphology. Optical properties including reflection, light emission, transmission, and absorption are determined by their electronic structure which in turn, depends on surface atoms [43, 44]. Lastly, mechanical behavior is characterized by high strength conditions and high speed plasticity, which are influenced by material structure, grain size, porosity, hardness, adhesion, elastic modulus, and friction [47]. Methods of synthesizing nanomaterials are top down and bottom up approaches.

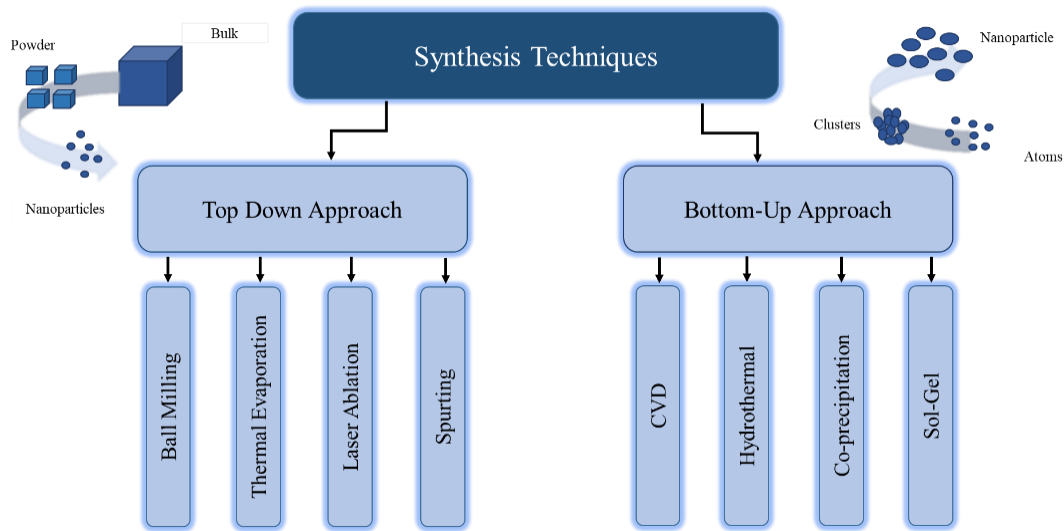


Fig. 2.1. Top-down and Bottom-up synthesis technique for nanostructure.

### 2.2.1. Top-Down Approach

This method involves converting bulk material into nano-sized particles. However, it is not very effective in producing irregular shapes and extremely small particles despite being relatively easy to use. Obtaining the required particle size and shape can be difficult, which is the main disadvantage of this approach [45]. This approach is more effective in fabricating thin films. These

techniques are frequently implemented when creating electrical circuits that require a high level of integration and connectivity [48].

#### 2.2.1.1. Mechanical Milling & Ball Milling Process

In the top-down approach, ball milling is the simplest and most efficient process to produce nanoparticles by attrition. The process transfers kinetic energy from the grinding medium to break down the material, producing various nanoparticles and metal alloys. The impact of the balls with one another and with the vessel walls can result in high-pressure and high-temperature conditions, driving severe phase transformations. A fixed quantity of powder materials is loaded into a milling jar and processed by the interaction between the jar and milling balls. A range of reactions can be produced that do not happen at ambient temperature. [43, 47, 48]. Ball milling is used for many purposes including reduction of particle size, change in the structure of particles, growth of particle size, and agglomeration. It can also be used to mix phases of two or more materials or modify fixed material characteristics like density, or work hardening, or flow ability. The temperature increases during milling due to several factors, including collisions between balls and powders, collisions between balls and walls, collisions between balls, and the frictional forces generated. The overall temperature rise of particles during milling can contribute to these factors [51]. The advantages of this process are lost if large crystallites form instead of nanocomposites due to high-temperature reactions taking place. To avoid an accident, it is crucial to understand the condition of exothermic reactions that may occur during the manufacturing process and lead to ignition. When it comes to milling energetic materials in powder particle form, this statement holds more significance [52]. In Fig. 2.2 the schematic diagram is shown.

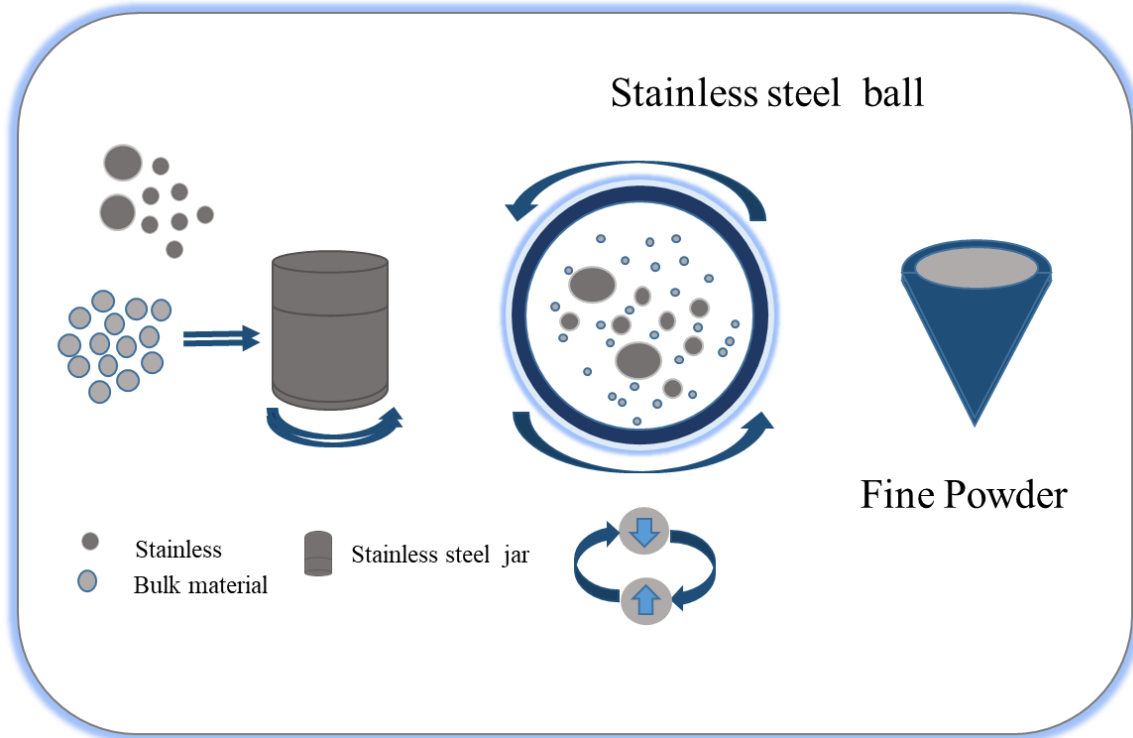


Fig. 2.2. Schematic diagram of ball milling technique.

#### 2.2.1.2. Thermal Evaporation

Thermal evaporation is a widely used technique for producing stable, uniformly dispersed suspensions that can self-assemble. The method relies on heat to break a chemical link in a molecule, leading to its breakdown. The thermal evaporation setup comprises an alumina crucible for powder containment, a resistive heating system, and a consistent distance between the source and substrates. Prior to the evaporation process, substrates are cleaned using acetone and ethanol. Key factors like furnace temperature, evaporation duration, and the gap between the source and substrate play a crucial role in influencing the outcome [45]. A significant benefit of this approach is that it avoids the use of solvents, ensuring uniform deposition on substrates, especially for ultrathin layers. It provides precise control over film thickness by monitoring the deposition rates of each precursor. This method is particularly well-suited for materials with low melting points. Shutters and masks were employed due to the line of sight trajectory and limited-area sources. The process allows for easy monitoring and control of the deposited material, with residual gases and vapors readily detectable during deposition [53].

### 2.2.1.3. Laser Ablation

This method's main goal is reducing the particle size to the nano level using laser irradiation. In this process, a solid material is coated with a thin layer and then subjected to pulsed laser irradiation. The most common lasers used for this method include Nd: YAG (neodymium-doped yttrium aluminum garnet), Ti: Sapphire (titanium-doped sapphire), and copper vapor lasers. When the laser irradiates the target material, it causes fragmentation of the solid material into nanoparticles, which remain in the liquid surrounding the target and assemble a colloidal solution. The laser pulse time and energy determine the amount of ablated particles and atoms formed. Moreover, various parameters including laser pulse time duration, wavelength, time of ablation, fluency of laser, and the surrounding liquid medium whether with or without surfactant can affect the efficiency of ablation and the characteristics of the resulting metal particles [54].

### 2.2.1.4. Sputtering

In this method, the sputtering process can be made more efficient by using magnetron sputtering. For this, a magnetic field is employed to deposit a thin film onto the substrate. By confining electrons within a magnetic field around the target, the plasma is intensified, leading to increased ionization of argon atoms and accelerated bombardment ions, thereby enhancing the deposition rate [55]. This method provides benefits such as uniformity, precise thickness control, rapid deposition rates, strong adhesion, and the capability to cover large areas effectively, suitable for both RF and DC sputtering techniques [56]. In ion sputtering, in an evacuated vacuum chamber sputtering gas is introduced and the pressure is maintained at 0.05 and 0.1 bar. A high voltage is applied to the target, or cathode causing free electrons to spiral around the magnetic system. These electrons collide with the sputtering gas usually argon, and cause ionization, resulting in the formation of glow discharge or plasma. The positively charged ions are attracted towards the target, where they continuously impinge. The process repeatedly occurs between metal atoms, gas molecules, a scattering of atoms, and forming a diffuse cloud. When the collision energy approaches the binding energy of the surface, an atom can be expelled [52, 55].

## 2.2.2. Bottom-Up Approaches

The bottom-up method is the opposite of top-down. Nanomaterials are formed through the self-assembly and growth of atoms and molecules as their building block resulting in well-defined shape, size, and chemical composition [45]. Ionic and molecular self-assembly is a typical example of a bottom-up approach, where physical or chemical forces are used to gather individual building blocks or molecules into larger ones through non covalent bonds like ionic and hydrogen bonds, Van der Waals forces, and water-mediated hydrogen bonding [48].

#### 2.2.2.1. Chemical Vapour Deposition (CVD)

In the bottom-up approach, nanomaterials are created through a simple materials process. A layer of gaseous reactant is applied onto a substrate using this method. When the gas or vapor interacts with a heated substrate, a reaction takes place inside a reaction chamber, leading to the formation of a thin layer on the substrate. This thin film is then etched out and utilized accordingly [45]. This reaction can be activated by thermal, plasma, laser, or photo-laser-methods. Thermal CVD activated at high temperatures above 900 employs a gas supply system, deposited chamber, and exhaust system. Plasma CVD involves plasma at a temperature between 300°C and 700°C to start the reaction, and laser CVD-activated pyrolysis happens by laser thermal energy and deposits materials on an absorbing substrate. Photo-laser-induced UV radiation reaches chemical bonds, allowing deposition at room temperature [58].

#### 2.2.2.2. Hydrothermal Method

The hydrothermal method which involves the reaction of aqueous solution vapors with solid materials at high-temperature and high-pressure, results in the deposition of nano-size particles. In this method, cations precipitate in polymeric hydroxide form, and these hydroxides undergo dehydration, and facilitate the formation of metal oxide crystal structures. The presence of a second metal cation helps control the formation process, preventing the formation of complex hydroxides by adding base in a metal salt solution [54]. This approach significantly advances science and technology by promoting homogeneous precipitation, offering an environmentally friendly solution, ensuring cost efficiency, scalability, and yielding a pure final product. Furthermore, this method can be divided into hydrothermal synthesis, treatment, crystal growth, organic waste treatment, crystal growth, and preparation of functional ceramic powder [45].



#### 2.2.2.3. Co-Precipitation

In this synthesis method, solid particles are produced by dissolving material into solvent. It is the simplest method for nanoparticles produced on a large scale, and cost effective among all the wet methods. This method can form both micro-particles and nanoparticles at low temperatures depend on the salts used. The process involves inorganic metal salts, like nitride and chloride, dissolved in water. These factors such as temperature, type of solvent pH value, mixing rate of reagent and solvent, and post-treatment may affect the properties of the final nanoparticle formed. However, controlling the particle size due to these factors' influence is not easy, leading to typically broad size distribution [43, 57].

#### 2.2.2.4. Sol-Gel Method

The sol-gel method is a widely used bottom-up approach for synthesizing nanomaterials due to its straightforward process. It combines two stages: sol and gel. In this technique, "sol" refers to a colloidal solution of solid particles dispersed in a liquid, while "gel" denotes a macromolecule dispersed in the liquid phase [45]. Colloidal particles used in this process are much larger than normal molecules and nanoparticles. However, when mixed with a liquid collide appears bulky, while nano-sized molecules look clean. The process involves the evolution of networks through the formation of a colloidal suspension (sol) and gelatin to create a network in a continuous liquid phase (gel). It involves the use of metal alkoxides and alkoxy silane ions, with tetraethoxysilane (TMOS) and tetraethoxysilanes (TEOS) being the most widely used ones for synthesizing silica gels. These are organic precursors that are used to form silica, aluminum, titanium, zirconium, and other materials. Mutual solvent alcohol is commonly used. Initially, a solution of one or more selected alkoxides is created. A catalyst is then used to initiate the reaction and control pH levels. This process consists of four stages: hydrolysis, condensation, particle growth, and particle agglomeration [57, 58].

### **2.3. Nanofluids Preparation Techniques**

The preparation of nanofluids is a crucial step in experimental studies with nanofluids. To produce nanofluids, nanometer-sized solid particles are dispersed into a base fluid like water, EG,

oil, etc. However, agglomeration is a major issue. It is necessary to prepare nanofluids delicately they have specific requirements, such as an even and stable suspension, low particle agglomeration, and no chemical changes in the fluid [8]. Adding nanoparticles in base fluids significantly improves thermal conductivity compared to those of conventional heat transfer fluids, and this makes nanofluids a promising option for enhancing heat transfer capabilities [43]. Nanofluids can be prepared using either by one-step or two-step method as shown in Fig 2.3. In one step method nanoparticles are directly dispersed in a base fluid and mainly through chemical means [61]. On the other hand, in the two-step method, nanoparticles are first prepared in the form of powder using physical or chemical methods and then suspended in a base fluid [4].

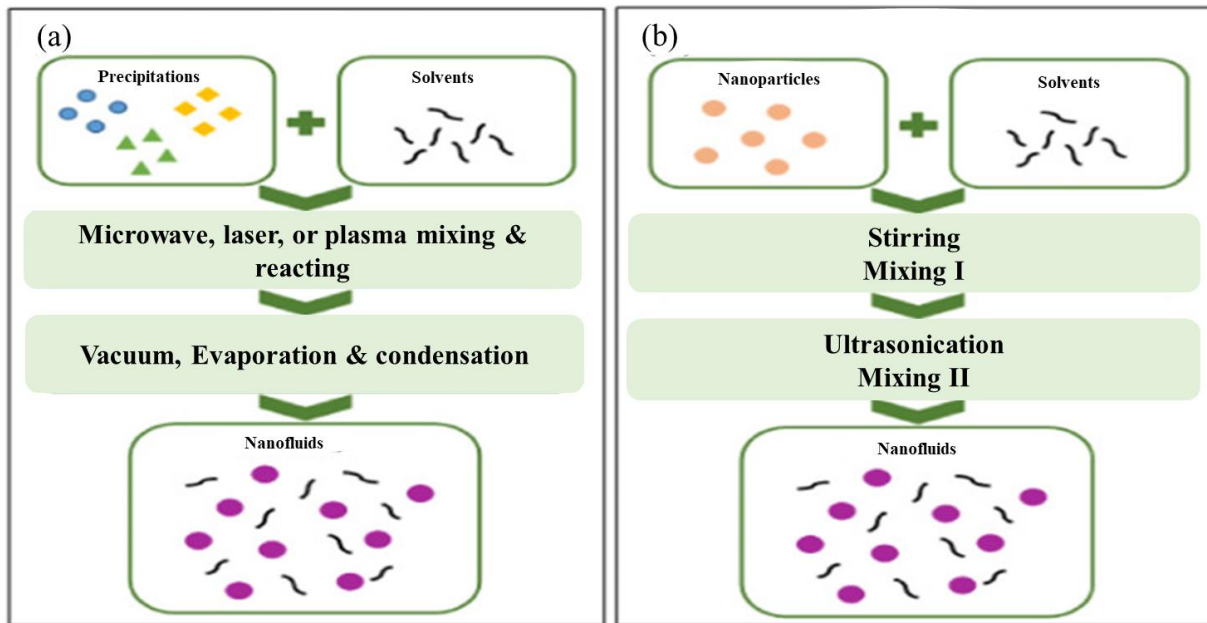


Fig. 2.3. Preparation Method (a) Single-step method (b) Two-step method [62].

### 2.3.1. Single-step Method of Nanofluid Preparation

In the one-step method, nanofluids' preparation involves producing particles while dispersion them directly into the base fluid [1]. This approach presents several advantages such as preventing oxidation of nanoparticles, achieving uniform dispersion, enhancing stability, and reducing accumulation during storage, drying, and transportation. However, there are some limitations to this method, such as a slow production process, restrictions to low-pressure fluids, and the possibility of nanoparticle collision at low concentrations in certain cases [22].

#### 2.3.1.1. Direct Evaporation Method

In this method, metals can be transformed into nanofluids through various techniques. One such technique involves heating the metals to their critical point and then subjecting them to base fluids. This technique involves passing a high voltage pulse of 300 V in a thin wire, causing it to evaporate and transform into plasma within microseconds. The plasma is subsequently condensed into nanoparticles by interaction with inert gases such as argon and nitrogen. The resulting is then combined with nanoparticles to develop a hybrid nanofluid [63]. Another method, for producing ultrafine nanoparticles is vacuum evaporation onto an oil substrate. In this method, metals or non-metals with high thermal conductivity are evaporated in a vacuum onto the surface of flowing oil, where ultrafine particles are subsequently formed on the oil's surface. VEROS offers several advantages, including the ability to produce extremely fine particles that are uniformly dispersed in oil or base fluids. The production rate is also faster than the gas evaporation method. The apparatus features a rotating disk within the work chamber, where oil or a base fluid is introduced at the disk's center. Centrifugal force drives the evaporation of metal atoms, which subsequently deposit onto the flowing oil. The resulting oil or base fluid, now infused with ultrafine metal particles, is then collected in a container [22].

#### 2.3.1.2. Physical Method

J. C. Kim et al. [64] studied a one-step physical method to prepare Cu nanofluid, synthesized through a one-step electrical explosion of wire in EG exhibits stable properties without surfactants. It has been reported the addition of only 0.1 vol% Cu nanoparticles dispersed into ethylene glycol can increase its thermal conductivity by up to 5.2%. Ho Chang et al. [65] studied utilizing the plasma arc discharge system to quickly vaporize aluminum by releasing a high-energy plasma arc. The control parameters for this process include working current, plasma gas, and protective gas flow rate. The pressure control system creates a pressure differential to transport vaporized particles into a collection chamber. To prevent excessive particle growth, the nanofluid collection and cooling system pre-condense deionized water, enabling low temperatures during nanofluid collection. The vaporized metal is then induced into a collection piping, where it mixes with pre-condensed deionized water, instantly condensing into nanoparticles to form a fully mixed nanofluid.

### 2.3.1.3. Chemical Method

Chemical methods have several advantages over physical ones, such as being more economical and faster. A recent study explored various kinds of chemical methods and summarized several of them in a section. For instance, the researchers investigated a pioneering work that utilized a single-step chemical method. To synthesize copper nanofluid, a mixture of 25 ml of 0.1 M  $\text{CuSO}_4 \cdot 5\text{H}_2\text{O}$  and 5 ml of 0.01 M polyvinylpyrrolidone in ethylene glycol was prepared. The mixture was then subjected to microwave for 5 min followed by the addition of 25 ml of 0.1 M sodium hypophosphite. The result is the color change from blue to dark red [66].

The mixture included 50 ppm of CuO, 96% WCO biodiesel, 3% water, and 1% ethylene glycol. They used a one-step chemical synthesis that involved dissolving 50 mg of copper acetate in 30 ml of distilled water and adding distilled water and adding diethanol amine and hydrazine hydrate. The resulting brownish-black CuO nanofluid was characterized using UV-visible spectroscopy, which showed absorption bands at 223 nm and 293 nm, confirming the formation of CuO. After that, transmission electron microscopy (TEM) revealed an average particle size of 6 nm.

### 2.3.2. Two-Step Method

In this method, dry nanoparticles are formed and then dispersed into a base fluid. However, since nanoparticles have a high surface energy, clustering, and aggregation are unavoidable and can easily occur. Eventually, the particles tend to settle at the bottom of the container, making it challenging to create a homogeneous dispersion using a two-step method. However, techniques such as high shear and ultrasound can be used to minimize this problem. Different methods to discussed for making nanofluids. The method is suitable for producing nanofluids containing oxide particles and carbon nanotubes. While this method works, well with oxide nanoparticles and is attractive to the industry due to its simple preparation method, it has the disadvantage of quickly agglomerated particles. Consequently, it presents many challenges nowadays. Since nanoparticles disperse partially, the dispersions are poor, and sedimentation occurs, requiring a high volume concentration to increase heat transfer (10 times per single step). As a result, the cost would be as much as loading [67]. The two-step method is useful for applications with particle concentrations

greater than 20 vol%, though it faces limitations with metal nanoparticles. However, some surface-treated nanoparticles showed excellent dispersion [68]. The first materials tried for nanofluid preparation were oxide nanoparticles, mainly because they are easy to make and chemically stable in solution [5].

#### 2.3.2.1. Ultrasonic Sonicator

Ultrasonication is the widely employed method for nanoparticle dispersion in nanofluid preparation, but there are no standardized procedures for the pulse on-off duration and amplitude percentage. Some researchers have found that indirect sonication, which involves an ultrasonic bath, may not be as effective for dispersing dry powders, especially in highly viscous base fluids. On the other hand, direct sonication using probe sonication is considered more suitable for preparation of nanofluid. The choice between direct and indirect sonication depends on various factors, such as the nature of the nanoparticle and the viscosity of the base fluid [22]. The delayed nanoparticle oxidation post-sonication is the cause of the scattered sedimentation in nanofluids at 10°C and 20°C. On the other hand, flocculated sedimentation in other samples results from particle oxidation during the preparation phase. The noticeable hydrogen generation is dispersed sedimentation nanofluids exhibit a distinct oxidation timing highlighting its connection to settling behavior [69].

#### 2.3.2.2. High-pressure homogenizer

The high-pressure homogenizer, which consists of two micro-channels that divide a liquid stream into two separate streams stream is then recombined in a reacting chamber. These streams are then recombined in a reacting chamber. The increased velocity of the pressurized liquid streams in the microchannel causes cavitation to form in the liquid, which in turn generates high energy that is used to break up clusters of nanoparticles. [70]. In this setup, tiny particles are pushed through a narrow tube into an even narrower microchannel, where they speed up dramatically and cavitation bubbles form. This fast flow, along with impacts on the chamber walls and high shear rates, breaks up particle clusters, resulting in highly homogeneous suspensions with reduced particle aggregation [22].

#### 2.3.2.3. Mechanical Stirring

Agglomeration among particles can be reduced by mechanical stirring or ultrasonication. Mechanical mixing aids in breaking large agglomerates into smaller agglomerates/particles and a well-dispersed nano-suspension is obtained. Methods such as high-pressure homogenizers, ultrasonic sonicator and mechanical stirrers are effective for preparing liquid samples under atmospheric conditions at room temperature. However, with this fluid in a gaseous phase, these methods may not be suitable. Some fluids like refrigerants can improve performance when mixed with ultrafine particles, forming a “nano-refrigerant”. The Shaker method is used for low-temperature fluids or those in the gaseous phase, but it may not improve stability. To keep the nano-refrigerant stable, it’s kept inside an orbital incubator shaker with a temperature control unit, and the temperature must be below the refrigerant’s boiling point to prevent vaporization [36].

## **2.4. Stability of Nanofluid**

The stability of nanofluids depends on maintaining dispersion, kinetic, and chemical stability. Dispersion stability relates to the aggregation of nanoparticles within the nanofluids, while kinetic stability relates to the Brownian motion of nanoparticles in the base fluid. This random motion helps to prevent sedimentation due to gravity. Chemical stability involves the potential chemical reactions between the nanoparticles themselves or between the nanoparticles and the base fluid. However, in cooling applications, any chemical reactions are undesirable [71]. Therefore, nanoparticle agglomeration leads to microchannel blockages and decreased thermal conductivity in nanofluids. Stability issues are therefore a significant concern, influencing the properties and performance of nanofluids, which requires detailed study of the factors affecting their dispersion stability [72]. The DLVO theory, proposed by Derjaguin, Landau, Verwey, and Overbeek, explained colloidal suspension stability. This theory is based on the following assumptions: (1) suspended particles are Van der Waals attractive forces and electrostatic forces, (2) the particle suspended in dilute, (3) gravity and buoyancy forces are neglected, (4) the colloidal suspension is homogeneous, and (5) the distribution of ion throughout the colloidal system is influenced by three factors: Brownian motion, and entropy-induced dispersion [44]. To enhance the stability of nanofluids, several techniques have been developed: Surfactants (These are cost-effective and require minimal amounts to alter the system surface characteristics), Modification techniques (This approach involved altering the surface properties of the nanoparticles), Steric

Repulsion and Electrostatic Repulsion (These mechanisms are used to prevent the aggregation of nanoparticles) [73].

#### 2.4.1. Stability Measuring Techniques

The stability of nanofluid solutions can sometimes be inferred from visual observations: a stable nanofluid typically appears as a homogeneous mixture, whereas an unstable one may exhibit inhomogeneity. However, due to the minute size of nanoparticles, more precise characterization techniques are necessary to predict stability and instability accurately [38].

#### 2.4.2. 3w Method

A recent study has demonstrated a method for evaluating the stability of nanofluids by observing the increase in thermal conductivity resulting from nanoparticle sedimentations across a broad range of nanoparticle volume fractions [74]. This method measures the thermal conductivity and stability of nanofluids. It involves introducing a sinusoidal heating. The metal's temperature variation with the same angular frequency as the substrate. Both the electrical resistance and the temperature of the metal have linear relations of temperature. By evaluating the temperature oscillation directly, the magnitude of the temperature can be used to calculate the substrate's thermal conductivity [22].

#### 2.4.3. Sedimentation and Centrifugation

Sedimentation is the technique for evaluating stability, which depends on sediment settling to the bottom of the container due to gravity. A longer time required for a nanofluid to form a precipitate indicates superior stability. Researchers have utilized sedimentation method to find stability of nanofluid. Centrifugation is a quick way to access the stability of nanofluid and is an alternative to sedimentation. In this technique, the centrifugal force far outweighs the gravitational force, enhancing the sedimentation process [44]. Numerous researchers have employed this method to test the durability of nanofluids. The stability time of water/EG-based  $\text{TiO}_2\text{-SiO}_2$  nanofluid exceeded one month, as visualized through the sedimentation method [75]. Ouikhalfan and Labihi [76] determined the stability period of CTAB and SDS-treated  $\text{TiO}_2$  nanofluid using

the sediment photograph technique. Thus capturing images of sedimentation has proven to be an effective means of assessing nanofluid stability.

#### 2.4.4. Zeta potential Measurement

The zeta potential measurement is used to assess the stability of colloidal dispersions [41,42]. Zeta potential refers to electrostatic repulsion between the surface of particles and the stationary layer of fluid surrounding them. The significance of zeta potential values is directly linked to the stability of nanofluids. High positive or negative zeta potential values are directly linked to the stability of nanofluids as shown in Table 2.1. High positive or negative zeta potential values indicate a stabilized condition, whereas low values suggest instability [30,43]. Therefore, zeta potential values of 0 mV, 15 mV, 30 mV, 45 mV, and 60 mV, correspond to unstable conditions, slightly stable conditions with rapid particle settlement, moderately stable conditions, slightly stable conditions with rapid particle settlement., moderately stable conditions, good stability, and excellent stability, respectively [79]. The water-based Al<sub>2</sub>O<sub>3</sub> nanofluid has a zeta potential ranging from -30 mV to -26 mV. When SDS surfactant is added to improve stability, the zeta potential changes to a range of 14 mV to 2 mV in surfactant-free nanofluids [80]. Given its importance as a measure of colloidal suspension durability, many researchers utilize the zeta potential test in their investigations [78–80].

Table 2.1. Zeta potential values.

Zeta potential	Stability
±20 mV	Poor Stability
±20–±40 mV	Moderate Stability
±40–±60 mV	High Stability
>±60 mV	Extreme Stability



#### 2.4.5. Absorbance and Transmittance Analysis

Spectral transmittance and absorbance measurements provide a quantities assessment of nanofluid stability. This evaluation method is typically employed when nanoparticles suspended in the base fluid exhibit an absorption peak between 200 and 1100 nm. Colloids and suspensions react differently to incident light due to the phonon vibrations of the particles [84].

The analysis of absorbance and transmittance can help predict the stability of nanofluids. According to the Beer-Lambert Law, absorbance intensity ( $A_\lambda$ ) has a linear relationship with the concentration of particles through which light passes:

$$A_\lambda = \log_{10}\left(\frac{I_0}{I}\right) = \alpha * l * c \quad (2.1)$$

Where  $A_\lambda$  is absorbance,  $l$  is the length of the light path,  $\alpha$  represents absorptivity, and  $c$  is the particle concentration,  $I_0$ ,  $I$ ,  $\alpha$ , and  $c$  [30,50].

Transmittance intensity is determined using this formula:

$$T_\lambda = I/I_0 \quad (2.2)$$

Where  $T_\lambda$  is transmittance,  $I$  is the laser intensity after incidence, and  $I_0$  is the incident laser light intensity.

A decrement in absorbance indicates an un-stable nanofluid, with measurements taken using a UV-vis spectrophotometer. Absorbance and transmittance depends on several properties, such as working temperature range, pH of the base fluid, and thermal conductivity. Some metal oxide nanoparticles yield good results using this method [86]. However, it is less effective for dark-colored nanoparticles and those with high concentrations [50].

#### 2.4.6. Electron Microscopy

Particle clustering or agglomeration can be studied through electron microscopy techniques, including scanning electron microscopy (SEM) and transmission electron microscopy

(TEM). These methods are instrumental in assessing the stability of nanofluids [87]. TEM is useful for observing particle agglomeration in nanofluids and can serve as an alternative measure for determining nanofluid stability through particle size distribution measurement. High-resolution TEM images provide detailed two dimensional visuals of nanoparticles suspended in the base fluid. Numerous Researchers have employed this technique to evaluate the extent of particle aggregation, and the shape and size of different nanofluids [85–87]. On the other hand, the procedure for SEM involves placing a nanofluid drop on sticky tape, fixing the tape onto a specimen holder, heating it in a vacuum heater, and then allowing it to dry naturally in the air. Once dried, the sample is placed in the SEM vacuum chamber for image capture [91]. Rubalaya Valentina et al. [92] examined two nanofluid samples (ZnO and ZnZrO in rice bran oil) using SEM, both with and without antioxidants. The ZnO samples demonstrated a uniform distribution, while the ZnZrO samples displayed significant aggregation.

#### 2.4.7. Dynamic Light Scattering

Dynamics light (DLS) is a technique used to measure the particle size distribution in colloidal suspensions. A DLS measurement setup includes key components such as a laser that illuminates the nanoparticles dispersed in a base fluid and a photon detector that monitors the scattered light fluctuations caused by the particles' Brownian motion. The diffusion coefficient is derived from these intensity fluctuations by using light scattering theory. This coefficient is then used to calculate the particle size through the Stokes-Einstein equation. [93]

$$R_H = \frac{k_B T}{6\pi\mu D} \quad (2.3)$$

$R_H$  is the hydrodynamic radius,  $D$  is the translational diffusion coefficient,  $k_B$  is the Boltzmann constant,  $T$  is the absolute temperature, and  $\mu$  is the viscosity.

By measuring particle size at different intervals over an extended period, DLS can indicate the tendency of nanoparticles to agglomerate. Instability in the nanofluid leads to cluster formation, which eventually results in sedimentation. Therefore, an increase in particle size over time can indicate nanofluid instability. For example, Kole et al. [94] observed a ~7 times increase in the cluster size of CuO nanoparticles in gear oil (base fluid) compared to their primary particle size, due to nanofluid instability.

## 2.5. Destabilization Factor and Mode

The performance of nanofluids can degrade irreversibly due to destabilization factors that affect their stability. These factors cause particles to irreversibly aggregate, deposit on surfaces, and change morphology, impacting the rheological, thermal, and optical properties of nanofluids. Understanding failure mechanisms and the factors causing colloidal and chemical destabilization is essential for designing robust nanofluids. Physical destabilization occurs through particle agglomeration, aggregation, surface deposition, sedimentation, and surface deposition, while processes like base fluid oxidation, particle oxidation, fragmentation and oxidative etching, drive chemical destabilization. The text below delves into these destabilization mechanisms.

### 2.5.1. Aging

Nanofluids tend to degrade with time because of various factors, including the agglomeration of the nanoparticles, which leads to kinetic instability. In perkinetic clustering dominated by Brownian motion, the energy barrier for particles to remain stable ranges from 15 - 25  $k_B T$ , indicative of kinetically stable colloidal dispersions [22]. The stability of nanofluids can span from a few seconds to several decades [43]. As storage duration increases, particle interactions become more pronounced, resulting in greater nanoparticle clustering.

The Smoluchowski equation models the changing concentration of particles as a function of time:

$$N(t) = \frac{3\mu_{bf}N(0)}{4k_bTN(t)+3\mu_{bf}} \quad (2.4)$$

Here,  $N(t)$  denotes the number of particles at time  $(t)$  in seconds,  $T$  is the temperature in Kelvin, and  $\mu_{bf}$  is the dynamic viscosity of the base fluid.

### 2.5.2. Concentration

The clustering frequency of particles, a key factor in destabilization, is directly related to the square of the particle number density. For instance, in two colloidal dispersions, one with 200 nm particles and the other with 20 nm particles, the latter will have 1000 times the particle concentration and a collision frequency 1,000,000 times higher. Increased particle concentration

leads to a higher clustering frequency. The average separation between particles can be calculated using Eq. (1):[95].

$$h_{ij} = D_p \left\{ \left( \left( \frac{\pi}{6\phi_p} \right)^{0.33} \right) + 1 \right\} \quad (2.5)$$

Where  $h_{ij}$  represents the mean static surface-to-surface interaction between particles distance  $i$  and  $j$ ,  $D_p$  is the particle diameter, and  $\phi_p$  is the volume fraction of particles. The study indicates that increasing particle concentration decreases the average separation, resulting in clustering. However, very much separation would be ineffective [96]. The particles concentration in nanofluids is related to the Reynolds number, with localized regions depending on the fluid's flow conditions [97].

### 2.5.3. Shear Rate

In nanofluids, a high shear rate can break down large nanoparticle clusters, reducing the viscosity of the base fluid. When the shear rate decreases, encourages clustering, contributing to increment viscosity. The shear rate also affects the rheology of nanofluids; higher shear rates tend to make nanofluids behave like Newtonian fluids, while lower shear rates can result in Newtonian and non-Newtonian behaviors [98]. Chen et al. highlighted the relationship between viscosity, stability, and shear rate. Shear stress can either break up or form clusters, and orthokinetic clustering, due to fluid movement under a velocity gradient, can increase the frequency of particle collisions. Brownian motion also contributes to this, though the impact of fluid circulation on clustering frequency is not fully understood [99]. This shearing phenomenon is also relevant to reducing drag in lubrication-related applications. Witharna et al. [100] reported that factors like particle concentration, temperature, shear rate, and duration of shear affect the stability of TiO<sub>2</sub>-EG nanofluid, noting that high shear rates and temperatures can alter particle cluster sizes.

### 2.5.4. Phase Change

The processes of evaporation and boiling in nanofluids can lead to particle deposition, affecting wettability and surface roughness, potentially causing severe fouling issues such as algae growth and corrosion [101]. At higher temperatures, the ionic strength increases as ionic particles

accumulate due to evaporation, compressing the Electrical Double Layer and reducing the electrostatic repulsion between nanoparticles. The impact of melting and freezing on nanofluids optical properties and stability has not been extensively explored. Xinxin et al. [102] suggested that combining glycols and water can effectively lower the freezing point of nanofluids, thereby minimize phase change instability.

#### 2.5.5. Solution Chemistry

Nano-materials particularly face the issue of chemical destabilization, such as oxidation, [103] which is a common issue in nanofluids. This effect often arises at elevated working temperatures or when minimal air infiltrates the fluid system, accelerating nanofluid oxidation. Variations in pH, [104] the presence of chemical entites, and electrolytes can also induce nanoparticle oxidation [101] and cause corrosion in the container walls [105]. Dissolved oxygen can significantly damage the spectral profile of nanofluids due to nanoparticle oxidation at elevated temperatures [106]. Furthermore, oxidation can lead to other physical and chemical issues [107]. For instance, Zhang et al. found that the rate at which citrate-coated silver nanoparticles clustered increased by 3–8 times due to surface oxidation. Additionally, oxygen presence can promote ionic etching and irregularities in nanostructures [103]. Changes in electrolyte and pH levels can neutralize surface charges by decreasing the electrical double layer around nanoparticles, leading to a sharp decrease in electrostatic repulsion [108].

#### 2.5.6. Surfactant

Surfactants are materials that lower the surface tension of liquids, which is essential for phase change distribution. They have a beneficial impact on both liquid -liquid and solid-liquid systems. When used to stabilize powdered particles in a liquid, these surfactants are called dispersants [109]. Surfactants consist of two components: one that is soluble and another that is insoluble. These components align so that the soluble part interacts with the liquid, while the insoluble part interacts with the solid surface. Dispersants are classified into four main categories based on the structure of their head group. However, there are some drawbacks to using dispersants for stabilizing nanofluids, such as the potential breakdown of the bond between nanoparticles and the surfactant [110]. Additionally, an excess amount of surfactant can adversely affect the thermal

properties of the nanofluid by decreasing thermal conductivity and increasing viscosity [111]. Research has demonstrated that the adding of surfactants like benzalkonium chloride, benzethonium chloride, and CTAB improves the stability and heat transfer efficiency of SiO<sub>2</sub> nanoparticles (15 nm in diameter) dispersed in synthetic oil and Therminol-66, with benzalkonium chloride offering the greatest stability [112].

## **2.6. Thermal Conductivity**

The thermal conductivity of nanofluids is influenced by various factors, including the size, shape, and material of the particles, the material of the base fluid, and the temperature.

### **Factor Affecting the Thermal Conductivity of Nanofluid**

#### **2.6.1. Particle Size**

The nanoparticle size has a major impact on the thermal conductivity properties of nanofluids, which consist of fluids mixed with nanoparticles. S. Sudarshan et al. [113] found that nanoparticles with diameter of 30 to 40 nm led to a significant increase in thermal conductivity, up to 100% with only 1.5 volume percent of nanoparticles. This suggests that nanoparticles in this size range are particularly effective at enhancing thermal conductivity in nanofluids. T P Teng et al. [114] investigated the thermal conductivity ratio of alumina (Al<sub>2</sub>O<sub>3</sub>)/water nanofluids with exploring particle sizes of 20, 50, and 100 nm concentrations (0.5, 1.0, 1.5, and 2.0 wt%). They also considered different temperatures (10°C, 30°C, and 50°C). Their results exhibited that smaller nanoparticle sizes correlated with higher thermal conductivity ratios. Additionally, they found that higher temperatures enhanced this effect, indicating an enhanced sensitivity to nanoparticle size at elevated temperatures.

#### **2.6.2. Particle Shape**

Normally the cylindrical nanoparticles, distinguished by their significant length-to-diameter ratio, play a key role in nanofluid studies. R Yun et al. [115] explored the impact of nanoparticle shapes, including nearly rectangular and spherical, on the thermal conductivity of ZnO nanofluids across various volume concentrations. At a 5.0 vol.% concentration, thermal

conductivity increased by up to 12% for spherical nanoparticles and 18% for nearly rectangular nanoparticles. P.B. Maheshwary et al. [116] also investigated the influence of nanoparticle shape on the thermal conductivity of TiO<sub>2</sub>-water-based nanofluids. They found that altering the shape of TiO<sub>2</sub> nanoparticles, particularly utilizing cubic shapes at 2.5 wt.%, resulted in the highest enhancement in thermal conductivity.

### 2.6.3. Particle Material and Base Fluid

Different categories of particle materials, including oxide metal carbides, nitrides, metals, ceramics, and non-metals, are utilized in the preparation of nanofluids. Carbon nanotubes, whether single or multiwall, are also employed as particle materials due to their notably high thermal conductivity. Base fluids commonly used for the preparation of nanofluids for heat transfer applications include water, ethylene/propylene glycols, bio-fluids, and engine oil.

### 2.6.4. Temperature

The thermal conductivity of nanofluids is influenced by both the temperature of the base fluid and the nanoparticles themselves. Temperature changes affect Brownian motion and clustering of nanoparticles, which in turn impact the thermal conductivity of the nanofluids. Wei Yu et al. [117] investigated how temperature affects the TC enhancement of nanofluids containing ZnO nanoparticles. They observed that as temperature increased, so did the thermal conductivity of the nanofluids. Similarly, T K Dey et al. [118] explored the TC enhancement of CuO-gear oil nanofluids, finding that it varied with temperature. At room temperature, the maximum enhancement was 10.4% with a 0.025 volume fraction of CuO nanoparticles, which increased to 11.9% at 80 °C. Rajan K S et al. [119] demonstrated higher TC of sand in PG with 46.2% enhancement for 2 vol% nanofluids at 10 °C.

### 2.6.5. Additives

Additives are employed to maintain nanoparticles dispersed and prevent their agglomeration, thereby facilitating thermal conductivity enhancement in nanofluids. W. H. Zhong et al. [120] explored the potential of various nanomaterials in augmenting fluidic heat transfer applications through investigations into thermal conductivity. Conductive nanomaterials like

copper nanoparticles (CuNPs), carbon nanotubes (CNTs), and gold nanoparticles (AuNPs), as well as their hybrids such as CuNP–CNT or AuNP–CNT, were utilized to boost the thermal conductivity of fluids. The study revealed that mono-nanoparticle suspensions exhibited the highest increase in TC, with CuNPs demonstrating the most significant improvement. Conversely, hybrid suspensions did not exhibit the same level of enhancement. Eastman et al. [121] tested Cu in EG both with and without additives. The findings indicated that additives could substantially enhance the thermal conductivity of nanofluids.

#### 2.6.6. Acidity (pH)

There is a limited amount of research exploring the influence of base fluid pH on the thermal conductivity of nanofluids. In their study, X F Li et al. [122] examined how pH and the presence of sodium dodecyl benzenesulfonate (SDBS) surfactant affect the thermal conductivity of nanofluids. Their findings indicated that the enhancement of thermal conductivity in Cu-H<sub>2</sub>O nanofluids is notably influenced by the nanoparticle weight fraction, pH levels, and SDBS surfactant concentration in the nano-suspensions. Xie et al. [123] were among the pioneers in investigating the impact of increasing pH on the thermal conductivity ratio, conducting tests on Al<sub>2</sub>O<sub>3</sub>/DIW nanofluids. Their findings demonstrated that the TC enhancement of Al<sub>2</sub>O<sub>3</sub>/DIW nanofluids ranged from 23% to 19% as the pH varied from 2 to 11.5.

#### 2.6.7. Clustering

Clustering represents another variable impacting the thermal conductivity of nanofluids. At higher concentrations and prolonged durations, nanofluids tend to form clusters, thereby diminishing the effective surface area for thermal interaction among particles, resulting in reduced fluid thermal conductivity. J. Philip et al. [124] investigated the thermal conductivity increment observed in nanofluids based on ethylene glycol and water. They attributed the substantial increase in thermal conductivity to the nanoparticles' finer size and uniform distribution. Experimental findings underscore the significant influence of nanoparticle size, polydispersity, cluster dimensions, and particle volume fraction on thermal conductivity.

### 2.7. Viscosity



Viscosity is crucial for heat transfer applications because it affects pressure drop and pumping power. It depends on the base fluid's viscosity, particle loading, particle size, temperature, and type of nanoparticles used. More research is essential to find the effects of these factors on the viscosity of nanofluids. Instruments such as rotational rheometer, piston-type rheometer, and capillary viscometers are widely used for nanofluid viscosity measurement. Understanding viscosity is important for designing efficient nanofluids for heat transfer because pressure drop and pumping power are influenced by it. Compared to studies on thermal conductivity, there have been fewer investigations into the rheological behavior of nanofluid [67].

## **Factor Affecting the Viscosity of Nanofluid**

### **2.7.1. Volume Concentration**

The concentration of nanofluids plays a important role in determining the viscosity of coolant media. Researchers have found that viscosity of nanofluid the viscosity of nanofluids is directly affected by the weight percentage of nanoparticles. Although the exact reason for non-linearity requires further investigation, it is found that different concentrations could be a possible reason for the increase in viscosity with an increase in particle concentration. Particle size also affects the density and viscosity of nanofluid, with viscosity showing a more significant difference. Experiments on viscosity were conducted over a wide temperature range to demonstrate their applicability in cold regions. The nanoparticle diameter can also affect the rheology of nanofluids, with non-Newtonian behavior observed at sub-zero temperatures for certain particle volume concentrations. Researchers have developed correlations between viscosity and particle volume percent and nanofluid temperature based on experimental data [104–106].

S Wongwises et al. [39] found that increase in viscosity is primarily due to the particle volume concentration. Hung and Chou [40] measured the suspension performance of nanofluids as influenced by additive concentrations, as demonstrated in experiments with MWCNTs and Chitosan in water. P Estelle et al. [41] measured the [36–38] viscosity of carbon nanotubes water-based nanofluids behave as shear-thinning materials for high particle content, while lower particle content shows Newtonian behavior. M.H.K Darvanjooghi et al. [42] investigated the effect of temperature and mass fraction on the viscosity of crude oil-based nanofluids containing oxide

nanoparticles increases significantly with higher-density nanoparticles. All nanofluid samples exhibit Newtonian behavior at different shear rates. Sardinia et al. [130] investigations into CuO-based oil nanofluids showed that particle weight fractions from 0.2% to 2% maintained Newtonian behavior under various temperature conditions.

### 2.7.2. Morphology

The morphology, including both shape and size, of nanoparticles can significantly affect the pumping power of a cooling system and viscosity. M Farbod et al. [131] examined CuO-engine oil nanofluid-containing nanoparticles with various nanostructures such as nanorhombics and nanorods. They found that the viscosity of the base oil and nanofluids, ranging from 0.2 to 1 wt.%, followed a Newtonian behavior and was influenced by the morphology of the nanoparticles. Specifically, the nanofluid containing 0.2 wt.% of nanorods exhibited higher viscosity compared to other nanostructures and the base fluid. Conversely, the nanofluid with nanorhombics demonstrated a lower viscosity than the base oil, indicating its potential suitability for lubrication purposes. Nguyen et al. [132] evaluate the impact of particle size, considering  $\text{Al}_2\text{O}_3$  nanoparticles with sizes of 36 nm and 47 nm their findings revealed that 47 nm  $\text{Al}_2\text{O}_3$  particles exhibited higher viscosity compared to the 36 nm particles.

### 2.7.3. Shear Rate

The influence of shear rate on viscosity in non-Newtonian nanofluids is a significant parameter. P Estelle et al. [133] investigated experimental investigations on the effect of shearing time on viscosity for  $\text{Al}_2\text{O}_3$ /water and CNT/water nanofluids at low concentrations and temperatures. They found that CNT water-based nanofluids exhibit Newtonian fluid behavior at a high shear rate, while  $\text{Al}_2\text{O}_3$  water-based nanofluids display non-Newtonian behavior within the investigated range of low temperatures. T X Phuoc et al. [134] observed the impact of particle volume fractions and shear rates on shear stress and viscosity in  $\text{Fe}_2\text{O}_3$ /DW nanofluids with Poly(ethylene oxide), PEO, as dispersants. They noted that  $\text{Fe}_2\text{O}_3$ /DW at 0.2% PVP nanofluids with particle volume fractions.

### 2.7.4. Temperature

Temperature is a critical factor influencing viscosity, as demonstrated in several studies. Karimipour et al. [135] investigated the impact of temperature on the dynamic viscosity of liquid paraffin-based nanofluids. Their findings revealed that as the nanoparticle concentration increased, the ratio of nanofluid dynamic viscosity to that of the base fluid also increased. However, as the temperature rose, the viscosity of the nanofluid notably decreased. M Afrand et al. [136] examined the viscosity of SWCNTs dispersed in EG from 30°C to 60°C for various solid volume fractions. They found that at 30°C and a volume fraction of 0.1%, the nanofluid's viscosity increased to 3.18 times that of the base fluid. S Wongwises et al. [137] studied TiO<sub>2</sub> nanoparticles dispersed in water and were investigated at 15°C to 35°C, with varying particle concentrations. Results indicated that both the viscosity and thermal conductivity of nanofluids increased with higher particle concentrations, surpassing those of the base liquids. Additionally, while thermal conductivity enhanced with rising temperatures of nanofluid, viscosity decreased. Suganthi and Rajan [138] experimentally studied ZnO nanoparticle-dispersed water nanofluids, focusing on temperature's effect on the hydrodynamic size distribution and zeta potential variations during heating and cooling cycles. Their results demonstrated a decrease in relative viscosity with increasing temperature within the range of 35°C to 55°C.

Below are the steps for making a new chapter. This will help to begin a new chapter using this template. This will also help to get the page numbers correctly.

## **2.8. Recent Studies of Different Research Groups**

Zyla et al. investigated the thermophysical properties of Si<sub>3</sub>N<sub>4</sub>-EG nanofluids with different nanoparticle volume fractions. They found that the nanofluids exhibited non-Newtonian shear thinning behavior, with thermal conductivity and refractive index increasing linearly, while electrical conductivity showed a strong nonlinear relationship. Absorption, especially in the UV region, improved with higher nanoparticle volume fractions. Zyla and J Fal [139] investigated the basic thermophysical properties of AlN – EG nanofluids, prepared using a two-step method with commercial AlN nanoparticles. The dynamic viscosity, thermal conductivity, and electrical conductivity were measured at 298.15 K, revealing a non-Newtonian behavior, a linear increase in thermal conductivity with nanoparticle concentration, and a significant rise in electrical conductivity with nanoparticle concentration.

Esmaeili et al. [140] synthesized aluminum nitride-carbon (AlN-C) nanocomposites using a green mechano-chemical method and dispersed them in ethylene glycol without surfactants. The nanofluids maintained outstanding stability for up to three months at a low concentration of 0.22 vol% and improved the heat transfer coefficient by 24% compared to the base fluid in a laminar flow regime. Zyla et al. [141] experimentally investigated the thermophysical properties of EG-based nanofluids with titanium nitride nanoparticles. It was found that smaller nanoparticles increased thermal conductivity and surface tension, while larger ones enhanced dielectric properties and electrical conductivity. The nanofluids transitioned from Newtonian to shear-thinning behavior with smaller nanoparticle sizes, and rheological properties varying based on nanoparticle concentration and size.

Villarejo et al. [142] investigated boron nitride nanotube-based nanofluids using Triton X-100 as a surfactant, achieving stable dispersions with particle sizes of 150 to 170 nm and a  $\zeta$  potential of around  $-25$  mV. The fluids exhibited Newtonian behavior and showed an 8% increase in isobaric-specific heat and a 10% increase in thermal conductivity, with no significant change in viscosity. This indicated their potential as effective options for thermal system applications due to their improved thermal properties and stable rheological behavior. Zyla et al. [143] conducted an experimental study on the thermal conductivity of boron nitride (BN) plate-like particles in EG, using a two-step method to prepare nanofluids. The study tested concentrations up to 20 wt.% and measured thermal conductivity from 293.15 K to 338.15 K. Results showed that increase in thermal conductivity with concentration of nanoparticle but varied minimally with temperature.

Villarejo et al. [144] prepared boron nitride nanotube-based nanofluids using a two-step method and assessed their stability, rheological, and thermal properties. The nanofluids remained stable for a month with no significant change in surface tension. It showed up to a 33% increase in thermal conductivity and an 18% improvement in heat transfer coefficients, indicating potential for solar thermal applications. A. K. Sleiti, et al. [144] investigated PAO oil combined with hexagonal Boron Nitride (hBN) to develop nanofluids for heat transfer and lubrication. The study found that PAO/hBN nanofluids exhibited Newtonian behavior, improved thermal conductivity, and enhanced heat transfer performance compared to pure PAO, although viscosity and specific heat were influenced by concentration and temperature. Heat transfer enhancement ranged from 10% to 29% based on hBN concentration, due to increased thermal conductivity.

Singh et al. [145] investigated silicon carbide-water nanofluid for heat transfer applications at a volume concentration of 4 vol. % to 7 vol. %. The viscosity of nanofluid did not notably change with the temperature tested up to 85°C and thermal conductivity increased 28% to make it useful for heat transfer. Ezekwem et al. [146] studied the thermal and electrical conductivity of silicon carbide-based nanofluid which had superior heat transfer properties than traditional fluids such as EG, water, and engine oil at concentrations of 0.5-5 vol% by using a two-step method. The highest absorbency for SiC/DW and SiC/EG nanofluids exhibits at 265 nm and 271 nm, and SiC/DW shows greater stability as compared to SiC/EG. The highest thermal conductivity is enhanced by 25% and 16% and electrical conductivity increases 58 and 148 times with SiC nanoparticles at 5% volume concentration.

Guo et al. [147] investigated silicon oxide nanofluids electrical and thermal conductivity in an ethylene glycol/water mixture. The two-step method was used to prepare nanofluid and variation in thermal and electrical conductivity as a function of EG concentration (0-100%, v/v) and temperature 25-45°C. The results showed that the thermal and electrical conductivity decreased as the percentage of EG content increased. Zyla et al. [148] investigated the viscosity, thermal, and electrical conductivity of SiO<sub>2</sub> nanoparticles suspended in ethylene glycol (EG). They measured the dynamic viscosity, electrical, and thermal conductivity across various particle fractions at 298.15 K, finding that all properties increased linearly with nanoparticle concentration. The study also evaluated heat transfer performance and the thermo-electrical conductivity (TEC) ratio based on the results.

H Jin et al. [149] investigated the physical properties of SiO<sub>2</sub>-mineral oil nanofluids with varying nanoparticle volume fractions. They found that the thermal conductivity increased with temperature, while the viscosity remained nearly unchanged above 20°C. P.K. Namburu et al. [127] investigated the viscosity and specific heat of SiO<sub>2</sub> nanoparticles with diameters of 20, 50, and 100 nm in a 60:40 ethylene glycol-water mixture. They examined nanofluids with particle volume percentages from 0 to 10%, observing non-Newtonian behavior at sub-zero temperatures. From the experimental data, they developed a new correlation relating viscosity to particle volume percentage and temperature. R Ranjbarzadeh et al. [150] conducted an experimental study where silica nanoparticles were synthesized from a rice plant source and used to produce eco-friendly water/silica nanofluids. The stability of the nanofluids was confirmed through DLS, TEM tests, and visual observation over six months, showing excellent stability. The thermal conductivity

enhancement reached a maximum of 38.2% at 55°C with a 3% solid volume fraction, with a novel correlation introduced for its prediction. R Mondragon et al. [151] studied the stability and agglomeration of silica nanofluids, which were prepared using an ultrasonic probe for effective dispersion. They found that solid content was the most critical factor, and despite agglomeration at high concentrations, nanofluids with low viscosity were achieved at 20% mass load. The stability of nanofluids was controlled by pH, with more stable conditions under basic pH values, far from the isoelectric point.

Table 2.2. Literature review of Silicon and nitride base nanofluids.

Nanoparticles	Base fluid	Surfactant	Stability	Thermal conductivity	Viscosity & Rheology	Concentrations	Ref.
Si <sub>3</sub> N <sub>4</sub>	EG	-	-	Increasing linearly with vol.%	Non-Newtonian at higher concentration	0.01-0.1 vol%	[152]
AlN	EG	-	-	4.2%	Non-Newtonian at higher concentration	0.05-0.20 vol%	[139]
AlN-C	EG	-	3 months	Increasing linearly with vol.%	Non-Newtonian at higher concentration	0.027-0.22 vol%	[140]
TiN	EG	-	-	Increasing linearly with vol.%	Newtonian	0.01-0.05 mass%	[141]
BN	Water	Triton X-100	25days	8.3%	Newtonian	0.01-0.03 vol%	[142]
BN	EG	-	-	Increasing linearly with vol.%	-	0.05-0.2 vol%	[143]
BNNTs	Biphenyl: Diphenyl oxide	Triton X-100	month	33%	decreases with temperature & Newtonian	0.35 vol%	[144]
hBN	Polyalpha-Olefin oil	-	-	decreases with temperature	decreases with temperature	0.25–1 vol%	[153]
SiC	DIW	-	-	28%	Decreases with temperature	4-7 vol%	[145]
SiC	EG, DW	-	SiC/DW more stable till 2 weeks	25% (SiC/EG) 16% ( SiC/EG	-	0.5-5 vol%	[146]
SiO <sub>2</sub>	EG: water	-	-	Decreases as EG content percentage increases	-	0.3 mass%	[147]
SiO <sub>2</sub>	EG	-	-	Increasing linearly with Vc	Newtonian	0.1-0.05 vol%	[148]
SiO <sub>2</sub>	mineral oil	-	month	Increasing linearly with Vc	negligible effect at above 20°C	0.01-0.1 vol%	[149]
SiO <sub>2</sub>	EG: water	-	-	-	Non-Newtonian	0-10 vol%	[127]
SiO <sub>2</sub>	water	-	6 months	38.2% increase	-	0.1- 3 vol%	[150]
SiO <sub>2</sub>	DIW	-	48 hours	-	Increase the mass of NPs increase	0.01- 0.20 w/w	[151]

## 2.9. Why silicon nitride?

Recent studies indicate that silicon-based nanoparticles have effectively improved stability and thermophysical properties. The positive results achieved with  $\text{SiO}_2$  [154] and  $\text{SiC}$  [9] nanoparticles inspire the exploration of silicon-based nanomaterials for similar advancements.  $\text{Si}_3\text{N}_4$  was selected due to a scarcity of literature, and its notable high thermal stability properties. According to the author, the investigations involving the physical properties of EG nanofluids incorporating  $\text{Si}_3\text{N}_4$  nanoparticles have been conducted by Zyla et al. [155]-[152] focusing on the isobaric heat capacity, density, thermal conductivity, optical, electrical, and rheological properties. However, the existing literature does not adequately address nanofluids' stability, surfactants' impact, and the exploration of various base fluids on the thermophysical properties of  $\text{Si}_3\text{N}_4$  nanofluids.

## 2.10. Research Gap

Despite considerable effort in working with silicon nitride nanoparticles suspended in deionized water and ethylene glycol, and testing their long-term stability with four different surfactants, it is important to investigate the effects of these nanoparticles on thermophysical properties like viscosity and thermal conductivity, alongside rheological properties and overall stability, both before and after addition of surfactant.

## Summary

Nanofluids can be synthesized using either a single-step or a two-step process. The single-step method involves the simultaneous preparation of nanoparticles and nanofluids, while the two-step method first creates nanoparticles separately before mixing them into a base fluid. Each method has its own set of advantages and disadvantages, depending on the intended application. Once prepared, assessing the stability of nanofluids is crucial. Different techniques, such as sedimentation analysis, zeta potential, and UV-VIS spectroscopy measurement, are employed to evaluate stability. To enhance stability, chemical methods like surfactant addition and pH adjustment, as well as mechanical techniques such as magnetic stirring, ultrasonication, and high-shear mixing, are applied. Additionally, it is essential to assess the thermophysical properties, including thermal conductivity, viscosity, density, and flow behavior (Newtonian or non-Newtonian) of nanofluids.



## CHAPTER 3: EXPERIMENTAL PROCEDURES

### 3.1. Materials

This study investigated the dispersion of silicon nitride ( $\text{Si}_3\text{N}_4$ ) nanoparticles in two different base fluids: De-ionized Water (DIW) and Ethylene Glycol (EG). Four different surfactants i.e. OLAM (Oleyl amine), SDS (Sodium dodecyl sulfate), SDBS (Sodium dodecyl benzene sulphonate), and Tween-80, were also used to investigate their effect on the stability of nanofluids. This research aims to understand the dispersing of silicon nitride nanoparticles, which has significant implications for various applications in material science and nanotechnology. The characteristics of the nanoparticles, base fluids, and surfactants utilized are outlined in Table 3.1.

Table 3.1. Characteristics of the nanoparticles, base fluids, and surfactants.

Materials Used	Chemical Formula	Type	Density	Molar mass	Supplier	Purity(%)
			( $\text{g}/\text{cm}^3$ )	( $\text{g}/\text{mol}$ )		
Silicon Nitride	$\text{Si}_3\text{N}_4$	Non-Polar	3.17	140.28	Sigma-Aldrich	$\geq 99$
EG	$\text{CH}_2(\text{OH})_2$	Polar	1.11	62.07	Merck KGaA	$\geq 99$
OLAM	$\text{C}_{18}\text{H}_{37}\text{N}$	Non-ionic	0.813	267.493	Sigma-Aldrich	$\geq 70$
SDS	$\text{NaC}_{12}\text{H}_{25}\text{SO}_4$	Ionic	1.01	288.38	Sigma-Aldrich	$\geq 98$
SDBS	$\text{C}_{18}\text{H}_{30}\text{NaO}_3\text{S}$	Ionic	1.02	348.48	Sigma-Aldrich	$\geq 99$
Tween-80	$\text{C}_{64}\text{H}_{124}\text{O}_{26}$	Non-ionic	1.06	1310	Sigma-Aldrich	$\geq 97$

### 3.2. Preparation of Nanofluids

Nanofluids were prepared through a two-step process. Initially, nanoparticles were produced as dry powders using chemical or physical approaches. These dry nanoparticles were then dispersed into a base fluid, undergoing intensive homogenization to achieve a stable and even distribution within the fluid. In this analysis considered three base fluids: DIW, a mixture of DIW and EG (60:40 and 40:60), and EG. For, a given percentage of volume concentration, the required quantity of nanoparticles was estimated using the formula [156].

$$\phi_1 = \frac{\left(\frac{m}{\rho}\right)_{Si_3N_4}}{\left(\frac{m}{\rho}\right)_{Si_3N_4} + \left(\frac{m}{\rho}\right)_{bf}} * 100 \quad (3.1)$$

Where ‘m’ represents the mass of the nanoparticle and mass of base fluid, ‘ $\phi$ ’ represents the volume concentration of nanofluid, and ‘ $\rho$ ’ is the density of the nanoparticle and base fluid.

The mass of the nanoparticles was accurately measured using a high-precision electronic balance (model AS 220, R2, RADWAG, with an accuracy  $\pm 0.2$  mg). Nanofluid were prepared by taking base fluid in a beaker and directly mixing the required quantity of  $Si_3N_4$  nanoparticles using a mechanical stirrer for 20 minutes. Subsequently, a 15-minute probe sonication was conducted using a probe sonicator (Q Sonica, LLC model Q500 operating at 500W/20kHz). This process was carried out within a cooling water cold water bath to regulate the temperature and prevent excessive heating. To further improve the stability of the nanofluid, 1-hour bath sonication was carried out using an Ultrasonic cleaner operating at 400W/50Hz. Four different surfactants, namely oleyl amine (OLAM), Sodium Dodecyl Sulfate (SDS), Tween 80, and sodium dodecyl benzene sulfonate (SDBS) were added to optimize stability. As suggested in the literature, all the surfactants were proportionally mixed at the same ratio ( $1/10^{th}$ ) of the number of nanoparticles [157]. First, the surfactant was mixed with DIW, a mixture of DIW and EG (60:40,40:60), and EG and stirred by a mechanical stirrer for 10 minutes to ensure a homogenous mixing surfactant with the base fluid. Then the nanoparticles were added and using the same surfactant the process was repeated for each of the nanofluids. The stability of nanofluid with different surfactants was assessed, and OLAM was selected for further experiments.

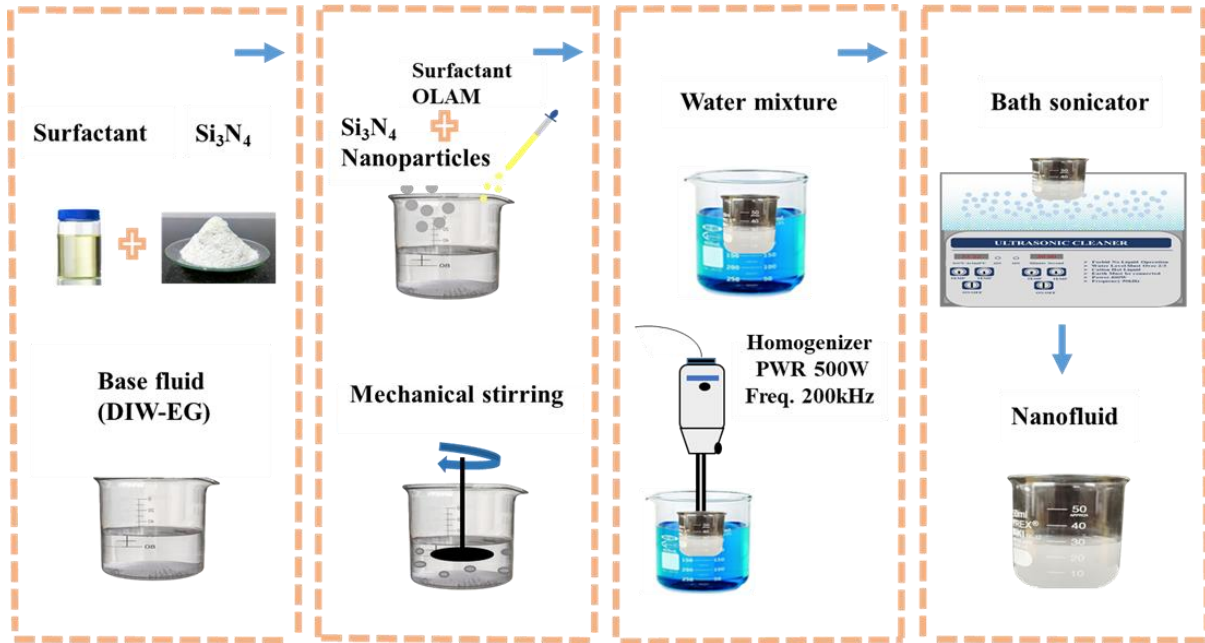


Fig. 3.1. Preparation of nanofluid by two-step method.

### 3.3. Characterization and Stability

The crystalline size of  $\text{Si}_3\text{N}_4$  is determined through X-ray diffraction (XRD) analysis using  $\text{Cu K}\alpha$  radiation, ranging from  $5^\circ$  to  $80^\circ$ , as shown in Fig. 2. The calculation, performed with the Debye-Scherrer equation (Eq. 4) and confirmed its presence in nanoparticle form,

$$D = (k \lambda) / (\beta \cos \theta) \quad (3.2)$$

Where ' $\lambda$ ' represents the X-ray wavelength, ' $\cos \theta$ ' denotes the diffraction angle, ' $k$ ' is typically a constant equal to 1 and  $\beta$  refers to the peak width known as Full Width at Half Maximum (FWHM) [158].

Photographic images of prepared  $\text{Si}_3\text{N}_4/\text{DIW}$ ,  $\text{Si}_3\text{N}_4/60 \text{ DIW}$ ,  $\text{Si}_3\text{N}_4/60 \text{ EG}$ , and  $\text{Si}_3\text{N}_4/\text{EG}$  nanofluids are shown in Fig. 4 with and without surfactant. The dispersion stability of nanofluid suspension was assessed using a UV-VIS spectrometer that operates within a wavelength range of 200 nm to 1100 nm. The absorbance measurements were obtained over time following the preparation of nanofluid to evaluate its stability. The UV-VIS spectrometer detects changes in the intensity of the light due to absorption and scattering in fluid. Initial background scans were taken with reference and sample solutions in the cuvette. Samples with high absorption were diluted before measurement to ensure light could pass through the

solution. Measurements are taken within 300 nm to 800 nm using the same cuvettes for consistency as shown in Fig. 4.4.

The zeta potential (WALLIS instruments, utilizing ZetaQ software, measuring range -200mV to 200 mV), representing electrostatic repulsion between nanoparticles and base fluid, is one of the key indicators of nanofluid stability. According to Babita et al. [159] a high zeta potential indicates stronger repulsive forces, inhibiting aggregate formation and ensuring greater stability. Nanofluids with zeta potential measurements over  $\pm 30$  mV indicate moderate stability and  $\pm 60$  mV demonstrate exceptional stability. In this study, four types of surfactants were employed: two ionic (SDBS and SDS) and two non-ionic (Tween-80 and OLAM). Surfactants were added at a ratio of  $1/10^{\text{th}}$  of the nanoparticle amount in the base fluid to enhance homogeneity. OLAM exhibits the highest zeta potential value indicating nanofluids have good stability shown in Fig. 6 and maintained a homogeneous mixture for over 40 days, unlike SDS, SDBS, and Tween-80 which failed to achieve through mixing with the nanoparticles.

### **3.4. Thermophysical Properties of Nanofluid**

This study involved the preparation of  $\text{Si}_3\text{N}_4$  nanofluid with a volume concentration of 0.06 vol. % by dispersing nanoparticles in various base fluids. The thermal conductivity of the prepared nanofluid samples was determined using the DTC 300 from TA Instruments across a temperature range from 30°C to 80°C. The 'Guarded Heat Flow Meter' method, following ASTM E1530 standards, was used for TC measurements, which had an accuracy between  $\pm 3\%$  to 8%.

AMETEX Brookfield's DV2T instrument was used to measure the nanofluids' viscosity and rheological behavior. The viscosity and rheological properties of the nanofluid were then measured across the temperature range from 30°C to 80°C. Additionally, viscosity and shear stress measurements were taken at various shear rates ranging from  $70 \text{ s}^{-1}$ ,  $100 \text{ s}^{-1}$ ,  $120 \text{ s}^{-1}$ ,  $150 \text{ s}^{-1}$ ,  $180 \text{ s}^{-1}$ , and  $220 \text{ s}^{-1}$ . To ensure accuracy, shear stress and viscosity measurements were taken three times. Subsequently, the nanofluids' average values for dynamic viscosity and shear stress were calculated.

Table 3.2. Specifications details of the instruments used.

Sr. No.	Instruments	Specifications
1	Electronic balance	Model Accuracy
		AS 220, R2, RADWAG ± 0.2 mg
2	XRD (By Bruker Germany)	Model X-ray source Wavelength Detector Time step Power
		D8-Advance Cu K $\alpha$ 5°-80° Lynxeye 0.1 Sec 12W
3	SEM (Made in Japan Company Jeol)	Model Magnification Accelerating voltage
		JSM-649A 0.5 $\mu$ m-10 $\mu$ m 20kV
4	Multiparameter with 10m cable probe (Made in ROMANIA)	pH range instrument drift
		2.00-19.99 <40 $\mu$ V/°C
5	Q Sonica LLC	Model Power Freq. Volts
		Q500 500W 20kHz 230V~AC 50/60 Hz 6.3A Max
6	Ultrasonic cleaner	Model Input Power
		FSF-080S 220V/50Hz 400W
7	UV-VIS spectroscopy	Wavelength range
		200nm-1100nm
8	WALLIS instruments (CORDOUAN technologies, France)	Model Software Range
		ZPA220901 ZetaQ -200mV to 200 mV
9	DV2T instrument by AMETEK Brookfield	Spindle speed Spindle type Accuracy Temperature sensing
		1-200rpm RV ±8% 0°C to 100°C
10	DTC 300 instrument by TA instruments	Method Thermal conductivity range Accuracy
		Guarded heat flux meter 20°C to 80°C ±3% to 8%

## Summary

Nanofluids were synthesized using a two-step method: initially, Si<sub>3</sub>N<sub>4</sub> nanoparticles were fabricated, and then these nanoparticles were dispersed in base fluids (DIW, DIW/EG mixtures, EG). The volume concentration of nanoparticles was calculated using their mass and

density. To improve nanofluid stability, surfactants (OLAM, SDS, Tween 30, SDBS) were added at a ratio of 1/10 relative to the nanoparticles, with OLAM proving to be the most effective stabilizer. The nanofluids were characterized using XRD to determine crystalline size, SEM for morphology analysis, and UV-VIS spectroscopy for dispersion stability. Zeta potential measurements revealed that OLAM-stabilized nanofluids exhibited the highest stability. Thermal conductivity was measured with the DTC 300, while the rheological properties and viscosity of all samples were evaluated using the AMETEX Brookfield DV2T instrument over temperatures ranging from 30°C to 80°C and various shear rates (70 s<sup>-1</sup>, 100 s<sup>-1</sup>, 120 s<sup>-1</sup>, 150 s<sup>-1</sup>, 180 s<sup>-1</sup>, and 220 s<sup>-1</sup>)

## CHAPTER 4: RESULTS AND DISCUSSION

### 4.1. Phase Analysis

The X-ray diffraction (XRD) analysis (Fig. 2) without further procurement of  $\text{Si}_3\text{N}_4$  reveals characteristic peaks at angles of  $13.4^\circ$ ,  $27.05^\circ$ ,  $33.62^\circ$ ,  $36.03^\circ$ ,  $38.94^\circ$ ,  $41.49^\circ$ ,  $52.13^\circ$  and  $70.12^\circ$  which are typically attributed to  $\beta\text{-Si}_3\text{N}_4$  crystal structure and also compared with JCPDS card no.33-1160 [160]. By employing Scherer's equation, which relates full width at half maximum (FWHM) of diffraction peaks to particle size, the average crystalline size of silicon nitride nanoparticles is determined to be less than 60 nm.

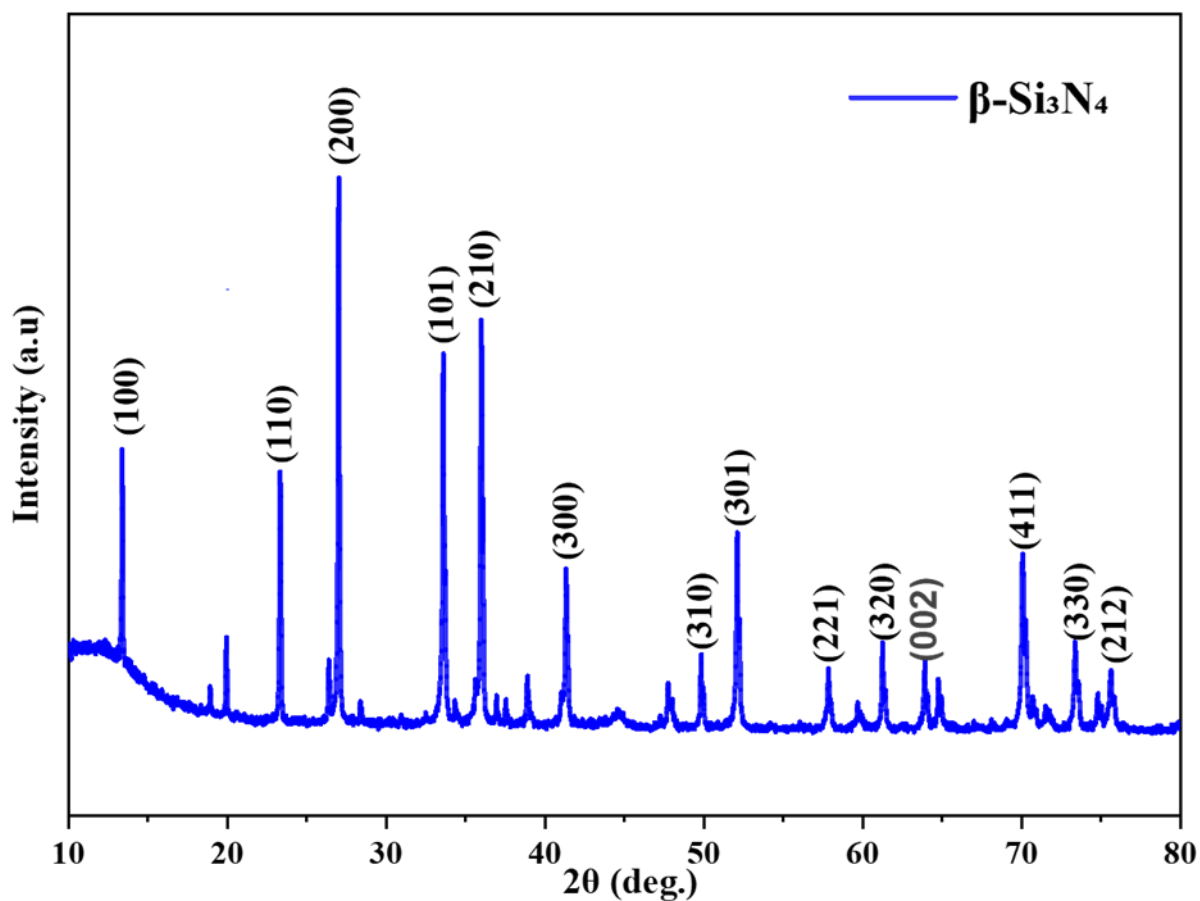


Fig. 4.1. XRD pattern of  $\text{Si}_3\text{N}_4$  nanoparticles.

### 4.2. Impact of Temperature on Ultra-Sonication

Ultrasonication is an effective technique for enhancing the dispersion of nanoparticles within a base fluid. Applying ultrasonic waves makes nanoparticles better distributed throughout the fluid, improving the resulting nanofluid's stability. Proper dispersion achieved through ultrasonication helps prevent issues like settling or clustering of nanoparticles. Maintaining this stability is essential for ensuring the nanofluid retains its desired properties over time. Optimal ultrasonication parameters, including time and power, are crucial for achieving long-term stability and performance of the nanofluid. Asadi et al. [161] found that using more efficient ultrasonic probe devices instead of ultrasonic baths and lower ultrasonication times and power led to better results. Unlike the dispersed cavitation that occurs in the fluids of ultrasonic baths, probe devices provide focused and intense ultrasonication directly beneath the probe, resulting in a more effective and controllable dispersion of nanoparticles. However, increasing the ultrasonication time and power can cause some nanofluids to become less stable. While ultrasonication is used to break down particle agglomerates and disperse particles more uniformly, excessive ultrasonication can have the reverse effect. Over time, the particles might agglomerate due to the high energy inputs leading to unstable suspensions. Moreover, the increasing temperature generated by both probe sonicator and bath sonicator can induce oxidation, a challenge encountered frequently during experimentation. To prevent heating during sonication and reduce the probability of oxidation, a cold water bath was used to control the temperature of the nanofluid. The heating issue was effectively resolved by maintaining the temperature below 25°C.

### **4.3. Stability Analysis Using Visual Sedimentation Method**

Silicon nitride nanofluid samples were prepared using DIW, EG, and DIW-EG ratios (60:40, 40:60) and were initially stable, as shown in Fig. 4.3 (a). The  $\text{Si}_3\text{N}_4/\text{DIW}$  nanofluid exhibited complete instability, leading to full sedimentation within 72 hours. On the other hand,  $\text{Si}_3\text{N}_4/60$  DIW,  $\text{Si}_3\text{N}_4/60$  EG, and  $\text{Si}_3\text{N}_4/\text{EG}$  nanofluids exhibited different levels of sedimentation.  $\text{Si}_3\text{N}_4/60$  EG nanofluid showed complete nanoparticle sedimentation after 5 days, whereas  $\text{Si}_3\text{N}_4/60$  DIW nanofluid exhibited entire nanoparticle agglomeration and sedimentation after 10 days.  $\text{Si}_3\text{N}_4/\text{EG}$  nanofluid demonstrated stability over 40 days with slight nanoparticle sedimentation, as shown in Fig. 4 (b) and (c).

After consulting literature, it was noted that the addition of surfactant could enhance the stability of nanofluid. Therefore, the impact of four different surfactants (OLAM, SDS,



Tween 80, and SDBS) on the stability of silicon nitride nanofluid was investigated. It was found that SDS, Tween 80, and SDBS were not effective in dispersing the  $\text{Si}_3\text{N}_4$  nanoparticles throughout the base fluid due to their low surface activity, leading to poor stabilization and dispersion [38]. OLAM, a non-ionic surfactant, offered steric stabilization by effectively dispersing the silicon nitride nanoparticles [22]. When OLAM was used, the  $\text{Si}_3\text{N}_4/\text{DIW}$  nanofluid remained stable for over five months without any sedimentation. Whereas,  $\text{Si}_3\text{N}_4/60$  DIW and  $\text{Si}_3\text{N}_4/60$  EG were stable for 20 days. It was concluded that OLAM was the only surfactant that provided the necessary surface activity to effectively coat the nanoparticles and prevent their agglomeration and sedimentation.

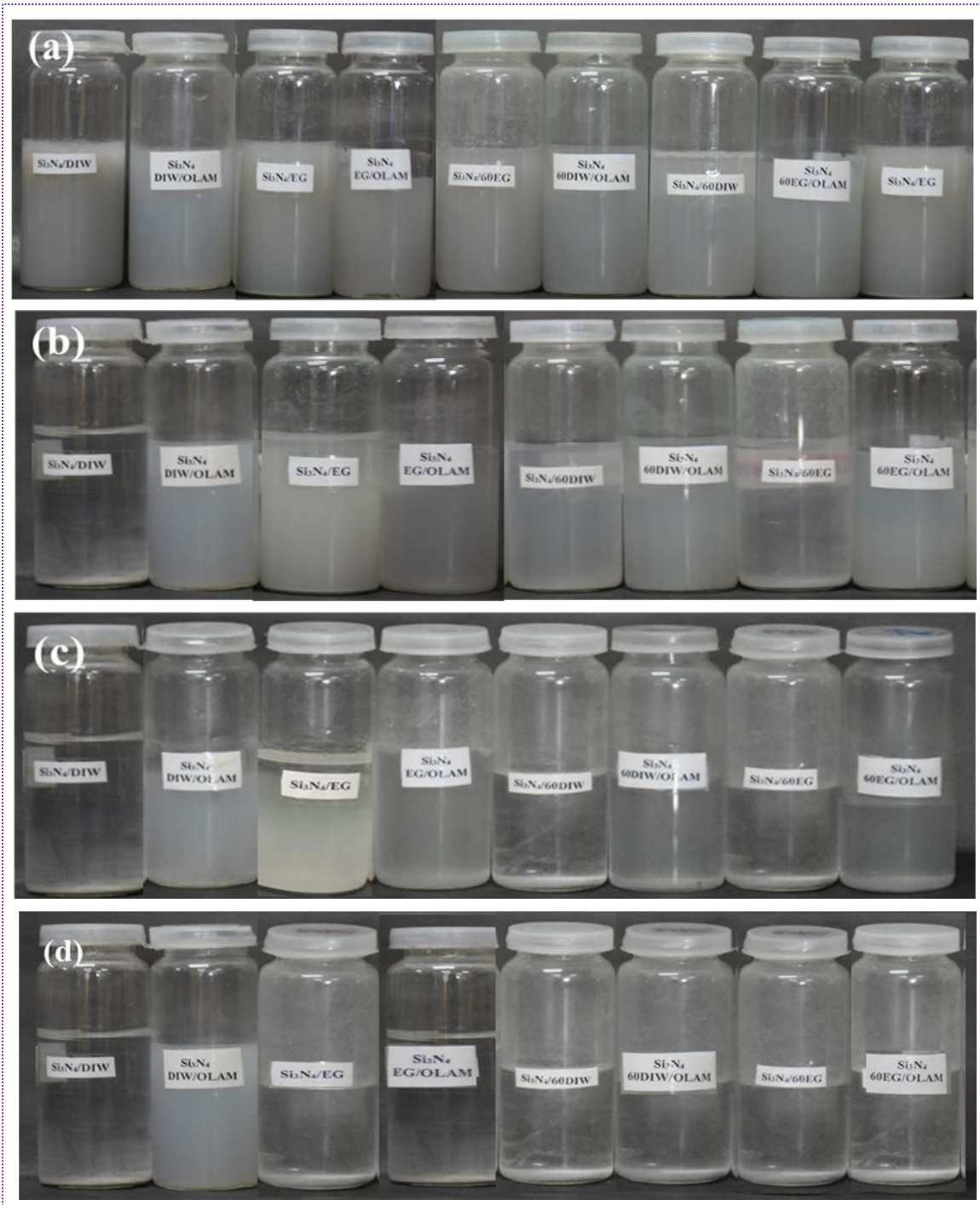


Fig. 4.3. Visual analysis of prepared nanofluids on (a) day 1, (b) day 20, (c) day 40, and month 5.

#### 4.4. Stability Analysis using UV-VIS Spectroscopy

UV-VIS spectrum, ranging in wavelength from 300 nm-800 nm was used to evaluate the nanofluid stability. Various experiments are conducted utilizing  $\text{Si}_3\text{N}_4$  nanoparticles with

different base fluids to investigate the impact of UV absorbance. The results show that higher absorbance correlates with more nanoparticle distribution within the nanofluid, indicating improved stability. However,  $\text{Si}_3\text{N}_4/60$  EG/OLAM nanofluid exhibits the highest absorbance peak on the first day followed by  $\text{Si}_3\text{N}_4/60$  DIW/OLAM,  $\text{Si}_3\text{N}_4/\text{EG}/\text{OLAM}$ ,  $\text{Si}_3\text{N}_4/\text{DIW}/\text{OLAM}$ ,  $\text{Si}_3\text{N}_4/\text{EG}$ ,  $\text{Si}_3\text{N}_4/60$  DIW,  $\text{Si}_3\text{N}_4/\text{DIW}$ , and  $\text{Si}_3\text{N}_4/60$  EG nanofluids. It was observed that adding of surfactant (OLAM) enhanced the absorptivity of nanofluids, contributing to stability. However, over time, the nanofluids observe a slight decrease in absorptivity. Even after 20 and 40 days, UV- VIS spectroscopy was performed again on all samples presented in Fig. 4.4. Even after 20 days,  $\text{Si}_3\text{N}_4/\text{DIW}/\text{OLAM}$  nanofluid demonstrates the same absorption peak, and other  $\text{Si}_3\text{N}_4/60$  EG/OLAM,  $\text{Si}_3\text{N}_4/60$  DIW/OLAM,  $\text{Si}_3\text{N}_4/\text{EG}/\text{OLAM}$  nanofluids show a slight drop of absorption where  $\text{Si}_3\text{N}_4/60$  DIW nanofluid shows maximum drop of absorption because of sedimentation and  $\text{Si}_3\text{N}_4/\text{DIW}$ ,  $\text{Si}_3\text{N}_4/60$  EG shows zero absorption peak because of complete sedimentation. After 40 days, UV-VIS was conducted again on stable samples, where  $\text{Si}_3\text{N}_4/\text{DIW}/\text{OLAM}$  showed the highest absorption peak, followed by  $\text{Si}_3\text{N}_4/60$  EG/OLAM,  $\text{Si}_3\text{N}_4/\text{EG}/\text{OLAM}$ ,  $\text{Si}_3\text{N}_4/60$  DIW/OLAM, and  $\text{Si}_3\text{N}_4/60$  DIW shows zero absorption because of complete sedimentation. Consequently, it was confirmed that  $\text{Si}_3\text{N}_4/\text{DIW}/\text{OLAM}$ ,  $\text{Si}_3\text{N}_4/60$  EG/OLAM,  $\text{Si}_3\text{N}_4/60$  DIW/OLAM,  $\text{Si}_3\text{N}_4/\text{EG}/\text{OLAM}$  and  $\text{Si}_3\text{N}_4/\text{EG}$  nanofluids are more stable than others. K Palanisamy et al. [162] used the prepared nanofluids characterized by UV–VIS Spectrophotometer. They found that over time, the nanofluids showed a significant reduction in light absorption strength.

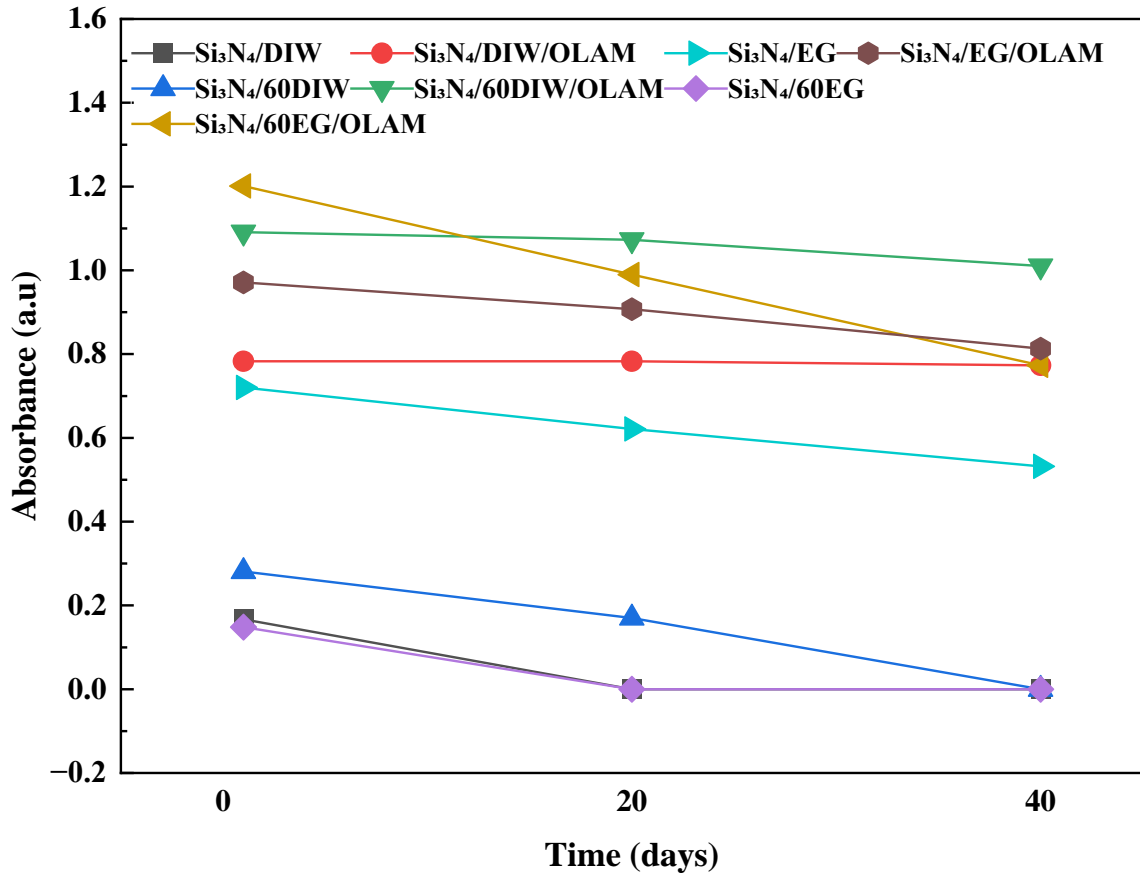


Fig. 4.4. UV-visible spectra of prepared nanofluids over various time intervals.

#### 4.5. Stability Analysis using Zeta Potential

Zeta potential measures the effective electric charge on the surface of the suspended nanoparticles in the base fluid [163]. A positive zeta potential indicates that particles will deposit on the cathode (the negative electrode), whereas a negative zeta potential, indicating the particles are expected to migrate toward the anode (the positive electrode) [164]. Generally, zeta potentials greater than  $\pm 30$  mV are considered good stability, meaning the nanoparticles will likely remain suspended for longer periods without significant aggregation [165].

The zeta potential of various nanofluids at day 1, day 20, and day 40 is shown in Fig. 4.5. On day 1, Si<sub>3</sub>N<sub>4</sub>/DIW/OLAM had the highest zeta potential value, indicating superior stability to all other samples. Si<sub>3</sub>N<sub>4</sub>/EG/OLAM, Si<sub>3</sub>N<sub>4</sub>/60 EG/OLAM, Si<sub>3</sub>N<sub>4</sub>/EG, and Si<sub>3</sub>N<sub>4</sub>/60 DIW showed moderate stability. However, Si<sub>3</sub>N<sub>4</sub>/60 DIW, Si<sub>3</sub>N<sub>4</sub>/60 EG, and Si<sub>3</sub>N<sub>4</sub>/DIW had the lowest zeta potential value, indicating the lowest stability.

After 20 days, the zeta potential value was assessed for stability.  $\text{Si}_3\text{N}_4/\text{DIW}/\text{OLAM}$  and  $\text{Si}_3\text{N}_4/60 \text{ EG}/\text{OLAM}$ , maintained their stability, with only slight decrement in zeta potential values.  $\text{Si}_3\text{N}_4/\text{EG}/\text{OLAM}$ ,  $\text{Si}_3\text{N}_4/\text{EG}$ , and  $\text{Si}_3\text{N}_4/60 \text{ DIW}$  exhibited the highest decrease in zeta potential.  $\text{Si}_3\text{N}_4/60 \text{ DIW}$ ,  $\text{Si}_3\text{N}_4/60 \text{ EG}$ , and  $\text{Si}_3\text{N}_4/\text{DIW}$  showed the lowest zeta potential value, indicating instability and suggesting them unsuitable for heat transfer applications.

After 40 days  $\text{Si}_3\text{N}_4/\text{DIW}/\text{OLAM}$  shows the highest zeta potential value and  $\text{Si}_3\text{N}_4/60 \text{ EG}/\text{OLAM}$ , whereas,  $\text{Si}_3\text{N}_4/\text{EG}/\text{OLAM}$ ,  $\text{Si}_3\text{N}_4/\text{EG}$ , and  $\text{Si}_3\text{N}_4/60 \text{ DIW}$  show a significant decrease of zeta potential value.  $\text{Si}_3\text{N}_4/60 \text{ DIW}$ ,  $\text{Si}_3\text{N}_4/60 \text{ EG}$ , and  $\text{Si}_3\text{N}_4/\text{DIW}$  show complete sedimentation.

The stability trend after 40 days was as follows:  $\text{Si}_3\text{N}_4/\text{DIW}/\text{OLAM} > \text{Si}_3\text{N}_4/60 \text{ EG}/\text{OLAM} > \text{Si}_3\text{N}_4/\text{EG}/\text{OLAM} > \text{Si}_3\text{N}_4/\text{EG} > \text{Si}_3\text{N}_4/60 \text{ DIW} > \text{Si}_3\text{N}_4/60 \text{ DIW} > \text{Si}_3\text{N}_4/60 \text{ EG} > \text{Si}_3\text{N}_4/\text{DIW}$ . Cauca et al. [166] evaluated the effect of surfactants on the zeta potential. The findings show nanofluid stability by electrostatic repulsion between  $\text{Si}_3\text{N}_4$  nanoparticles and show that OLAM surfactants provide optimal dispersion conditions based on their zeta potential values, ensuring excellent stability. High zeta potential values indicated that the nanofluids are well-stabilized, with  $\text{Si}_3\text{N}_4$  nanoparticles effectively repelling each other sufficient to overcome the natural tendency of particles to aggregate due to van der Waals attractive forces, thus remaining evenly dispersed.

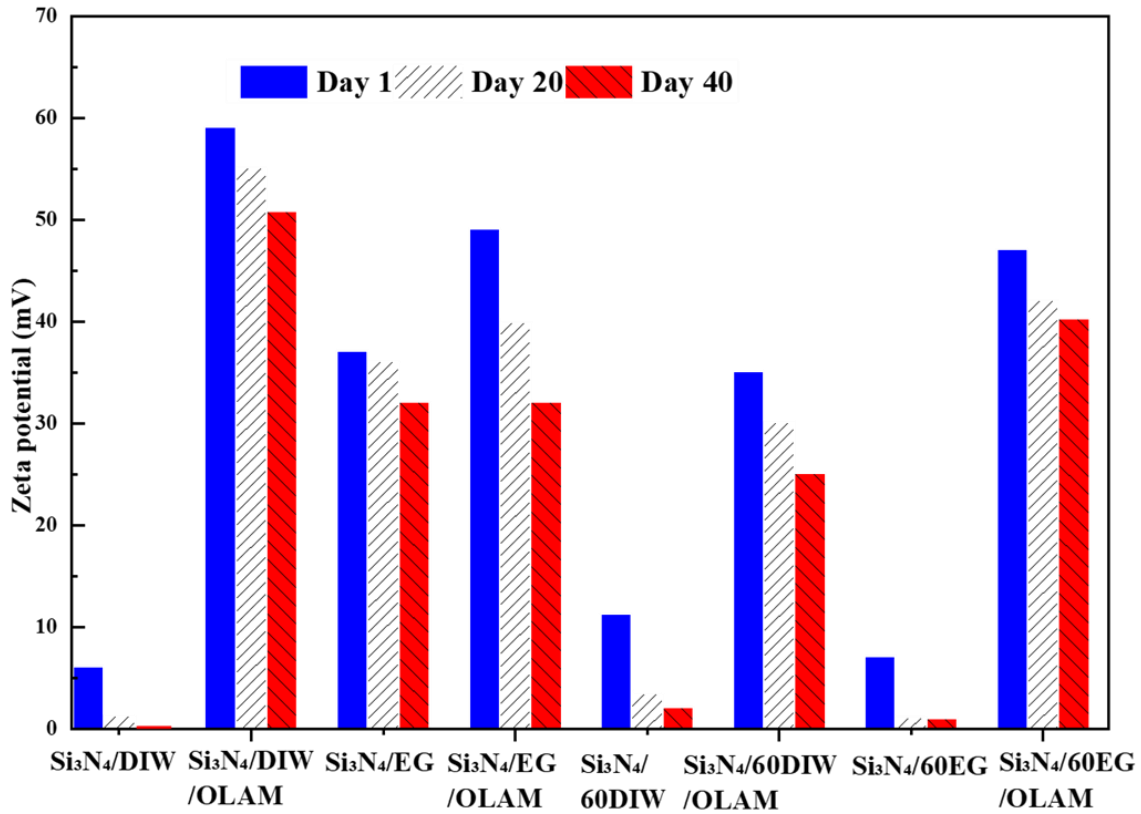


Fig. 4.5. Zeta potential graph of prepared nanofluids.

#### 4.6. Thermal Conductivity

The thermal conductivity results of Si<sub>3</sub>N<sub>4</sub>/nanofluids across a temperature range of 30°C to 80°C had been examined. The thermal conductivity (TC) of DIW-based nanofluids increases with the adding of Si<sub>3</sub>N<sub>4</sub> nanoparticles, achieving a 2.5% enhancement at 80°C. When the OLAM surfactant was added to the Si<sub>3</sub>N<sub>4</sub> nanofluids, thermal conductivity improved significantly at 80°C, showing 14% and 11.07% increases compared to DIW and Si<sub>3</sub>N<sub>4</sub>/DIW, respectively. This improvement was due to the greater stability of Si<sub>3</sub>N<sub>4</sub>/DIW/OLAM nanofluids which maintains particle suspension and enhances both convection and heat transfer. In contrast, Si<sub>3</sub>N<sub>4</sub>/DIW nanofluids exhibit low stability and cluster formation, as shown in Fig. 4.6 (a). This clustering reduces Brownian motion, negatively affecting convection and decreasing thermal conductivity. Almitani et al. [167] investigated the effect of different surfactants (CTAB, SLS, and PS20) on the thermal conductivity of aqueous silica nanofluid. The findings indicate that the TC increases with increasing temperature and volume

concentration of nanoparticles. The optimum surfactant ratio significantly impacts the TC of nanofluids.

In Fig. 4.6. (b), the thermal conductivity of EG increased by 4.69% with the addition of  $\text{Si}_3\text{N}_4$  nanoparticles. However, it decreased by 1.44% when the surfactant OLAM was added compared to pure EG. When the surfactant was introduced to the  $\text{Si}_3\text{N}_4/\text{EG}$  nanofluid, a significant increase in viscosity was observed compared to any other nanofluid under study. This increase in viscosity was attributed to the strong interaction between the surfactant and nanoparticles, which reduces the Brownian motion. Consequently, this reduction in Brownian motion limits convection, thereby decreasing the thermal conductivity.

Subsequently, the TC of  $\text{Si}_3\text{N}_4$  nanoparticles with different DIW and EG ratios is evaluated. In Fig. 4.6. (c), adding  $\text{Si}_3\text{N}_4$  nanoparticles to 60 DIW decreases TC by 5.6%, and adding surfactant OLAM results in a further decrease of 9.4% than the base fluid 60 DIW. The  $\text{Si}_3\text{N}_4/60$  DIW nanofluid was visually unstable due to sedimentation, which reduces TC. The addition of OLAM surfactant in  $\text{Si}_3\text{N}_4/60$  DIW can change the heat transfer mechanisms within the fluid because OLAM molecules can hinder the movement of fluid molecules, thus decreasing the convective heat transfer component.

In Fig. 4.6. (d), adding  $\text{Si}_3\text{N}_4$  nanoparticles to 60 EG increases TC by 8.1% at 80°C, and adding surfactant OLAM results in a further increase of 9.4% compared to 60 DIW and by 1.21% compared to  $\text{Si}_3\text{N}_4/60$  EG. The  $\text{Si}_3\text{N}_4/60$  EG enhanced the heat transfer properties of the fluid through Brownian motion, facilitating better energy transport. The addition of surfactant increases the nanoparticle's surface area and provides a greater interface for heat transfer between the fluid and the particles.

Finally, it is concluded that nanofluid containing  $\text{Si}_3\text{N}_4$  nanoparticles at a volume concentration of 0.06% has exhibited a maximum enhancement of thermal conductivity of 14% by using OLAM compared to DIW due to the highest stability. Furthermore, the enhancement is observed at 9.4% compared to a mixture of 60% EG and 40% DIW by using an OLAM surfactant. Additionally, it shows an 8.1 % increase relative to 60 EG and 4.7% compared to pure EG without surfactant.

The overall trend of TC is  $\text{Si}_3\text{N}_4/\text{DIW}/\text{OLAM} > \text{Si}_3\text{N}_4/60 \text{ EG}/\text{OLAM} > \text{Si}_3\text{N}_4/60 \text{ EG} > \text{Si}_3\text{N}_4/\text{EG} > \text{Si}_3\text{N}_4/\text{DIW}$

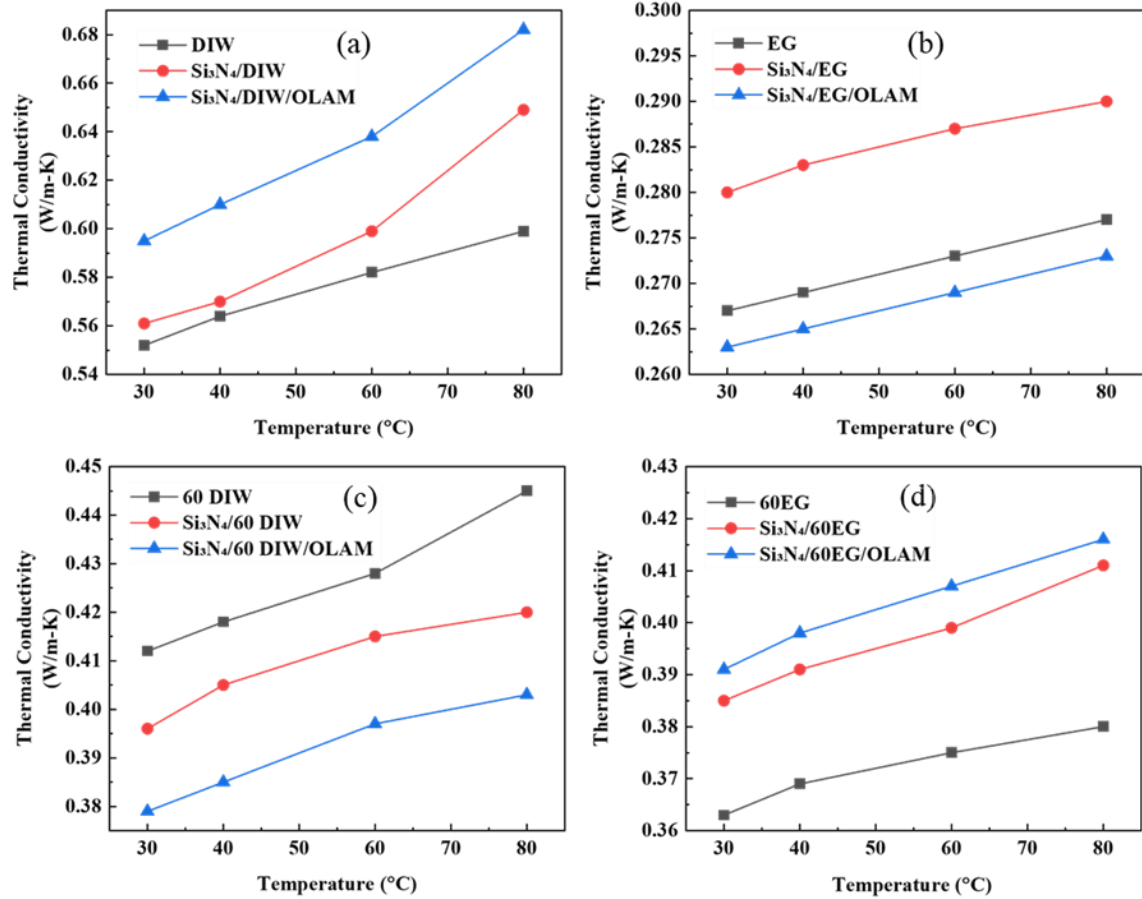


Fig. 4.6. Thermal conductivity of nanofluid with the influence of temperature (a) Si<sub>3</sub>N<sub>4</sub>/DIW, (b) Si<sub>3</sub>N<sub>4</sub>/60DIW, (c) Si<sub>3</sub>N<sub>4</sub>/60EG, and (d) Si<sub>3</sub>N<sub>4</sub>/EG.

#### 4.7. Rheological Behavior of Nanofluids

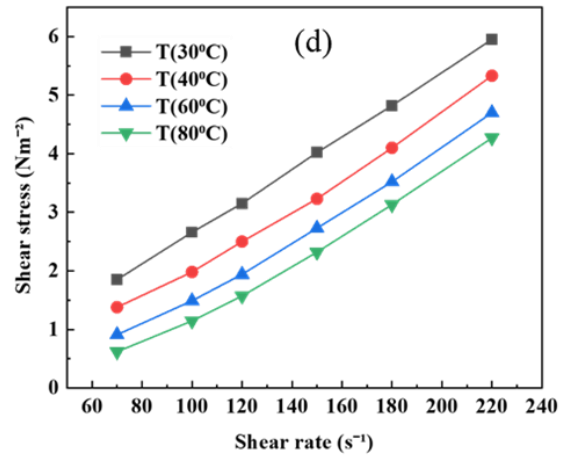
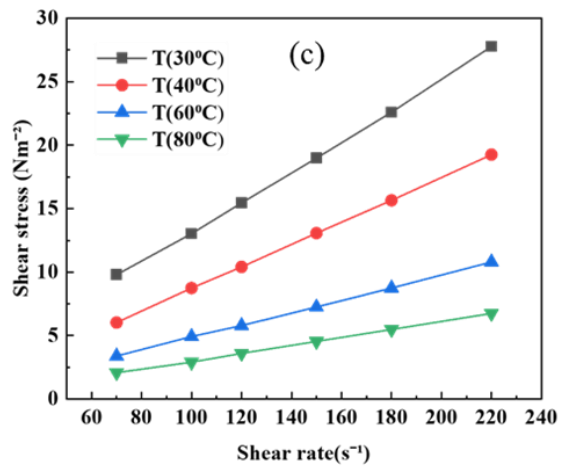
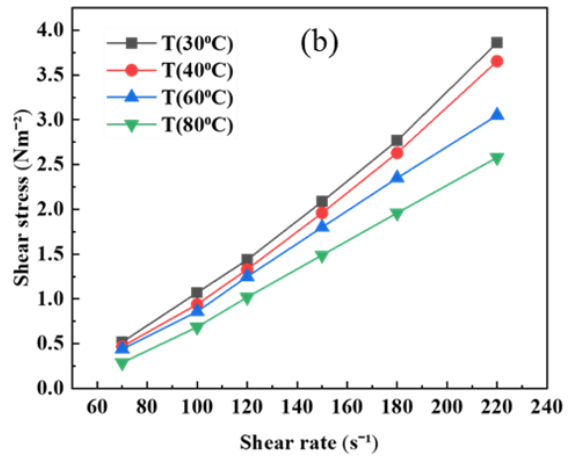
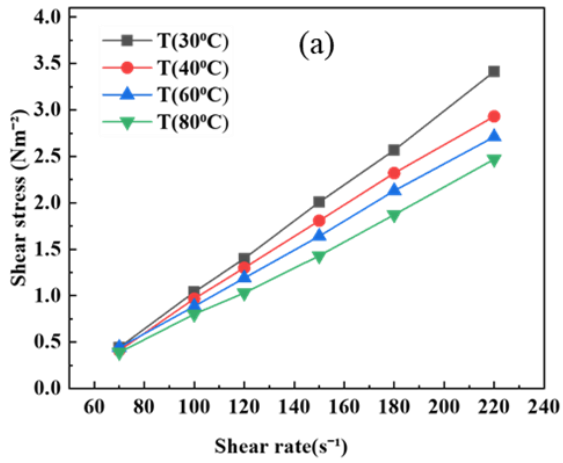
Rheological behavior describes the relationship between shear stress ( $\tau$ ) and shear rate ( $\dot{\gamma}$ ), with viscosity ( $\eta$ ) representing the fluid's resistance to flow. Newtonian fluids show linear behavior while non-Newtonian fluids exhibit non-linear behavior between shear stress and shear rate [168].

The rheological properties of 0.06 vol. % Si<sub>3</sub>N<sub>4</sub> nanofluids are observed at the 30°C to 80°C temperature range. The shear stress trend at various shear rates (70 s<sup>-1</sup>, 100 s<sup>-1</sup>, 120 s<sup>-1</sup>, 150 s<sup>-1</sup>, 180 s<sup>-1</sup>, and 220 s<sup>-1</sup>). In Fig.8, the plotted graph shows the result of shear stress against the shear rate and for a clear understanding, the data for each temperature is plotted across all shear rates. The data in Fig.8 (a-d), indicates a linear relationship between shear rate and shear stress, showing Newtonian behavior. These findings highlighted the consistent Newtonian



behavior across temperature ranges. This characteristic was essential for applications where the fluid was subjected to varying shear conditions, but a steady viscosity is required for reliable performance. Similar observations had been reported by Ghasemi and Karimipour [135], for increasing shear rate ( $13 \text{ s}^{-1}$ ,  $27 \text{ s}^{-1}$ ,  $39 \text{ s}^{-1}$ ,  $66 \text{ s}^{-1}$ ,  $93 \text{ s}^{-1}$ , and  $132 \text{ s}^{-1}$  using CuO nanoparticles in liquid paraffin, demonstrating Newtonian behavior and viscosity reduction with increasing temperature.

Fig. 4.7. (b) shows that adding OLAM to  $\text{Si}_3\text{N}_4/\text{EG}$  nanofluid changes its flow behavior from Newtonian to dilatant. The alteration arises from modification in internal structure and interactions among EG molecules. Specifically, changes in the internal structure involve variations in hydrogen bonding networks or the relative orientation of hydroxyl groups, affecting flow behavior. W. Tseng and S. Li [169] observed a similar change from Newtonian to dilatant behavior in  $\text{BaTiO}_3/\text{distilled water}$  nanofluid when  $\text{NH}_4\text{PA}$  was used as a surfactant.



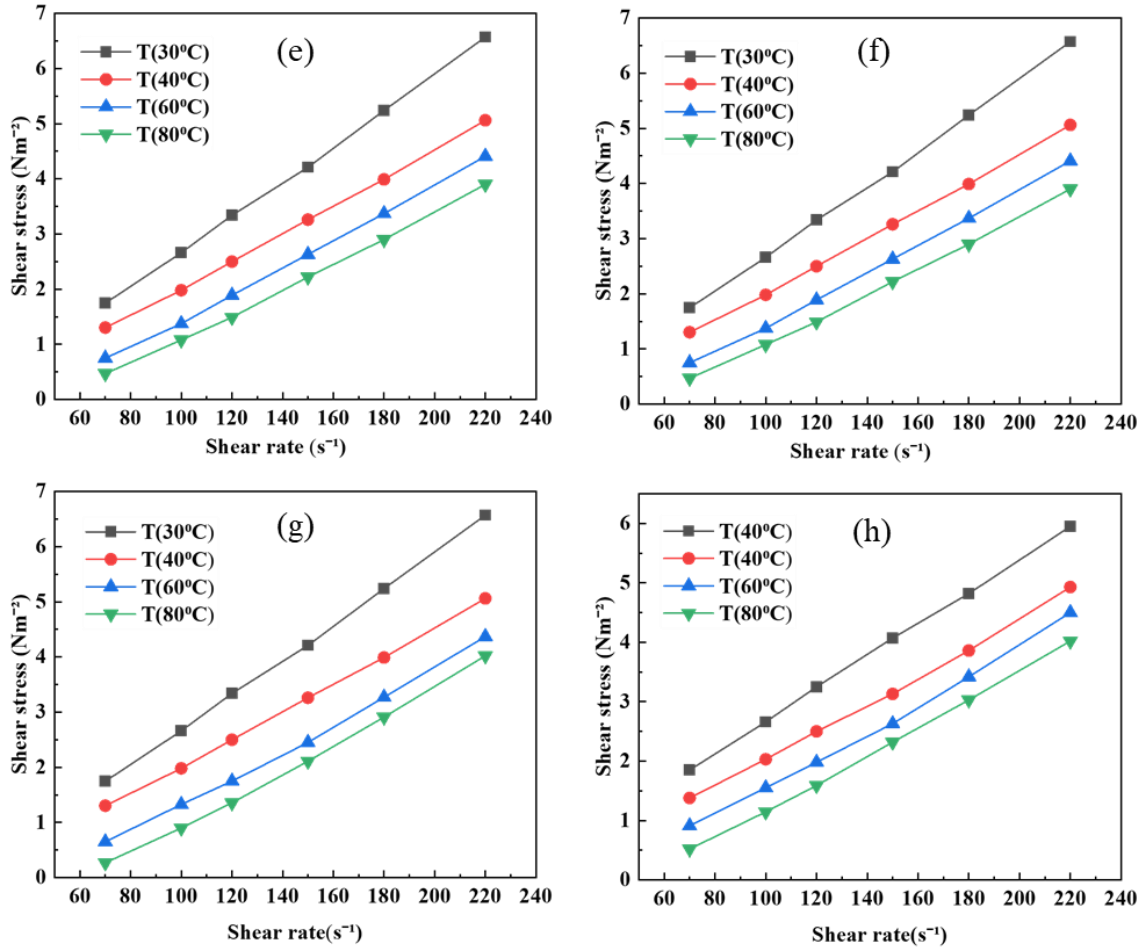


Fig. 4.7. Rheological behavior of nanofluid at different temperatures (a) Si<sub>3</sub>N<sub>4</sub>/DIW, (b) Si<sub>3</sub>N<sub>4</sub>/DIW/OLAM, (c) Si<sub>3</sub>N<sub>4</sub>/EG, (d) Si<sub>3</sub>N<sub>4</sub>/EG/OLAM, (e) Si<sub>3</sub>N<sub>4</sub>/60DIW, (f) Si<sub>3</sub>N<sub>4</sub>/60DIW/OLAM, (g) Si<sub>3</sub>N<sub>4</sub>/60EG, and (h) Si<sub>3</sub>N<sub>4</sub>/60EG/OLAM.

#### 4.8. Viscosity

As mentioned before, the viscosity of nanofluid is another property that needs to be studied because of its significant effect on heat transfer and pressure drops. Similar, to conventional fluids, temperature was the main effective parameter on the viscosity of nanofluids. Fig. 4.8, illustrates the relationship between viscosity and temperature

The viscosity of nanofluids by dispersing Si<sub>3</sub>N<sub>4</sub> with and without surfactant at 0.06 vol.% is measured over a temperature range of 30°C to 80°C at various shear rates (70 s<sup>-1</sup>, 100 s<sup>-1</sup>, 120 s<sup>-1</sup>, 150 s<sup>-1</sup>, 180 s<sup>-1</sup> and 220 s<sup>-1</sup>). According to the findings, the viscosity of the nanofluid-containing surfactant was higher than that of the mono nanofluid without surfactant. However, the viscosity results showed that each of the eight prepared nanofluids viscosity decreased with

the increasing temperature across all shear rates due to the reduction in intermolecular and adhesion forces between nanoparticles. Similar behavior was observed by P.S Kishore et al. [170] viscosity decreased when the temperature increased.

From Fig. 4.8. (a-d) the viscosity trend is described as follows:  $\text{Si}_3\text{N}_4/\text{EG}/\text{OLAM} > \text{Si}_3\text{N}_4/\text{EG} > \text{Si}_3\text{N}_4/60 \text{ EG} > \text{Si}_3\text{N}_4/60 \text{ EG}/\text{OLAM} > \text{Si}_3\text{N}_4/60 \text{ DIW}/\text{OLAM} > \text{Si}_3\text{N}_4/60 \text{ DIW} > \text{Si}_3\text{N}_4/\text{DIW}/\text{OLAM} > \text{Si}_3\text{N}_4/\text{DIW}$ . This was mainly due to the higher viscosity of EG when compared to water. Additionally, the impact of OLAM varies in viscosity depending on the type of base fluid used [171]. This study showed that the addition of OLAM surfactant increases the viscosity of nanofluids at all shear rates. This was because OLAM surfactant improves the interaction between nanoparticles and the base fluid, leading to greater resistance to flow and increased viscosity. The reduced viscosity behavior at all shear rates is only observed in the case of a base fluid 60:40 EG-DIW ratio. When added to a 60 EG, OLAM molecules align at the boundary between the 60 EG and  $\text{Si}_3\text{N}_4$  nanoparticles. This alignment reduced the attractive forces between the 60 EG molecules on the surface, consequently reducing surface tension. This decrease in surface tension led to resistance to flow, resulting in lower viscosity. Whereas, all other nanofluids exhibited increased viscosity upon the addition of surfactant OLAM.

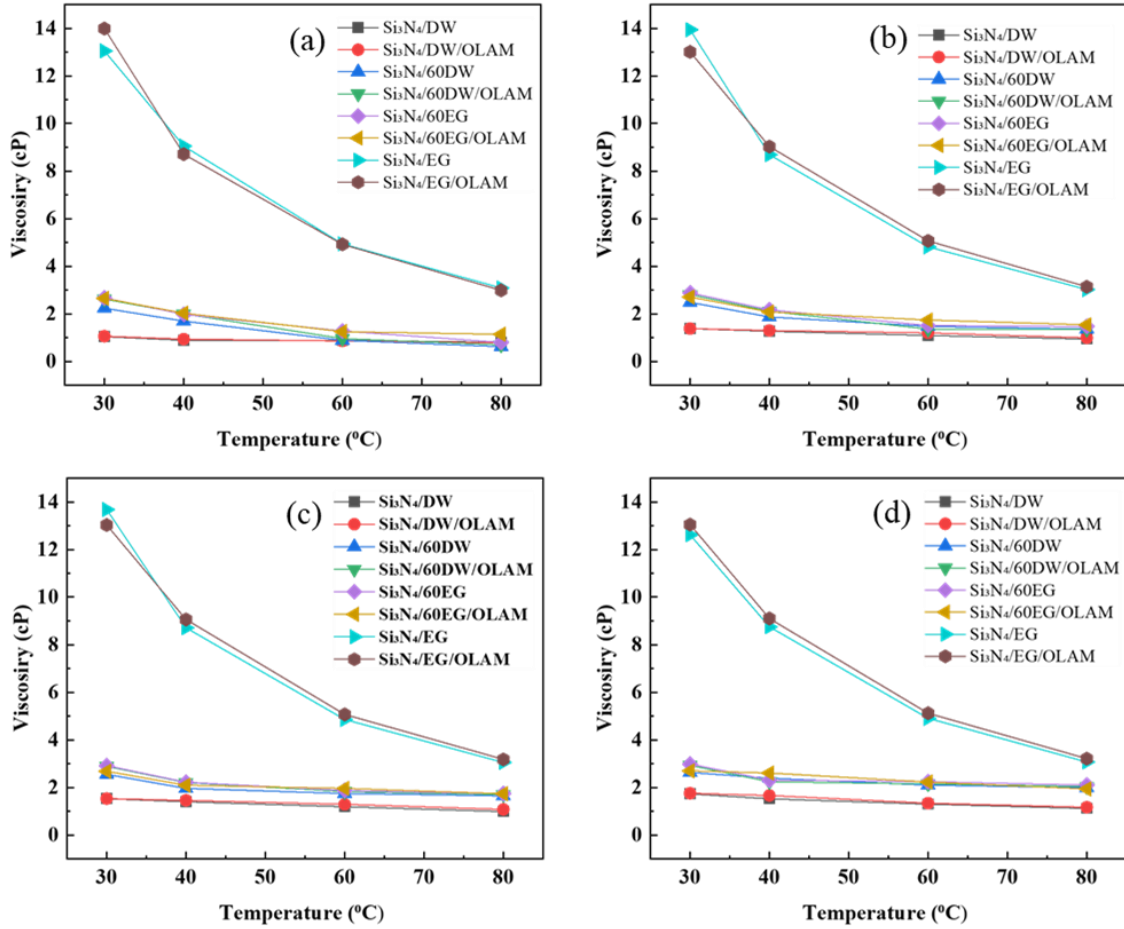


Fig. 4.8. Viscosity of nanofluid at shear rate (a)  $100\text{s}^{-1}$ , (b)  $150\text{s}^{-1}$ , (c)  $180\text{s}^{-1}$  and (d)  $220\text{s}^{-1}$ .

## Relative Analysis

In this study, we have examined various base fluids, their different ratios, and surfactant's impact on the stability and thermophysical properties of  $\text{Si}_3\text{N}_4$  nanofluids. Table 2 provides a comparative analysis with previous literature, focusing on nanomaterials impact on thermophysical properties and stability.

Table 4.1. A summary of previous literature on nanofluid.

<b>Nanoparticles</b>	<b>Base fluid</b>	<b>Concentrations</b>	<b>Surfactant</b>	<b>Stability</b>	<b>Thermal conductivity</b>	<b>Viscosity &amp; Rheology</b>	<b>Ref.</b>
<b>Si<sub>3</sub>N<sub>4</sub></b>	EG	0.01-0.1 vol%	-	-	0.2665 Wm <sup>-1</sup> K <sup>-1</sup>	Non-Newtonian at higher concentration	[152]
<b>Si<sub>3</sub>N<sub>4</sub></b>	EG	0.06vol%	-	-	0.29 Wm <sup>-1</sup> K <sup>-1</sup>	Newtonian	This study
<b>AlN</b>	EG	0.05-0.20 vol%	-	-	0.2969 Wm <sup>-1</sup> K <sup>-1</sup>	Non-Newtonian at higher concentration	[139]
<b>AlN-C</b>	EG	0.027-0.22 vol%	-	3 months	Increasing linearly with vol. %	Non-Newtonian at higher concentration	[140]
<b>TiN</b>	EG	0.01-0.05 mass%	-	-	0.2585 Wm <sup>-1</sup> K <sup>-1</sup>	Newtonian	[141]
<b>BN</b>	Water	0.01-0.03 vol%	Triton X-100	25 days	0.635 Wm <sup>-1</sup> K <sup>-1</sup>	Newtonian	[142]
<b>BN</b>	EG	0.05-0.2 vol%	-	-	0.6453 Wm <sup>-1</sup> K <sup>-1</sup>	-	[143]
<b>BNNTs</b>	Biphenyl: Diphenyl oxide	0.35vol%	Triton X-100	month	0.19 Wm <sup>-1</sup> K <sup>-1</sup>	Decreases with temperature & Newtonian	[144]

<b>hBN</b>	Polyalpha-Olefin oil	0.25–1 vol%	-	-	0.169 Wm <sup>-1</sup> K <sup>-1</sup>	Decreases with temperature	[153]
<b>SiC</b>	EG, DW	0.5-5vol%	-	SiC/DW more stable till 2 weeks	0.32 Wm <sup>-1</sup> K <sup>-1</sup> (SiC/EG)	-	[146]
<b>SiO<sub>2</sub></b>	EG: water	0.3 mass%	-	-	0.64 Wm <sup>-1</sup> K <sup>-1</sup>	-	[147]
<b>Si<sub>3</sub>N<sub>4</sub></b>	DIW, EG	0.06vol%	OLAM	-	0.682 and 0.29 Wm <sup>-1</sup> K <sup>-1</sup>	Newtonian	This study
<b>SiO<sub>2</sub></b>	EG	0.1-0.05 vol%	-	-	0.2526 Wm <sup>-1</sup> K <sup>-1</sup>	Newtonian	[148]

## Summary

The XRD patterns of nanoparticles were analyzed and validated against existing literature. We investigated the stability, rheology, and thermophysical properties of various nanofluids. Among these, Si<sub>3</sub>N<sub>4</sub>/DIW with OLAM demonstrated exceptional stability for over 5 months, with a zeta potential of 59.18 mV. OLAM also enhanced the viscosity and thermal conductivity of all samples at 80°C. All samples displayed Newtonian behavior, characterized by a linear relationship between shear rate and stress. However, OLAM modified the flow behavior of Si<sub>3</sub>N<sub>4</sub>/EG, causing it to become dilatant. The addition of surfactants generally led to an increase in viscosity, though viscosity decreased with rising temperature. In contrast, thermal conductivity increased with temperature.



## CHAPTER 5: CONCLUSIONS AND RECOMMENDATION

### 5.1. Conclusions

The study employed a two-step method to prepare  $\text{Si}_3\text{N}_4$  nanofluids with different base fluids: DIW, EG, 60 DIW, and 60 EG at a concentration of 0.06 vol.%. Different surfactants, including OLAM, Tween-80, and SDBS, were incorporated into the base fluids to enhance stability. The stability of the nanofluids was determined using visual sedimentation, zeta potential analysis, and UV–VIS spectroscopy. Additionally, the thermophysical properties of the nanofluids were measured across a temperature range from 30°C to 80°C, while viscosity and rheological characteristics were assessed at shear rates ranging from 70  $\text{s}^{-1}$  to 220  $\text{s}^{-1}$ . Results can be listed as follows:

- $\text{Si}_3\text{N}_4$ /DIW with OLAM shows excellent visual stability for over 5 months, as OLAM prevents particle aggregation and sedimentation.  $\text{Si}_3\text{N}_4$ /60 EG with OLAM remains visually stable for around 40 days, indicating that the combination of 60 EG and OLAM provides less stability than DIW.  $\text{Si}_3\text{N}_4$ /EG without surfactant stays stable for about 20 days after which a transparent layer appears, indicating the start of particle settling or aggregation.
- Zeta potential values remain consistent and correlated with UV-VIS absorptions.  $\text{Si}_3\text{N}_4$ /DIW nanofluids exhibit a zeta potential of 59.18 mV after adding OLAM, while  $\text{Si}_3\text{N}_4$  /60 EG shows 47.15 mV. Conversely,  $\text{Si}_3\text{N}_4$ /EG without surfactant has 35.5 mV.
- The thermal conductivity is enhanced as the temperature increases. The  $\text{Si}_3\text{N}_4$ /DIW/OLAM nanofluid shows a maximum enhancement of 14% at a concentration of 0.06 vol. % and a temperature of 80°C. Additionally, the enhancement in thermal conductivity is observed to be 9.4% for  $\text{Si}_3\text{N}_4$ /60 EG/OLAM and 4.7% for  $\text{Si}_3\text{N}_4$ /EG nanofluids.

- All samples exhibit Newtonian behavior, with a linear relation between shear stress and shear rate. However, adding OLAM to the Si<sub>3</sub>N<sub>4</sub>/EG nanofluid changed its flow behavior from Newtonian to dilatant.
- The addition of OLAM increased the viscosity of all nanofluids. However, the viscosity decreases only in the case of the Si<sub>3</sub>N<sub>4</sub>/60EG/OLAM nanofluid. This is because the base fluid aligns OLAM molecules at the interface with Si<sub>3</sub>N<sub>4</sub> nanoparticles, which reduces surface tension and viscosity. Additionally, as the temperature increases, the viscosity decreases further.

In this study, the stability of Si<sub>3</sub>N<sub>4</sub>/DIW nanofluid is enhanced by adding surfactant for long-term applications. It is evident from the results that OLAM is one of the most promising surfactant for Si<sub>3</sub>N<sub>4</sub> due to its excellent stability, moderate viscosity, and thermal conductivity. It enhances TC by 14 % at 80°C and increases viscosity at 30°C. However, its stability is more than 5 months making it appropriate for prolonged heat transfer applications.

## **5.2. Future Recommendation**

This study examines various base fluids such as DIW, EG, and ratios of DIW-EG (60:40 and 40:60) to determine the most effective surfactant for Si<sub>3</sub>N<sub>4</sub> mono nanofluid. However, preparing hybrid nanofluids with Si<sub>3</sub>N<sub>4</sub> nanoparticles remains a challenging task for further research.

## REFERENCES

- [1] M. Gupta, V. Singh, R. Kumar, and Z. Said, “A review on thermophysical properties of nanofluids and heat transfer applications,” *Renew. Sustain. Energy Rev.*, vol. 74, pp. 638–670, 2017, doi: <https://doi.org/10.1016/j.rser.2017.02.073>.
- [2] S. Qazi, *Solar Thermal Electricity and Solar Insolation*. 2017. doi: 10.1016/b978-0-12-803022-6.00007-1.
- [3] N. E. Helwig, S. Hong, and E. T. Hsiao-wecksler, *No 主観的健康感を中心とした在宅高齢者における健康関連指標に関する共分散構造分析* Title.
- [4] S. K R, A. S. Nair, V. K M, S. T R, and S. C. Nair, “an Overview of Recent Nanofluid Research,” *Int. Res. J. Pharm.*, vol. 5, no. 4, pp. 239–243, 2014, doi: 10.7897/2230-8407.050451.
- [5] S. K. Das, S. U. S. Choi, and H. E. Patel, “Heat transfer in nanofluids - A review,” *Heat Transf. Eng.*, vol. 27, no. 10, pp. 3–19, 2006, doi: 10.1080/01457630600904593.
- [6] S. U. S. Choi, 1, and J. A. Eastman, “Jam 1 1 19s5,” p. 6, 1995, [Online]. Available: [https://www.researchgate.net/profile/Jeffrey\\_Eastman/publication/236353373\\_Enhancing\\_thermal\\_conductivity\\_of\\_fluids\\_with\\_nanoparticles/links/0f3175336e78aa9c4c000000/Enhancing-thermal-conductivity-of-fluids-with-nanoparticles.pdf](https://www.researchgate.net/profile/Jeffrey_Eastman/publication/236353373_Enhancing_thermal_conductivity_of_fluids_with_nanoparticles/links/0f3175336e78aa9c4c000000/Enhancing-thermal-conductivity-of-fluids-with-nanoparticles.pdf)

- [7] M. U. Sajid and H. M. Ali, "Thermal conductivity of hybrid nanofluids: A critical review," *Int. J. Heat Mass Transf.*, vol. 126, pp. 211–234, 2018, doi: <https://doi.org/10.1016/j.ijheatmasstransfer.2018.05.021>.
- [8] D. K. Devendiran and V. A. Amirtham, "A review on preparation, characterization, properties and applications of nanofluids," *Renew. Sustain. Energy Rev.*, vol. 60, pp. 21–40, 2016, doi: <https://doi.org/10.1016/j.rser.2016.01.055>.
- [9] A. Ghafouri and D. Toghraie, "Experimental study on thermal conductivity of SiC-ZnO/ ethylene glycol hybrid nanofluid: Proposing an optimized multivariate correlation," *J. Taiwan Inst. Chem. Eng.*, vol. 148, p. 104824, 2023, doi: <https://doi.org/10.1016/j.jtice.2023.104824>.
- [10] A. Gaikwad, A. Sathe, and S. Sanap, "A design approach for thermal enhancement in heat sinks using different types of fins: A review," *Front. Therm. Eng.*, vol. 2, no. January, pp. 1–13, 2023, doi: [10.3389/fther.2022.980985](https://doi.org/10.3389/fther.2022.980985).
- [11] N. Sezer, M. A. Atieh, and M. Koç, "A comprehensive review on synthesis, stability, thermophysical properties, and characterization of nanofluids," *Powder Technol.*, vol. 344, pp. 404–431, 2019, doi: <https://doi.org/10.1016/j.powtec.2018.12.016>.
- [12] Z. Haddad, C. Abid, H. F. Oztop, and A. Mataoui, "A review on how the researchers prepare their nanofluids," *Int. J. Therm. Sci.*, vol. 76, pp. 168–189, 2014, doi: <https://doi.org/10.1016/j.ijthermalsci.2013.08.010>.
- [13] S. Handschuh-Wang, F. J. Stadler, and X. Zhou, "Critical Review on the Physical Properties of Gallium-Based Liquid Metals and Selected Pathways for Their

- Alteration,” *J. Phys. Chem. C*, vol. 125, no. 37, pp. 20113–20142, 2021, doi: 10.1021/acs.jpcc.1c05859.
- [14] Q. Wang, Y. Yu, and J. Liu, “Preparations, Characteristics and Applications of the Functional Liquid Metal Materials,” *Adv. Eng. Mater.*, vol. 20, no. 5, pp. 1–21, 2018, doi: 10.1002/adem.201700781.
- [15] K. Ma and J. Liu, “Liquid metal cooling in thermal management of computer chips,” *Front. Energy Power Eng. China*, vol. 1, pp. 384–402, Oct. 2007, doi: 10.1007/s11708-007-0057-3.
- [16] S. Lee, S. Choi, S. Li, and J. Eastman, “Measuring Thermal Conductivity of Fluids Containing Oxide Nanoparticles,” *Heat Transf.*, vol. 121, no. May 1999, pp. 280–289, 2013.
- [17] M.-S. Liu, M. Ching-Cheng Lin, I.-T. Huang, and C.-C. Wang, “Enhancement of thermal conductivity with carbon nanotube for nanofluids,” *Int. Commun. Heat Mass Transf.*, vol. 32, no. 9, pp. 1202–1210, 2005, doi: <https://doi.org/10.1016/j.icheatmasstransfer.2005.05.005>.
- [18] A. Das and D. Basak, “Efficacy of Ion Implantation in Zinc Oxide for Optoelectronic Applications: A Review,” *ACS Appl. Electron. Mater.*, vol. 3, no. 9, pp. 3693–3714, 2021, doi: 10.1021/acsaelm.1c00393.
- [19] R. Jalal, E. K. Goharshadi, M. Abareshi, M. Moosavi, A. Yousefi, and P. Nancarrow, “ZnO nanofluids: Green synthesis, characterization, and antibacterial activity,” *Mater. Chem. Phys.*, vol. 121, no. 1, pp. 198–201, 2010, doi:

<https://doi.org/10.1016/j.matchemphys.2010.01.020>.

- [20] S. Choudhary, A. Sachdeva, and P. Kumar, “Influence of stable zinc oxide nanofluid on thermal characteristics of flat plate solar collector,” *Renew. Energy*, vol. 152, pp. 1160–1170, 2020, doi: <https://doi.org/10.1016/j.renene.2020.01.142>.
- [21] E. C. Okonkwo, I. Wole-Osho, I. W. Almanassra, Y. M. Abdullatif, and T. Al-Ansari, *An updated review of nanofluids in various heat transfer devices*, vol. 145, no. 6. Springer International Publishing, 2021. doi: 10.1007/s10973-020-09760-2.
- [22] Z. Said *et al.*, “Recent advances on the fundamental physical phenomena behind stability, dynamic motion, thermophysical properties, heat transport, applications, and challenges of nanofluids,” *Phys. Rep.*, vol. 946, pp. 1–94, 2022, doi: 10.1016/j.physrep.2021.07.002.
- [23] N.-D. Jaji, H. L. Lee, M. H. Hussin, H. M. Akil, M. R. Zakaria, and M. B. H. Othman, “Advanced nickel nanoparticles technology: From synthesis to applications,” vol. 9, no. 1, pp. 1456–1480, 2020, doi: doi:10.1515/ntrev-2020-0109.
- [24] P. K. Khanna, S. Gaikwad, P. V Adhyapak, N. Singh, and R. Marimuthu, “Synthesis and characterization of copper nanoparticles,” *Mater. Lett.*, vol. 61, no. 25, pp. 4711–4714, 2007, doi: <https://doi.org/10.1016/j.matlet.2007.03.014>.
- [25] B. Wang, X. Wang, W. Lou, and J. Hao, “Ionic liquid-based stable nanofluids containing gold nanoparticles,” *J. Colloid Interface Sci.*, vol. 362, no. 1, pp. 5–14, 2011, doi: <https://doi.org/10.1016/j.jcis.2011.06.023>.

- [26] D. Philip, “Biosynthesis of Au, Ag and Au–Ag nanoparticles using edible mushroom extract,” *Spectrochim. Acta Part A Mol. Biomol. Spectrosc.*, vol. 73, no. 2, pp. 374–381, 2009, doi: <https://doi.org/10.1016/j.saa.2009.02.037>.
- [27] “Effects of nanofluids containing graphene\_graphene-oxide nanosheets on critical heat flux \_ Applied Physics Letters \_ AIP Publishing.”
- [28] S. Akbarzadeh, M. Farhadi, K. Sedighi, and M. Ebrahimi, “Experimental investigation on the thermal conductivity and viscosity of ZnO Nanofluid and Development of New Correlations,” *Challenges in Nano and Micro Scale Science and Technology*, vol. 2, no. 2, pp. 149–160, 2014.
- [29] A. Ahmadi Nadooshan, “An experimental correlation approach for predicting thermal conductivity of water-EG based nanofluids of zinc oxide,” *Phys. E Low-Dimensional Syst. Nanostructures*, vol. 87, no. November 2016, pp. 15–19, 2017, doi: [10.1016/j.physe.2016.11.004](https://doi.org/10.1016/j.physe.2016.11.004).
- [30] M. Jebali, G. Colangelo, and A. I. Gómez-Merino, “Green Synthesis, Characterization, and Empirical Thermal Conductivity Assessment of ZnO Nanofluids for High-Efficiency Heat-Transfer Applications,” *Materials (Basel)*, vol. 16, no. 4, 2023, doi: [10.3390/ma16041542](https://doi.org/10.3390/ma16041542).
- [31] M. Sepehrnia, K. Mohammadzadeh, M. M. Veyseh, E. Agah, and M. Amani, “Rheological behavior of engine oil based hybrid nanofluid containing MWCNTs and ZnO nanopowders: Experimental analysis, developing a novel correlation, and neural network modeling,” *Powder Technol.*, vol. 404, p. 117492, 2022, doi:

10.1016/j.powtec.2022.117492.

- [32] X. Wang *et al.*, “Vegetable oil-based nanofluid minimum quantity lubrication turning: Academic review and perspectives,” *J. Manuf. Process.*, vol. 59, pp. 76–97, 2020, doi: <https://doi.org/10.1016/j.jmapro.2020.09.044>.
- [33] N. A. C. Sidik, H. A. Mohammed, O. A. Alawi, and S. Samion, “A review on preparation methods and challenges of nanofluids,” *Int. Commun. Heat Mass Transf.*, vol. 54, pp. 115–125, 2014, doi: <https://doi.org/10.1016/j.icheatmasstransfer.2014.03.002>.
- [34] A. K. Sharma, A. K. Tiwari, and A. R. Dixit, “Effects of Minimum Quantity Lubrication (MQL) in machining processes using conventional and nanofluid based cutting fluids: A comprehensive review,” *J. Clean. Prod.*, vol. 127, pp. 1–18, 2016, doi: <https://doi.org/10.1016/j.jclepro.2016.03.146>.
- [35] W. K. Shafi and M. S. Charoo, “An overall review on the tribological, thermal and rheological properties of nanolubricants,” *Tribology - Materials, Surfaces and Interfaces*, vol. 15, no. 1, pp. 20–54, 2021. doi: 10.1080/17515831.2020.1785233.
- [36] M. U. Sajid and H. M. Ali, “Recent advances in application of nanofluids in heat transfer devices: A critical review,” *Renew. Sustain. Energy Rev.*, vol. 103, pp. 556–592, 2019, doi: <https://doi.org/10.1016/j.rser.2018.12.057>.
- [37] M. S. Bretado-de los Rios, C. I. Rivera-Solorio, and K. D. P. Nigam, “An overview of sustainability of heat exchangers and solar thermal applications with nanofluids: A review,” *Renew. Sustain. Energy Rev.*, vol. 142, p. 110855, 2021, doi:



<https://doi.org/10.1016/j.rser.2021.110855>.

- [38] N. A. Che Sidik, M. N. A. Witri Mohd Yazid, and R. Mamat, “Recent advancement of nanofluids in engine cooling system,” *Renew. Sustain. Energy Rev.*, vol. 75, pp. 137–144, 2017, doi: <https://doi.org/10.1016/j.rser.2016.10.057>.
- [39] M. Rafati, A. A. Hamidi, and M. Shariati Niaser, “Application of nanofluids in computer cooling systems (heat transfer performance of nanofluids),” *Appl. Therm. Eng.*, vol. 45–46, pp. 9–14, 2012, doi: <https://doi.org/10.1016/j.applthermaleng.2012.03.028>.
- [40] M. Bahiraei and S. Heshmatian, “Electronics cooling with nanofluids: A critical review,” *Energy Convers. Manag.*, vol. 172, pp. 438–456, 2018, doi: <https://doi.org/10.1016/j.enconman.2018.07.047>.
- [41] Q. He, S. Wang, M. Tong, and Y. Liu, “Experimental study on thermophysical properties of nanofluids as phase-change material (PCM) in low temperature cool storage,” *Energy Convers. Manag.*, vol. 64, pp. 199–205, 2012, doi: <https://doi.org/10.1016/j.enconman.2012.04.010>.
- [42] M. S. Patil, J. H. Seo, S. J. Kang, and M. Y. Lee, “Review on synthesis, thermo-physical property, and heat transfer mechanism of nanofluids,” *Energies*, vol. 9, no. 10, pp. 1–17, 2016, doi: 10.3390/en9100840.
- [43] D. Dhinesh Kumar and A. Valan Arasu, “A comprehensive review of preparation, characterization, properties and stability of hybrid nanofluids,” *Renew. Sustain. Energy Rev.*, vol. 81, no. August 2016, pp. 1669–1689, 2018, doi:

10.1016/j.rser.2017.05.257.

- [44] S. Chakraborty and P. K. Panigrahi, “Stability of nanofluid: A review,” *Appl. Therm. Eng.*, vol. 174, p. 115259, 2020, doi: <https://doi.org/10.1016/j.applthermaleng.2020.115259>.
- [45] N. Abid *et al.*, “Synthesis of nanomaterials using various top-down and bottom-up approaches, influencing factors, advantages, and disadvantages: A review,” *Adv. Colloid Interface Sci.*, vol. 300, no. December 2021, p. 102597, 2022, doi: [10.1016/j.cis.2021.102597](https://doi.org/10.1016/j.cis.2021.102597).
- [46] S. P. Patil and V. V. Burungale, “2 - Physical and chemical properties of nanomaterials,” in *Micro and Nano Technologies*, N. D. Thorat and J. B. T.-N. for B. C. T. Bauer, Eds., Elsevier, 2020, pp. 17–31. doi: <https://doi.org/10.1016/B978-0-12-820016-2.00002-1>.
- [47] A. Reghunadhan, N. Kalarikkal, and S. Thomas, “Chapter 7 - Mechanical Property Analysis of Nanomaterials,” in *Micro and Nano Technologies*, S. Mohan Bhagyaraj, O. S. Oluwafemi, N. Kalarikkal, and S. B. T.-C. of N. Thomas, Eds., Woodhead Publishing, 2018, pp. 191–212. doi: <https://doi.org/10.1016/B978-0-08-101973-3.00007-9>.
- [48] V. Harish *et al.*, “Nanoparticle and Nanostructure Synthesis and Controlled Growth Methods,” *Nanomaterials*, vol. 12, no. 18, pp. 1–30, 2022, doi: [10.3390/nano12183226](https://doi.org/10.3390/nano12183226).
- [49] Y. Chen, J. Fitz Gerald, J. S. Williams, and S. Bulcock, “Synthesis of boron nitride

- nanotubes at low temperatures using reactive ball milling,” *Chem. Phys. Lett.*, vol. 299, no. 3, pp. 260–264, 1999, doi: [https://doi.org/10.1016/S0009-2614\(98\)01252-4](https://doi.org/10.1016/S0009-2614(98)01252-4).
- [50] L. G. Austin and V. K. Bhatia, “Experimental methods for grinding studies in laboratory mills,” *Powder Technol.*, vol. 5, no. 5, pp. 261–266, 1972, doi: [https://doi.org/10.1016/0032-5910\(72\)80029-9](https://doi.org/10.1016/0032-5910(72)80029-9).
- [51] R. Hogg, A. J. Dynys, and H. Cho, “Fine grinding of aggregated powders,” *Powder Technol.*, vol. 122, no. 2, pp. 122–128, 2002, doi: [https://doi.org/10.1016/S0032-5910\(01\)00407-7](https://doi.org/10.1016/S0032-5910(01)00407-7).
- [52] L. Takacs, “Self-sustaining reactions induced by ball milling,” *Prog. Mater. Sci.*, vol. 47, no. 4, pp. 355–414, 2002, doi: [https://doi.org/10.1016/S0079-6425\(01\)00002-0](https://doi.org/10.1016/S0079-6425(01)00002-0).
- [53] S. Wang, X. Li, J. Wu, W. Wen, and Y. Qi, “Fabrication of efficient metal halide perovskite solar cells by vacuum thermal evaporation: A progress review,” *Curr. Opin. Electrochem.*, vol. 11, pp. 130–140, 2018, doi: <https://doi.org/10.1016/j.coelec.2018.10.006>.
- [54] P. G. Jamkhande, N. W. Ghule, A. H. Bamer, and M. G. Kalaskar, “Metal nanoparticles synthesis: An overview on methods of preparation, advantages and disadvantages, and applications,” *J. Drug Deliv. Sci. Technol.*, vol. 53, p. 101174, 2019, doi: <https://doi.org/10.1016/j.jddst.2019.101174>.
- [55] A. Zhou, “2 - Methods of MAX-phase synthesis and densification – II,” I. M. B. T.-

- A. in S. and T. of M. P. Low, Ed., Woodhead Publishing, 2012, pp. 21–46. doi: <https://doi.org/10.1533/9780857096012.21>.
- [56] M. M. Zagho, H. D. Dawoud, N. Bensalah, and T. M. Altahtamouni, “A brief overview of RF sputtering deposition of boron carbon nitride (BCN) thin films,” *Emergent Mater.*, vol. 2, no. 1, pp. 79–93, 2019, doi: 10.1007/s42247-018-0018-9.
- [57] D. M. Mattox, “Physical vapor deposition (PVD) processes,” *Met. Finish.*, vol. 100, pp. 394–408, 2002, doi: [https://doi.org/10.1016/S0026-0576\(02\)82043-8](https://doi.org/10.1016/S0026-0576(02)82043-8).
- [58] Mr Sharad Kamble, Miss Kaveri Bhosale, Mr Mahesh Mohite, and Mrs Swapnali Navale, “Methods of Preparation of Nanoparticles,” *Int. J. Adv. Res. Sci. Commun. Technol.*, vol. 7, no. 4, pp. 121–127, 2023, doi: 10.48175/ijarsct-9485.
- [59] N. Wang, J. Y. H. Fuh, S. T. Dheen, and A. Senthil Kumar, “Synthesis methods of functionalized nanoparticles: a review,” *Bio-Design Manuf.*, vol. 4, no. 2, pp. 379–404, 2021, doi: 10.1007/s42242-020-00106-3.
- [60] H. M. Ali, H. Babar, T. R. Shah, M. U. Sajid, M. A. Qasim, and S. Javed, “Preparation techniques of TiO<sub>2</sub> nanofluids and challenges: A review,” *Appl. Sci.*, vol. 8, no. 4, 2018, doi: 10.3390/app8040587.
- [61] G. Paul, J. Philip, B. Raj, P. K. Das, and I. Manna, “Synthesis, characterization, and thermal property measurement of nano-Al<sub>19</sub>Zn<sub>05</sub> dispersed nanofluid prepared by a two-step process,” *Int. J. Heat Mass Transf.*, vol. 54, no. 15, pp. 3783–3788, 2011, doi: <https://doi.org/10.1016/j.ijheatmasstransfer.2011.02.044>.

- [62] Z. Said *et al.*, “Nanofluids-based solar collectors as sustainable energy technology towards net-zero goal: Recent advances, environmental impact, challenges, and perspectives,” *Chem. Eng. Process. - Process Intensif.*, vol. 191, p. 109477, 2023, doi: <https://doi.org/10.1016/j.cep.2023.109477>.
- [63] G.-J. Lee, C. K. Kim, M. K. Lee, C. K. Rhee, S. Kim, and C. Kim, “Thermal conductivity enhancement of ZnO nanofluid using a one-step physical method,” *Thermochim. Acta*, vol. 542, pp. 24–27, 2012, doi: <https://doi.org/10.1016/j.tca.2012.01.010>.
- [64] L. H. Bac, K. S. Yun, J. S. Kim, J. C. Kim, and C. K. Rhee, “One-step Physical Method for Synthesis of Cu Nanofluid in Ethylene Glycol,” *J. Korean Powder Metall. Inst.*, vol. 17, no. 6, pp. 464–469, 2010, doi: 10.4150/kpmi.2010.17.6.464.
- [65] H. Chang and Y.-C. Chang, “Fabrication of Al<sub>2</sub>O<sub>3</sub> nanofluid by a plasma arc nanoparticles synthesis system,” *J. Mater. Process. Technol.*, vol. 207, no. 1, pp. 193–199, 2008, doi: <https://doi.org/10.1016/j.jmatprotec.2007.12.070>.
- [66] H. T. Zhu, Y. S. Lin, and Y. S. Yin, “A novel one-step chemical method for preparation of copper nanofluids,” *J. Colloid Interface Sci.*, vol. 277, no. 1, pp. 100–103, 2004, doi: 10.1016/j.jcis.2004.04.026.
- [67] A. Ghadimi, R. Saidur, and H. S. C. Metselaar, “A review of nanofluid stability properties and characterization in stationary conditions,” *Int. J. Heat Mass Transf.*, vol. 54, no. 17, pp. 4051–4068, 2011, doi: <https://doi.org/10.1016/j.ijheatmasstransfer.2011.04.014>.

- [68] E. J. Swanson, J. Tavares, and S. Coulombe, “Improved Dual-Plasma Process for the Synthesis of Coated or Functionalized Metal Nanoparticles,” *IEEE Trans. Plasma Sci.*, vol. 36, no. 4, pp. 886–887, 2008, doi: 10.1109/TPS.2008.924549.
- [69] N. Ali, J. A. Teixeira, and A. Addali, “Aluminium Nanofluids Stability: A Comparison between the Conventional Two-Step Fabrication Approach and the Controlled Sonication Bath Temperature Method,” *J. Nanomater.*, vol. 2019, p. 3930572, 2019, doi: 10.1155/2019/3930572.
- [70] Y. Hwang *et al.*, “Production and dispersion stability of nanoparticles in nanofluids,” *Powder Technol.*, vol. 186, no. 2, pp. 145–153, 2008, doi: <https://doi.org/10.1016/j.powtec.2007.11.020>.
- [71] S. Mukherjee, P. C. Mishra, and P. Chaudhuri, “Stability of Heat Transfer Nanofluids – A Review,” *ChemBioEng Rev.*, vol. 5, no. 5, pp. 312–333, 2018, doi: 10.1002/cben.201800008.
- [72] W. Yu and H. Xie, “A Review on Nanofluids: Preparation, Stability Mechanisms, and Applications,” *J. Nanomater.*, vol. 2012, p. 435873, 2012, doi: 10.1155/2012/435873.
- [73] G. Xia, H. Jiang, R. Liu, and Y. Zhai, “Effects of surfactant on the stability and thermal conductivity of Al<sub>2</sub>O<sub>3</sub>/de-ionized water nanofluids,” *Int. J. Therm. Sci.*, vol. 84, pp. 118–124, 2014, doi: <https://doi.org/10.1016/j.ijthermalsci.2014.05.004>.
- [74] S. Mukherjee and S. Paria, “Preparation and Stability of Nanofluids-A Review,” vol. 9, no. 2, pp. 63–69, 2013.

- [75] M. F. Nabil, W. H. Azmi, K. A. Hamid, and R. Mamat, "Experimental investigation of heat transfer and friction factor of TiO<sub>2</sub>-SiO<sub>2</sub> nanofluids in water:ethylene glycol mixture," *Int. J. Heat Mass Transf.*, vol. 124, pp. 1361–1369, 2018, doi: <https://doi.org/10.1016/j.ijheatmasstransfer.2018.04.143>.
- [76] M. Ouikhalfan *et al.*, "Stability and thermal conductivity enhancement of aqueous nanofluid based on surfactant-modified TiO<sub>2</sub>," *J. Dispers. Sci. Technol.*, vol. 41, no. 3, pp. 374–382, Feb. 2020, doi: 10.1080/01932691.2019.1578665.
- [77] W. Yu and H. Xie, "A review on nanofluids: Preparation, stability mechanisms, and applications," *J. Nanomater.*, vol. 2012, 2012, doi: 10.1155/2012/435873.
- [78] J. Sarkar, "A critical review on convective heat transfer correlations of nanofluids," *Renew. Sustain. Energy Rev.*, vol. 15, no. 6, pp. 3271–3277, 2011, doi: <https://doi.org/10.1016/j.rser.2011.04.025>.
- [79] J.-H. Lee *et al.*, "Effective viscosities and thermal conductivities of aqueous nanofluids containing low volume concentrations of Al<sub>2</sub>O<sub>3</sub> nanoparticles," *Int. J. Heat Mass Transf.*, vol. 51, no. 11, pp. 2651–2656, 2008, doi: <https://doi.org/10.1016/j.ijheatmasstransfer.2007.10.026>.
- [80] R. Choudhary, D. Khurana, A. Kumar, and S. Subudhi, "Stability analysis of Al<sub>2</sub>O<sub>3</sub>/water nanofluids," *J. Exp. Nanosci.*, vol. 12, no. 1, pp. 140–151, Jan. 2017, doi: 10.1080/17458080.2017.1285445.
- [81] X. J. Wang, X. Li, and S. Yang, "Influence of pH and SDBS on the stability and thermal conductivity of nanofluids," *Energy and Fuels*, vol. 23, no. 5, pp. 2684–

2689, 2009, doi: 10.1021/ef800865a.

- [82] M. F. Zawrah, R. M. Khattab, L. G. Girgis, H. El Daidamony, and R. E. Abdel Aziz, “Stability and electrical conductivity of water-base Al<sub>2</sub>O<sub>3</sub> nanofluids for different applications,” *HBRC J.*, vol. 12, no. 3, pp. 227–234, 2016, doi: <https://doi.org/10.1016/j.hbrcj.2014.12.001>.
- [83] H. J. Kim, I. C. Bang, and J. Onoe, “Characteristic stability of bare Au-water nanofluids fabricated by pulsed laser ablation in liquids,” *Opt. Lasers Eng.*, vol. 47, no. 5, pp. 532–538, 2009, doi: <https://doi.org/10.1016/j.optlaseng.2008.10.011>.
- [84] W. Chamsa-ard, S. Brundavanam, C. C. Fung, D. Fawcett, and G. Poinern, “Nanofluid Types, Their Synthesis, Properties and Incorporation in Direct Solar Thermal Collectors: A Review,” *Nanomaterials*, vol. 7, no. 6, 2017. doi: 10.3390/nano7060131.
- [85] D. F. Swinehart, “The Beer-Lambert Law,” *J. Chem. Educ.*, vol. 39, no. 7, p. 333, Jul. 1962, doi: 10.1021/ed039p333.
- [86] M. Milanese, G. Colangelo, A. Cretì, M. Lomascolo, F. Iacobazzi, and A. de Risi, “Optical absorption measurements of oxide nanoparticles for application as nanofluid in direct absorption solar power systems – Part II: ZnO, CeO<sub>2</sub>, Fe<sub>2</sub>O<sub>3</sub> nanoparticles behavior,” *Sol. Energy Mater. Sol. Cells*, vol. 147, pp. 321–326, 2016, doi: <https://doi.org/10.1016/j.solmat.2015.12.030>.
- [87] L. Kong, J. Sun, and Y. Bao, “Preparation, characterization and tribological mechanism of nanofluids,” *RSC Adv.*, vol. 7, no. 21, pp. 12599–12609, 2017, doi:



10.1039/c6ra28243a.

- [88] S. Chakraborty, I. Sarkar, D. K. Behera, S. K. Pal, and S. Chakraborty, “Experimental investigation on the effect of dispersant addition on thermal and rheological characteristics of TiO<sub>2</sub> nanofluid,” *Powder Technol.*, vol. 307, pp. 10–24, 2017, doi: <https://doi.org/10.1016/j.powtec.2016.11.016>.
- [89] S. Chakraborty, I. Sengupta, I. Sarkar, S. K. Pal, and S. Chakraborty, “Effect of surfactant on thermo-physical properties and spray cooling heat transfer performance of Cu-Zn-Al LDH nanofluid,” *Appl. Clay Sci.*, vol. 168, pp. 43–55, 2019, doi: <https://doi.org/10.1016/j.clay.2018.10.018>.
- [90] N. Ali, J. A. Teixeira, and A. Addali, “A Review on Nanofluids: Fabrication, Stability, and Thermophysical Properties,” *J. Nanomater.*, vol. 2018, p. 6978130, 2018, doi: [10.1155/2018/6978130](https://doi.org/10.1155/2018/6978130).
- [91] D. Dey, P. Kumar, and S. Samantaray, “A review of nanofluid preparation, stability, and thermo-physical properties,” *Heat Transf. - Asian Res.*, vol. 46, no. 8, pp. 1413–1442, 2017, doi: [10.1002/htj.21282](https://doi.org/10.1002/htj.21282).
- [92] S. Rubalya Valantina, K. Arockia Jayalatha, D. R. Phebee Angeline, S. Uma, and B. Ashvanth, “Synthesis and characterisation of electro-rheological property of novel eco-friendly rice bran oil and nanofluid,” *J. Mol. Liq.*, vol. 256, pp. 256–266, 2018, doi: <https://doi.org/10.1016/j.molliq.2018.01.183>.
- [93] S. Bhattacharjee, “DLS and zeta potential – What they are and what they are not?,” *J. Control. Release*, vol. 235, pp. 337–351, 2016, doi: <https://doi.org/10.1016/j.jconrel.2016.05.016>.

<https://doi.org/10.1016/j.jconrel.2016.06.017>.

- [94] M. Kole and T. K. Dey, “Effect of aggregation on the viscosity of copper oxide–gear oil nanofluids,” *Int. J. Therm. Sci.*, vol. 50, no. 9, pp. 1741–1747, 2011, doi: <https://doi.org/10.1016/j.ijthermalsci.2011.03.027>.
- [95] C. T. Crowe, J. D. Schwarzkopf, M. Sommerfeld, and Y. Tsuj, *Multi-phase Flows with Droplets and Particles*. 1998.
- [96] N. M. Kovalchuk, D. Johnson, V. Sobolev, N. Hilal, and V. Starov, “Interactions between nanoparticles in nanosuspension,” *Adv. Colloid Interface Sci.*, vol. 272, p. 102020, 2019, doi: <https://doi.org/10.1016/j.cis.2019.102020>.
- [97] O. Z. Sharaf, A. N. Al-Khateeb, D. C. Kyritsis, and E. Abu-Nada, “Numerical investigation of nanofluid particle migration and convective heat transfer in microchannels using an Eulerian–Lagrangian approach,” *J. Fluid Mech.*, vol. 878, pp. 62–97, 2019, doi: DOI: 10.1017/jfm.2019.606.
- [98] H. Chen, Y. Ding, and C. Tan, “Rheological behaviour of nanofluids,” *New J. Phys.*, vol. 9, no. 10, p. 367, 2007, doi: 10.1088/1367-2630/9/10/367.
- [99] M. Bortolato *et al.*, “Investigation of a single wall carbon nanohorn-based nanofluid in a full-scale direct absorption parabolic trough solar collector,” *Energy Convers. Manag.*, vol. 150, pp. 693–703, 2017, doi: <https://doi.org/10.1016/j.enconman.2017.08.044>.
- [100] S. Witharana, H. Chen, and Y. Ding, “Stability of nanofluids in quiescent and shear

flow fields,” *Nanoscale Res. Lett.*, vol. 6, no. 1, p. 231, 2011, doi: 10.1186/1556-276X-6-231.

- [101] M. J. Nine, H. Chung, M. R. Tanshen, N. A. B. A. Osman, and H. Jeong, “Is metal nanofluid reliable as heat carrier?,” *J. Hazard. Mater.*, vol. 273, pp. 183–191, 2014, doi: <https://doi.org/10.1016/j.jhazmat.2014.03.055>.
- [102] X. Xu, C. Xu, J. Liu, X. Fang, and Z. Zhang, “A direct absorption solar collector based on a water-ethylene glycol based nanofluid with anti-freeze property and excellent dispersion stability,” *Renew. Energy*, vol. 133, pp. 760–769, 2019, doi: <https://doi.org/10.1016/j.renene.2018.10.073>.
- [103] A. Krupa *et al.*, “High-Energy Ball Milling as Green Process To Vitrify Tadalafil and Improve Bioavailability,” *Mol. Pharm.*, vol. 13, no. 11, pp. 3891–3902, Nov. 2016, doi: 10.1021/acs.molpharmaceut.6b00688.
- [104] N. Singh and V. Khullar, “Efficient Volumetric Absorption Solar Thermal Platforms Employing Thermally Stable - Solar Selective Nanofluids Engineered from Used Engine Oil,” *Sci. Rep.*, vol. 9, no. 1, p. 10541, 2019, doi: 10.1038/s41598-019-47126-3.
- [105] J. Piquot, U. Nithiyantham, Y. Grosu, and A. Faik, “Spray-graphitization as a protection method against corrosion by molten nitrate salts and molten salts based nanofluids for thermal energy storage applications,” *Sol. Energy Mater. Sol. Cells*, vol. 200, p. 110024, 2019, doi: <https://doi.org/10.1016/j.solmat.2019.110024>.
- [106] N. E. Hjerrild, J. A. Scott, R. Amal, and R. A. Taylor, “Exploring the effects of heat

- and UV exposure on glycerol-based Ag-SiO<sub>2</sub> nanofluids for PV/T applications,” *Renew. Energy*, vol. 120, pp. 266–274, 2018, doi: <https://doi.org/10.1016/j.renene.2017.12.073>.
- [107] W. Zhang, Y. Yao, K. Li, Y. Huang, and Y. Chen, “Influence of dissolved oxygen on aggregation kinetics of citrate-coated silver nanoparticles,” *Environ. Pollut.*, vol. 159, no. 12, pp. 3757–3762, 2011, doi: <https://doi.org/10.1016/j.envpol.2011.07.013>.
- [108] H. D. Koca, S. Doganay, A. Turgut, I. H. Tavman, R. Saidur, and I. M. Mahbulul, “Effect of particle size on the viscosity of nanofluids: A review,” *Renew. Sustain. Energy Rev.*, vol. 82, pp. 1664–1674, 2018, doi: <https://doi.org/10.1016/j.rser.2017.07.016>.
- [109] B. Munkhbayar, M. R. Tanshen, J. Jeoun, H. Chung, and H. Jeong, “Surfactant-free dispersion of silver nanoparticles into MWCNT-aqueous nanofluids prepared by one-step technique and their thermal characteristics,” *Ceram. Int.*, vol. 39, no. 6, pp. 6415–6425, 2013, doi: <https://doi.org/10.1016/j.ceramint.2013.01.069>.
- [110] L. Chen, H. Xie, Y. Li, and W. Yu, “Nanofluids containing carbon nanotubes treated by mechanochemical reaction,” *Thermochim. Acta*, vol. 477, no. 1, pp. 21–24, 2008, doi: <https://doi.org/10.1016/j.tca.2008.08.001>.
- [111] Z. Mingzheng, X. Guodong, L. Jian, C. Lei, and Z. Lijun, “Analysis of factors influencing thermal conductivity and viscosity in different kinds of surfactant solutions,” *Exp. Therm. Fluid Sci.*, vol. 36, pp. 22–29, 2012, doi:

<https://doi.org/10.1016/j.expthermflusci.2011.07.014>.

- [112] E. V Timofeeva, M. R. Moravek, and D. Singh, “Improving the heat transfer efficiency of synthetic oil with silica nanoparticles,” *J. Colloid Interface Sci.*, vol. 364, no. 1, pp. 71–79, 2011, doi: <https://doi.org/10.1016/j.jcis.2011.08.004>.
- [113] M. Chopkar, S. Sudarshan, P. K. Das, and I. Manna, “Effect of Particle Size on Thermal Conductivity of Nanofluid,” *Metall. Mater. Trans. A*, vol. 39, no. 7, pp. 1535–1542, 2008, doi: [10.1007/s11661-007-9444-7](https://doi.org/10.1007/s11661-007-9444-7).
- [114] T.-P. Teng, Y.-H. Hung, T.-C. Teng, H.-E. Mo, and H.-G. Hsu, “The effect of alumina/water nanofluid particle size on thermal conductivity,” *Appl. Therm. Eng.*, vol. 30, no. 14, pp. 2213–2218, 2010, doi: <https://doi.org/10.1016/j.applthermaleng.2010.05.036>.
- [115] J. Jeong, C. Li, Y. Kwon, J. Lee, S. H. Kim, and R. Yun, “Particle shape effect on the viscosity and thermal conductivity of ZnO nanofluids,” *Int. J. Refrig.*, vol. 36, no. 8, pp. 2233–2241, 2013, doi: <https://doi.org/10.1016/j.ijrefrig.2013.07.024>.
- [116] P. B. Maheshwary, C. C. Handa, and K. R. Nemade, “A comprehensive study of effect of concentration, particle size and particle shape on thermal conductivity of titania/water based nanofluid,” *Appl. Therm. Eng.*, vol. 119, pp. 79–88, 2017, doi: <https://doi.org/10.1016/j.applthermaleng.2017.03.054>.
- [117] W. Yu, H. Xie, L. Chen, and Y. Li, “Investigation of thermal conductivity and viscosity of ethylene glycol based ZnO nanofluid,” *Thermochim. Acta*, vol. 491, no. 1, pp. 92–96, 2009, doi: <https://doi.org/10.1016/j.tca.2009.03.007>.

- [118] M. Kole and T. K. Dey, "Role of interfacial layer and clustering on the effective thermal conductivity of CuO–gear oil nanofluids," *Exp. Therm. Fluid Sci.*, vol. 35, no. 7, pp. 1490–1495, 2011, doi: <https://doi.org/10.1016/j.expthermflusci.2011.06.010>.
- [119] M. S, S. A, and R. KS, "Thermo-physical properties of engineered dispersions of nano-sand in propylene glycol," *Colloids Surfaces A Physicochem. Eng. Asp.*, vol. 449, pp. 8–18, 2014, doi: <https://doi.org/10.1016/j.colsurfa.2014.02.040>.
- [120] S. Jana, A. Salehi-Khojin, and W.-H. Zhong, "Enhancement of fluid thermal conductivity by the addition of single and hybrid nano-additives," *Thermochim. Acta*, vol. 462, no. 1, pp. 45–55, 2007, doi: <https://doi.org/10.1016/j.tca.2007.06.009>.
- [121] J. A. Eastman, S. U. S. Choi, S. Li, W. Yu, and L. J. Thompson, "Anomalously increased effective thermal conductivities of ethylene glycol-based nanofluids containing copper nanoparticles," *Appl. Phys. Lett.*, vol. 78, no. 6, pp. 718–720, 2001, doi: 10.1063/1.1341218.
- [122] X. F. Li, D. S. Zhu, X. J. Wang, N. Wang, J. W. Gao, and H. Li, "Thermal conductivity enhancement dependent pH and chemical surfactant for Cu-H<sub>2</sub>O nanofluids," *Thermochim. Acta*, vol. 469, no. 1, pp. 98–103, 2008, doi: <https://doi.org/10.1016/j.tca.2008.01.008>.
- [123] H. Xie, J. Wang, T. Xi, Y. Liu, F. Ai, and Q. Wu, "Thermal conductivity enhancement of suspensions containing nanosized alumina particles," *J. Appl.*

*Phys.*, vol. 91, no. 7, pp. 4568–4572, 2002, doi: 10.1063/1.1454184.

- [124] N. R. Karthikeyan, J. Philip, and B. Raj, “Effect of clustering on the thermal conductivity of nanofluids,” *Mater. Chem. Phys.*, vol. 109, no. 1, pp. 50–55, 2008, doi: <https://doi.org/10.1016/j.matchemphys.2007.10.029>.
- [125] Y. He, Y. Jin, H. Chen, Y. Ding, D. Cang, and H. Lu, “Heat transfer and flow behaviour of aqueous suspensions of TiO<sub>2</sub> nanoparticles (nanofluids) flowing upward through a vertical pipe,” *Int. J. Heat Mass Transf.*, vol. 50, no. 11, pp. 2272–2281, 2007, doi: <https://doi.org/10.1016/j.ijheatmasstransfer.2006.10.024>.
- [126] N. Ahammed, L. G. Asirvatham, and S. Wongwises, “Effect of volume concentration and temperature on viscosity and surface tension of graphene–water nanofluid for heat transfer applications,” *J. Therm. Anal. Calorim.*, vol. 123, no. 2, pp. 1399–1409, 2016, doi: 10.1007/s10973-015-5034-x.
- [127] P. K. Namburu, D. P. Kulkarni, A. Dandekar, and D. K. Das, “Experimental investigation of viscosity and specific heat of silicon dioxide nanofluids,” *Micro Nano Lett.*, vol. 2, no. 3, pp. 67–71, 2007, doi: 10.1049/mnl:20070037.
- [128] H. Attari, F. Derakhshanfard, and M. H. K. Darvanjooghi, “Effect of temperature and mass fraction on viscosity of crude oil-based nanofluids containing oxide nanoparticles,” *Int. Commun. Heat Mass Transf.*, vol. 82, pp. 103–113, 2017, doi: <https://doi.org/10.1016/j.icheatmasstransfer.2017.02.007>.
- [129] Y.-H. Hung and W.-C. Chou, “Chitosan for Suspension Performance and Viscosity of MWCNTs,” *Int. J. Chem. Eng. Appl.*, vol. 3, no. 5, pp. 347–353, 2012, doi:

10.7763/ijcea.2012.v3.215.

- [130] M. Saeedinia, M. A. Akhavan-Behabadi, and P. Razi, “Thermal and rheological characteristics of CuO–Base oil nanofluid flow inside a circular tube,” *Int. Commun. Heat Mass Transf.*, vol. 39, no. 1, pp. 152–159, 2012, doi: <https://doi.org/10.1016/j.icheatmasstransfer.2011.08.001>.
- [131] M. Farbod, R. Kouhpeymani asl, and A. R. Noghreh abadi, “Morphology dependence of thermal and rheological properties of oil-based nanofluids of CuO nanostructures,” *Colloids Surfaces A Physicochem. Eng. Asp.*, vol. 474, pp. 71–75, 2015, doi: <https://doi.org/10.1016/j.colsurfa.2015.02.049>.
- [132] C. T. Nguyen *et al.*, “Viscosity data for Al<sub>2</sub>O<sub>3</sub>–water nanofluid—hysteresis: is heat transfer enhancement using nanofluids reliable?,” *Int. J. Therm. Sci.*, vol. 47, no. 2, pp. 103–111, 2008, doi: <https://doi.org/10.1016/j.ijthermalsci.2007.01.033>.
- [133] B. Aladag, S. Halelfadl, N. Doner, T. Maré, S. Duret, and P. Estellé, “Experimental investigations of the viscosity of nanofluids at low temperatures,” *Appl. Energy*, vol. 97, pp. 876–880, 2012, doi: <https://doi.org/10.1016/j.apenergy.2011.12.101>.
- [134] T. X. Phuoc and M. Massoudi, “Experimental observations of the effects of shear rates and particle concentration on the viscosity of Fe<sub>2</sub>O<sub>3</sub>–deionized water nanofluids,” *Int. J. Therm. Sci.*, vol. 48, no. 7, pp. 1294–1301, 2009, doi: <https://doi.org/10.1016/j.ijthermalsci.2008.11.015>.
- [135] S. Ghasemi and A. Karimipour, “Experimental investigation of the effects of temperature and mass fraction on the dynamic viscosity of CuO-paraffin nanofluid,”



- Appl. Therm. Eng.*, vol. 128, pp. 189–197, 2018, doi: <https://doi.org/10.1016/j.applthermaleng.2017.09.021>.
- [136] M. Baratpour, A. Karimipour, M. Afrand, and S. Wongwises, “Effects of temperature and concentration on the viscosity of nanofluids made of single-wall carbon nanotubes in ethylene glycol,” *Int. Commun. Heat Mass Transf.*, vol. 74, pp. 108–113, 2016, doi: <https://doi.org/10.1016/j.icheatmasstransfer.2016.02.008>.
- [137] W. Duangthongsuk and S. Wongwises, “Measurement of temperature-dependent thermal conductivity and viscosity of TiO<sub>2</sub>-water nanofluids,” *Exp. Therm. Fluid Sci.*, vol. 33, no. 4, pp. 706–714, 2009, doi: <https://doi.org/10.1016/j.expthermflusci.2009.01.005>.
- [138] K. S. Suganthi and K. S. Rajan, “Temperature induced changes in ZnO–water nanofluid: Zeta potential, size distribution and viscosity profiles,” *Int. J. Heat Mass Transf.*, vol. 55, no. 25, pp. 7969–7980, 2012, doi: <https://doi.org/10.1016/j.ijheatmasstransfer.2012.08.032>.
- [139] G. Żyła and J. Fal, “Experimental studies on viscosity, thermal and electrical conductivity of aluminum nitride–ethylene glycol (AlN–EG) nanofluids,” *Thermochim. Acta*, vol. 637, pp. 11–16, 2016, doi: <https://doi.org/10.1016/j.tca.2016.05.006>.
- [140] E. Esmacili, S. A. Rounaghi, W. Gruner, and J. Eckert, “The preparation of surfactant-free highly dispersed ethylene glycol-based aluminum nitride-carbon nanofluids for heat transfer application,” *Adv. Powder Technol.*, vol. 30, no. 10, pp.

2032–2041, 2019, doi: <https://doi.org/10.1016/j.appt.2019.06.008>.

- [141] G. Żyła, J. Fal, and P. Estellé, “Thermophysical and dielectric profiles of ethylene glycol based titanium nitride (TiN–EG) nanofluids with various size of particles,” *Int. J. Heat Mass Transf.*, vol. 113, pp. 1189–1199, 2017, doi: <https://doi.org/10.1016/j.ijheatmasstransfer.2017.06.032>.
- [142] R. Gómez-Villarejo, T. Aguilar, S. Hamze, P. Estellé, and J. Navas, “Experimental analysis of water-based nanofluids using boron nitride nanotubes with improved thermal properties,” *J. Mol. Liq.*, vol. 277, pp. 93–103, 2019, doi: <https://doi.org/10.1016/j.molliq.2018.12.093>.
- [143] G. Żyła, J. Fal, J. Traciak, M. Gizowska, and K. Perkowski, “Huge thermal conductivity enhancement in boron nitride – ethylene glycol nanofluids,” *Mater. Chem. Phys.*, vol. 180, pp. 250–255, 2016, doi: <https://doi.org/10.1016/j.matchemphys.2016.06.003>.
- [144] R. Gómez-Villarejo, P. Estellé, and J. Navas, “Boron nitride nanotubes-based nanofluids with enhanced thermal properties for use as heat transfer fluids in solar thermal applications,” *Sol. Energy Mater. Sol. Cells*, vol. 205, p. 110266, 2020, doi: <https://doi.org/10.1016/j.solmat.2019.110266>.
- [145] D. Singh *et al.*, “An investigation of silicon carbide-water nanofluid for heat transfer applications,” *Journal of Applied Physics*, vol. 105, no. 6. 2009. doi: 10.1063/1.3082094.
- [146] C. Ezekwem and A. Dare, “Thermal and electrical conductivity of silicon carbide

- nanofluids,” *Energy Sources, Part A Recover. Util. Environ. Eff.*, pp. 1–19, doi: 10.1080/15567036.2020.1792591.
- [147] Y. Guo, T. Zhang, D. Zhang, and Q. Wang, “Experimental investigation of thermal and electrical conductivity of silicon oxide nanofluids in ethylene glycol/water mixture,” *Int. J. Heat Mass Transf.*, vol. 117, pp. 280–286, 2018, doi: <https://doi.org/10.1016/j.ijheatmasstransfer.2017.09.091>.
- [148] G. Żyła and J. Fal, “Viscosity, thermal and electrical conductivity of silicon dioxide–ethylene glycol transparent nanofluids: An experimental studies,” *Thermochim. Acta*, vol. 650, pp. 106–113, 2017, doi: <https://doi.org/10.1016/j.tca.2017.02.001>.
- [149] H. Jin, T. Andritsch, I. A. Tsekmes, R. Kochetov, P. H. F. Morshuis, and J. J. Smit, “Properties of Mineral Oil based Silica Nanofluids,” *IEEE Trans. Dielectr. Electr. Insul.*, vol. 21, no. 3, pp. 1100–1108, 2014, doi: 10.1109/TDEI.2014.6832254.
- [150] R. Ranjbarzadeh, A. Moradikazerouni, R. Bakhtiari, A. Asadi, and M. Afrand, “An experimental study on stability and thermal conductivity of water/silica nanofluid: Eco-friendly production of nanoparticles,” *J. Clean. Prod.*, vol. 206, pp. 1089–1100, 2019, doi: <https://doi.org/10.1016/j.jclepro.2018.09.205>.
- [151] R. Mondragon, J. E. Julia, A. Barba, and J. C. Jarque, “Characterization of silica–water nanofluids dispersed with an ultrasound probe: A study of their physical properties and stability,” *Powder Technol.*, vol. 224, pp. 138–146, 2012, doi: <https://doi.org/10.1016/j.powtec.2012.02.043>.
- [152] G. Żyła, J. Fal, S. Bikić, and M. Wanic, “Ethylene glycol based silicon nitride

nanofluids: An experimental study on their thermophysical, electrical and optical properties,” *Phys. E Low-Dimensional Syst. Nanostructures*, vol. 104, no. July, pp. 82–90, 2018, doi: 10.1016/j.physe.2018.07.023.

- [153] A. K. Sleiti, “Heat transfer measurements of Polyalpha-Olefin- boron nitride nanofluids for thermal management and lubrication applications,” *Case Stud. Therm. Eng.*, vol. 22, p. 100776, 2020, doi: <https://doi.org/10.1016/j.csite.2020.100776>.
- [154] G. Yalçın, S. Öztuna, A. S. Dalkılıç, and S. Wongwises, “Measurement of thermal conductivity and viscosity of ZnO–SiO<sub>2</sub> hybrid nanofluids,” *J. Therm. Anal. Calorim.*, vol. 147, no. 15, pp. 8243–8259, 2022, doi: 10.1007/s10973-021-11076-8.
- [155] G. Żyła, J. P. Vallejo, and L. Lugo, “Isobaric heat capacity and density of ethylene glycol based nanofluids containing various nitride nanoparticle types: An experimental study,” *J. Mol. Liq.*, vol. 261, pp. 530–539, 2018, doi: <https://doi.org/10.1016/j.molliq.2018.04.012>.
- [156] L. S. Sundar, M. H. Farooky, S. N. Sarada, and M. K. Singh, “Experimental thermal conductivity of ethylene glycol and water mixture based low volume concentration of Al<sub>2</sub>O<sub>3</sub> and CuO nanofluids,” *Int. Commun. Heat Mass Transf.*, vol. 41, pp. 41–46, 2013, doi: <https://doi.org/10.1016/j.icheatmasstransfer.2012.11.004>.
- [157] A. Rehman *et al.*, “Effect of surfactants on the stability and thermophysical properties of Al<sub>2</sub>O<sub>3</sub>+TiO<sub>2</sub> hybrid nanofluids,” *J. Mol. Liq.*, vol. 391, no. PB, p.

123350, 2023, doi: 10.1016/j.molliq.2023.123350.

- [158] S. Todorova *et al.*, “Mesoporous CuO-Fe<sub>2</sub>O<sub>3</sub> composite catalysts for complete n-hexane oxidation,” in *Scientific Bases for the Preparation of Heterogeneous Catalysts*, E. M. Gaigneaux, M. Devillers, S. Hermans, P. A. Jacobs, J. A. Martens, and P. B. T.-S. in S. S. and C. Ruiz, Eds., Elsevier, 2010, pp. 547–550. doi: [https://doi.org/10.1016/S0167-2991\(10\)75105-3](https://doi.org/10.1016/S0167-2991(10)75105-3).
- [159] Babita, S. K. Sharma, and S. M. Gupta, “Preparation and evaluation of stable nanofluids for heat transfer application: A review,” *Exp. Therm. Fluid Sci.*, vol. 79, pp. 202–212, 2016, doi: <https://doi.org/10.1016/j.expthermflusci.2016.06.029>.
- [160] O. A. Lukianova, A. A. Parkhomenko, V. V. Krasilnikov, A. N. Khmara, and A. P. Kuzmenko, “New method of free silicon determination in pressureless sintered silicon nitride by Raman spectroscopy and XRD,” *Ceram. Int.*, vol. 45, no. 11, pp. 14338–14346, 2019, doi: <https://doi.org/10.1016/j.ceramint.2019.04.148>.
- [161] A. Asadi *et al.*, “Effect of sonication characteristics on stability, thermophysical properties, and heat transfer of nanofluids: A comprehensive review,” *Ultrason. Sonochem.*, vol. 58, p. 104701, 2019, doi: <https://doi.org/10.1016/j.ultsonch.2019.104701>.
- [162] P. C. Mukesh Kumar, K. Palanisamy, and V. Vijayan, “Stability analysis of heat transfer hybrid/water nanofluids,” *Mater. Today Proc.*, vol. 21, pp. 708–712, 2020, doi: <https://doi.org/10.1016/j.matpr.2019.06.743>.
- [163] S. Rajeshkumar, L. V. Bharath, and R. Geetha, “Chapter 17 - Broad spectrum

antibacterial silver nanoparticle green synthesis: Characterization, and mechanism of action,” in *Micro and Nano Technologies*, A. K. Shukla and S. B. T.-G. S. Iravani Characterization and Applications of Nanoparticles, Eds., Elsevier, 2019, pp. 429–444. doi: <https://doi.org/10.1016/B978-0-08-102579-6.00018-6>.

- [164] A. Hajizadeh *et al.*, “Electrophoretic deposition as a fabrication method for Li-ion battery electrodes and separators – A review,” *J. Power Sources*, vol. 535, p. 231448, 2022, doi: <https://doi.org/10.1016/j.jpowsour.2022.231448>.
- [165] R. H. Müller and C. Jacobs, “Buparvaquone mucoadhesive nanosuspension: preparation, optimisation and long-term stability,” *Int. J. Pharm.*, vol. 237, no. 1, pp. 151–161, 2002, doi: [https://doi.org/10.1016/S0378-5173\(02\)00040-6](https://doi.org/10.1016/S0378-5173(02)00040-6).
- [166] K. Cagua, F. Ordoñez, C. Zapata, B. Herrera, E. Pabón, and R. Buitrago-Sierra, “Surfactant concentration and pH effects on the zeta potential values of alumina nanofluids to inspect stability,” *Colloids Surfaces A Physicochem. Eng. Asp.*, vol. 583, p. 123960, 2019, doi: <https://doi.org/10.1016/j.colsurfa.2019.123960>.
- [167] K. H. Almitani, N. H. Abu-Hamdeh, S. Etedali, A. Abdollahi, A. S. Goldanlou, and A. Golmohammadzadeh, “Effects of surfactant on thermal conductivity of aqueous silica nanofluids,” *J. Mol. Liq.*, vol. 327, p. 114883, 2021, doi: <https://doi.org/10.1016/j.molliq.2020.114883>.
- [168] A. K. Sharma, A. K. Tiwari, and A. R. Dixit, “Rheological behaviour of nanofluids: A review,” *Renew. Sustain. Energy Rev.*, vol. 53, pp. 779–791, 2016, doi: <https://doi.org/10.1016/j.rser.2015.09.033>.

- [169] W. J. Tseng and S.-Y. Li, “Rheology of colloidal BaTiO<sub>3</sub> suspension with ammonium polyacrylate as a dispersant,” *Mater. Sci. Eng. A*, vol. 333, no. 1, pp. 314–319, 2002, doi: [https://doi.org/10.1016/S0921-5093\(01\)01856-1](https://doi.org/10.1016/S0921-5093(01)01856-1).
- [170] P. S. Kishore, V. Sireesha, V. Sree Harsha, V. Dharma Rao, and A. Brusly Solomon, “Preparation, characterization and thermo-physical properties of Cu-graphene nanoplatelets hybrid nanofluids,” *Mater. Today Proc.*, vol. 27, pp. 610–614, 2020, doi: <https://doi.org/10.1016/j.matpr.2019.12.108>.
- [171] L. T. Fogang, A. S. Sultan, and M. S. Kamal, “Understanding viscosity reduction of a long-tail sulfobetaine viscoelastic surfactant by organic compounds,” *RSC Adv.*, vol. 8, no. 8, pp. 4455–4463, 2018, doi: [10.1039/c7ra12538k](https://doi.org/10.1039/c7ra12538k).
- [172] H. W. Xian, N. A. C. Sidik, and R. Saidur, “Impact of different surfactants and ultrasonication time on the stability and thermophysical properties of hybrid nanofluids,” *Int. Commun. Heat Mass Transf.*, vol. 110, p. 104389, 2020, doi: <https://doi.org/10.1016/j.icheatmasstransfer.2019.104389>.

## LIST OF PUBLICATION

Action  	Manuscript Number 	Title 	Initial Date Submitted 	Status Date 	Current Status 
<a href="#">View Submission</a> <a href="#">Manuscript Analysis Services</a> <a href="#">View Reference Checking Results</a> <a href="#">Send E-mail</a>	MOLLIQ-D-24-09020	Investigation of the Stability and Thermophysical Properties of Si3N4 – Water/EG Nanofluids	Nov 05, 2024	Nov 20, 2024	Under Review